MITNE-207
C.2

NUCLEAR ENGINEERING
READING ROOM - M.I.T.

NEUTRONIC SENSITIVITY STUDIES ON MEKIN, AN ACCIDENT ANALYSIS COMPUTER CODE FOR NUCLEAR REACTORS

by

Craig E. Barbehenn, David D. Lanning

August 1977

Department of Nuclear Engineering
Massachusetts Institute of Technology
Cambridge, Massachusetts 02139

Electric Power Research Institute

MIT Libraries
Document Services

Room 14-0551
77 Massachusetts Avenue
Cambridge, MA 02139
Ph: 617.253.2800
Email: docs@mit.edu
http://libraries.mit.edu/docs

DISCLAIMER OF QUALITY

Due to the condition of the original material, there are unavoidable flaws in this reproduction. We have made every effort possible to provide you with the best copy available. If you are dissatisfied with this product and find it unusable, please contact Document Services as soon as possible.

Thank you.

Some pages in the original document contain pictures, graphics, or text that is illegible.

MITNE-207

NUCLEAR ENGINEERING
READING ROOM - M.I.T.

NEUTRONIC SENSITIVITY STUDIES ON MEKIN, AN ACCIDENT ANALYSIS COMPUTER CODE FOR NUCLEAR REACTORS

by

Craig E. Barbehenn, David D. Lanning

August 1977

Department of Nuclear Engineering
Massachusetts Institute of Technology
Cambridge, Massachusetts 02139

Electric Power Research Institute

ABSTRACT

Neutronic sensitivity studies have been made with respect to the use of the computer code MEKIN (MIT-EPRI Kinetics Code). This code is a tool for nuclear reactor safety analysis which couples neutron physics with thermal-hydraulics in time and three-dimensional space. These sensitivity results can be used as a guide with respect to three user inputs: neutronic spatial mesh size, neutronic time step size, and the linear cross section feedback parameters.

As the neutronic spatial mesh interval is decreased, the power distribution always converges to accurate solutions. For large problems with material discontinuities, a high degree of accuracy appears extremely expensive. For well-behaved and converged solutions, the required number of neutronic time steps may also be very costly. The solution is found to be particularly sensitive to time step size when the power-time behavior deviates from an exponential. The linear cross section feedback approximation cannot be depended upon, apriori, to accurately (i.e., within 10%) predict power level and energy deposition.

TABLE OF CONTENTS

TABLE OF CONTENTS (continued)

LIST OF FIGURES

LIST OF FIGURES (continued)

LIST OF FIGURES (continued)

LIST OF TABLES

LIST OF TABLES (continued)

ACKNOWLEDGEMENTS

Financial assistance for this work was generously provided by the Electric Power Research Institute.

Andrew Cook sacrificed a great deal of his own research time to offer everything from valuable theoretical suggestions to computer assistance, and his efforts are sincerely appreciated. Professor Allan F. Henry gave excellent advice with respect to neutronics while Tom Rodack and Professor Lothar Wolf were very helpful in the area of thermal hydraulics. George Solan of Yankee Atomic Power Company gathered much of the reactor data. Rachel Morton's aid was invaluable in regard to computer work.

CHAPTER 1

INTRODUCTION

Sensitivity studies with the computer code MEKIN (2) form the basis of this thesis. MEKIN is a nuclear reactor safety analysis code which couples neutron physics with thermal-hydraulics in time and three-dimensional space. Specifically, the code models light water reactor cores during postulated transients. The objective of this research project was to investigate and describe how certain neutronic input parameters effect the solution. The motivation behind the work and a general outline are provided in the next paragraphs.

Nuclear reactor safety has received a great deal of attention form this country's reactor vendors and public utilities. In addition, the government and general public have been constantly studying and questioning the issue. Complete experimental verification of safety is impractical or even impossible. As a result, computer codes have been the primary means of nuclear reactor accident analysis. Codes introduce compromises via numerical approximations and simplified physical models. The incentive for such compromising is both theoretical and economic; the mathematics or physics necessary for an exact solution may not be understood, while financial restraints limit computational time. Some compromises are built into the code, while others are options selected by the user. Either way, code users generally wish to attain a certain accuracy with the least amount of trouble. Therefore,

the user must have some idea on the extent that the solution is effected as the caluculation is simplified. This is the mode of thought which led to the problem addressed in this thesis: sensitivity studies with MEKIN.

This thesis is broken down into seven chapters. Chapter 2 provides a brief description of the MEKIN code in terms geometry and calculational strategy. This chapter can be skipped by those familiar with the code, and the MEKIN manual should be consulted if more detail is desired. Chapter 2 also addresses several areas of input preparation which warranted special attention in this study and may demand extra consideration by future code users. Chapter 3 gives an indication of the sensitivity of solution to the steady state convergence criteria. Chapter 4 gives a discussion of the sensitibity of solution to the neutronic mesh spacing. Chapter 5 gives a description of the sensitivity of solution to the neutronic time step size. Chapter 6 sets forth the sensitivity of solution to the cross section feedback parameters. Finally, Chapter 7 offers recommendations and conclusions.

CHAPTER 2

THE MEKIN CODE DESCRIPTION AND INPUT PREPARATION

MEKIN is a safety analysis code which couples neutron physics with thermal hydraulics in time and three-dimensional space. Specifically, this code represents cores of light-water nuclear reactors during postulated transients. A complete code description is contained in the MEKIN manual. Volume I consists of a theoretical explanation of the code's capabilities and caluclational strategy. Volumes II and III are made up of articles written while MEKIN was being developed.

This chapter highlights MEKIN and discusses several aspects of input preparation which deserve special attention. For more detail, the reader should consult the MEKIN manual.

2.1 MEKIN GEOMETRY

When using or discussing a code similar to MEKIN, an accepted nomenclature greatly enhances understanding and communication. Below is an explanation of the reactor geometry in MEKIN and a presentation of definitions employed throughout this thesis as well as in the code manual.

The core is represented as a mass of three-dimensional reactor regions. Every region is the same size, each is neutronically homogeneous, and each is rectangular parallel-piped. A region occupies a square box in the X-Y (horizontal) plane and an axial segment in the z (vertical) direction. The user supplies a set of cross-sections and related constants for each

region.

Superimposed on this region-geometry is a neutronic fine mesh geometry. As a result, each homogeneous region is subdivided into axial mesh intervals and horizontal square mesh increments. Both axial intervals and square increments must be uniform throughout the reactor. However, the set of axial intervals and the set of square increments may be varied independently. These intervals and squares all contain a centered neutronic mesh point. Turning back to three dimensions, a mesh increment of volume must also have a geometrically centered mesh point. Thus, a uniform number of mesh points are contained within each and every reactor region. Values of neutron flux, delayed neutron precursor concentration, and equilibrium xenon concentration are computed for each mesh point in the reactor.

Within the core, thermal-hydraulic regions are indentical to the neutronically homogeneous reactor regions discussed above. Both have the same size, same shape, and same locations. Outside the core, additional thermal-hydraulic regions may (user option) occupy volumes not considered in the neutronic analysis. A thermal-hydraulic channel is a vertical combination of regions. Average values of coolant density, coolant temperature, and fuel temperature are computed and stored for each thermal-hydraulic region.

Perhaps a summation of the geometrical model will clarify the nomenclature. A region should be visualized as a volume whose neutronic and thermal-hydraulic constants are smeared

over this volume. The neutron flux solution is computed at discrete mesh points within the region, while the radial temperature profile is calculated at discrete nodes within the region's average pin. Such a description is consistent with MEKIN's required input. The user specifies a uniform size of the regions, a uniform number of axial and horizontal mesh points per region, and a uniform number of radial fuel nodes per pin. Chapter 4 deals with the sensitivity of the neutronic mesh spacing in detail. Illustrations of the MEKIN geometry are privided on Figs. 2.1 and 2.2.

2.2 THE MEKIN CALCULATION

The calculational sequences can be subdivided into three classes: neutronics, thermal-hydraulics, and the transmission of information between the two. The neutronic model is transient neutron diffusion theory. The user can choose a calculation involving one or two neutron energy groups and from zero to six delayed neutron families. The thermal-hydraulic model is identifcal to the COBRA III-C/MIT code (14).

The steady state and transient calculational strategies require separate explanations. As a brief description, the next two paragraphs and associated figures include material taken directly from Volume I, Part I, pages 9-13 of the MEKIN manual.

The steady state reactor calculation involves an iteration between neutronic and thermal-hydraulic calculations. This iteration is required because neutronic parameters (e.g., cross sections) are functions of thermal-hydraulic state vari-

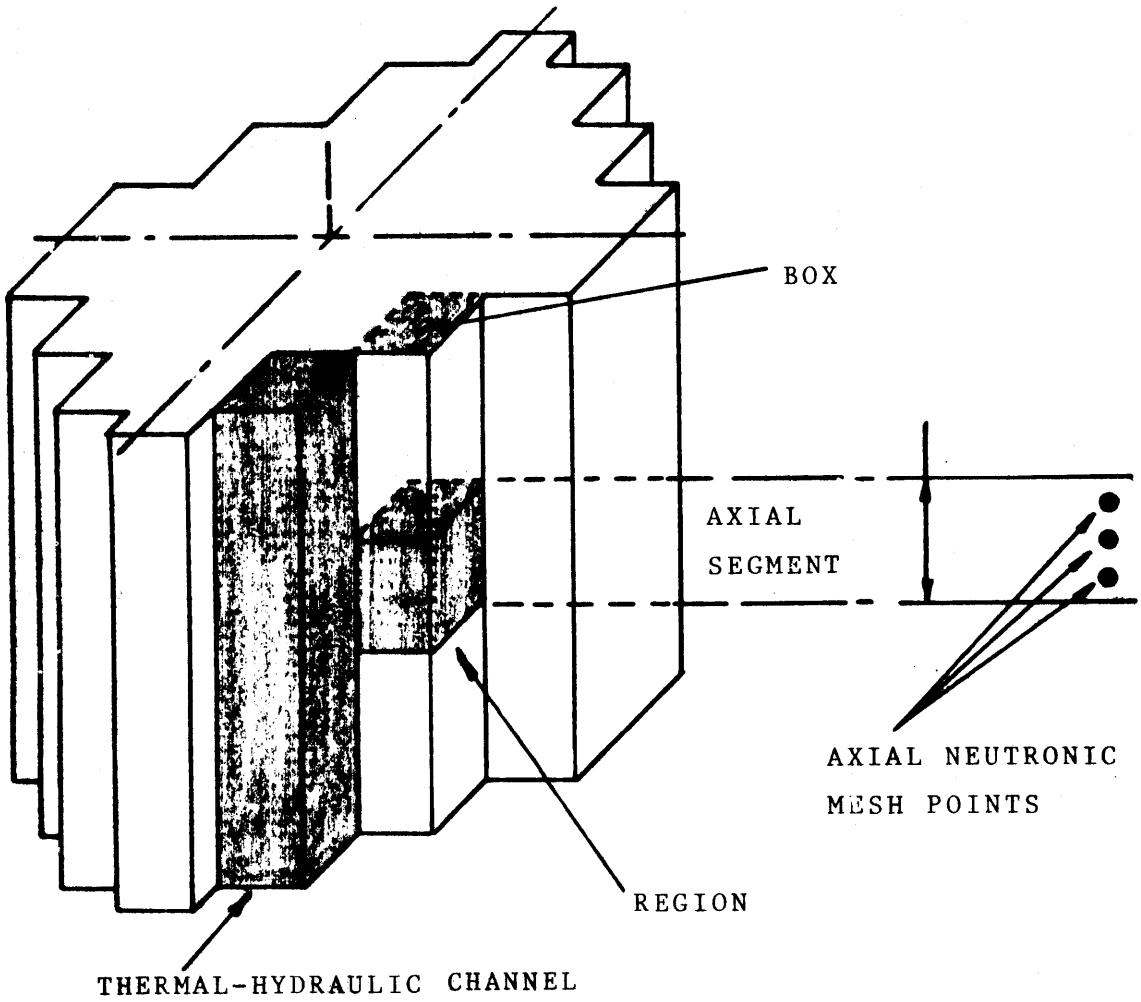

FIG. 2.1: REACTOR GEOMETRY IN MEKIN.

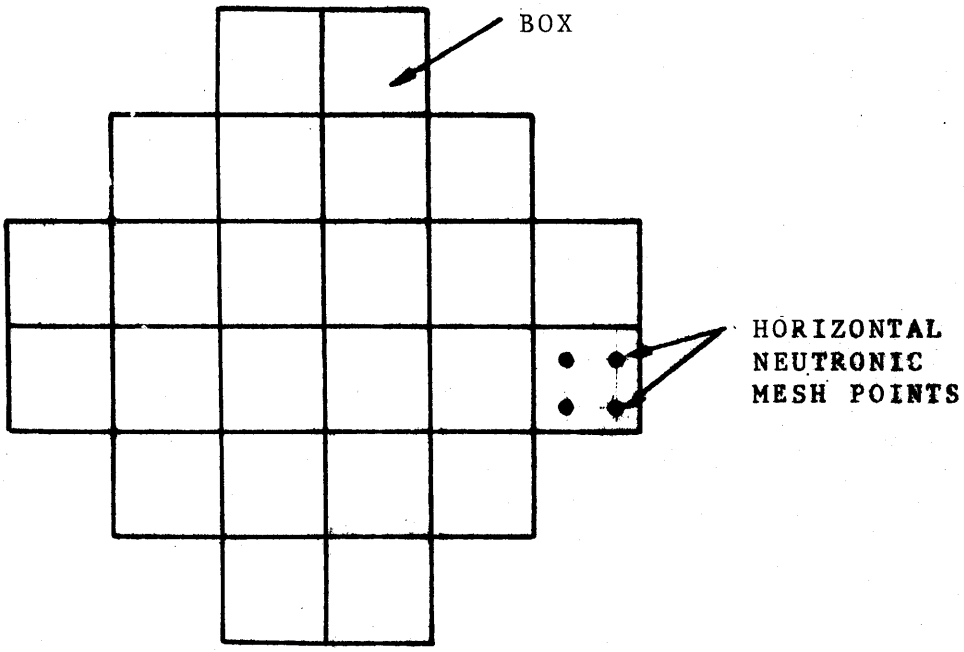

FIG. 2.2: HORIZONTAL REACTOR GEOMETRY IN MEKIN.

ables (e.g., temperatures and densities). Furthermore, the sensible power (i.e., heat) distribution is a function of the fission distribution. The sequence of calculations is illustrated in Fig. 2.3. Total reactor power is a user input and the static neutronic calculation is performed as a K-effective search. This calculation is based on user specified convergence criteria, which are discussed further in Chapter 3.

The general sequence of calculations required to update the reactor state over one time interval is illustrated in Fig. 2.4. Beginning in the lower, left-hand portion of the figure, the most recently computed thermal-hydraulic state variables (e_c, T_c, T_m) and correlated data are used to evaluate neutronic parameters. These parameters are modified to reflect external neutronic perturbations (e.g., control rod movement). The neutron flux (ϕ), delayed neutron precurser concentrations (C), and fission distribution (F) are updated in the transient neutronic calculation. The sensible power is computed. Thermal-hydraulic parameters and boundary conditions are modified to reflect the effect of external thermal-hydraulic perturbations (e.g., reduction of flow). Thethermal-hydraulic state variables are then computed. This sequence is repeated for successive thermal-hydraulic time intervals, and the user may specify multiple neutronic time steps within one thermal-hydraulic interval.

The sensitivity of the time interval between neutronic calculations is discussed in depth in Chapter 5 of this thesis. The sensitivity of the technique for updating the cross sections is considered in Chapter 6.

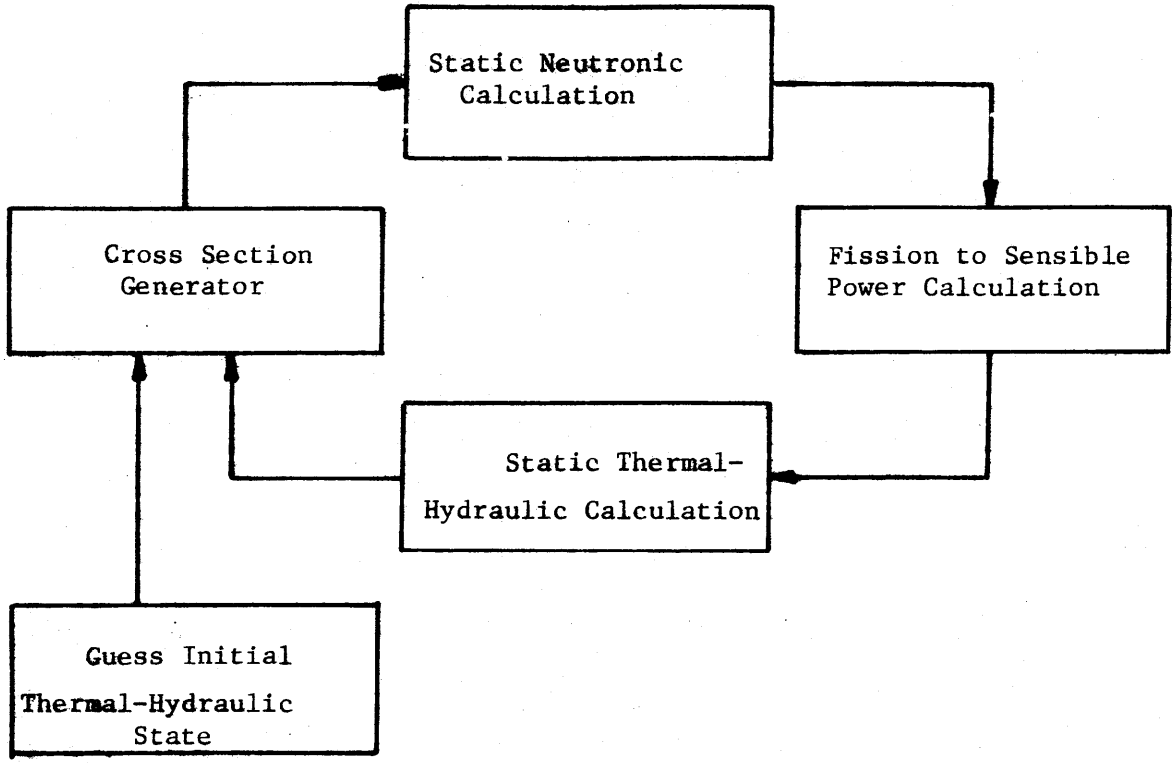

FIG. 2.3: STEADY STATE CALCULATION (2).

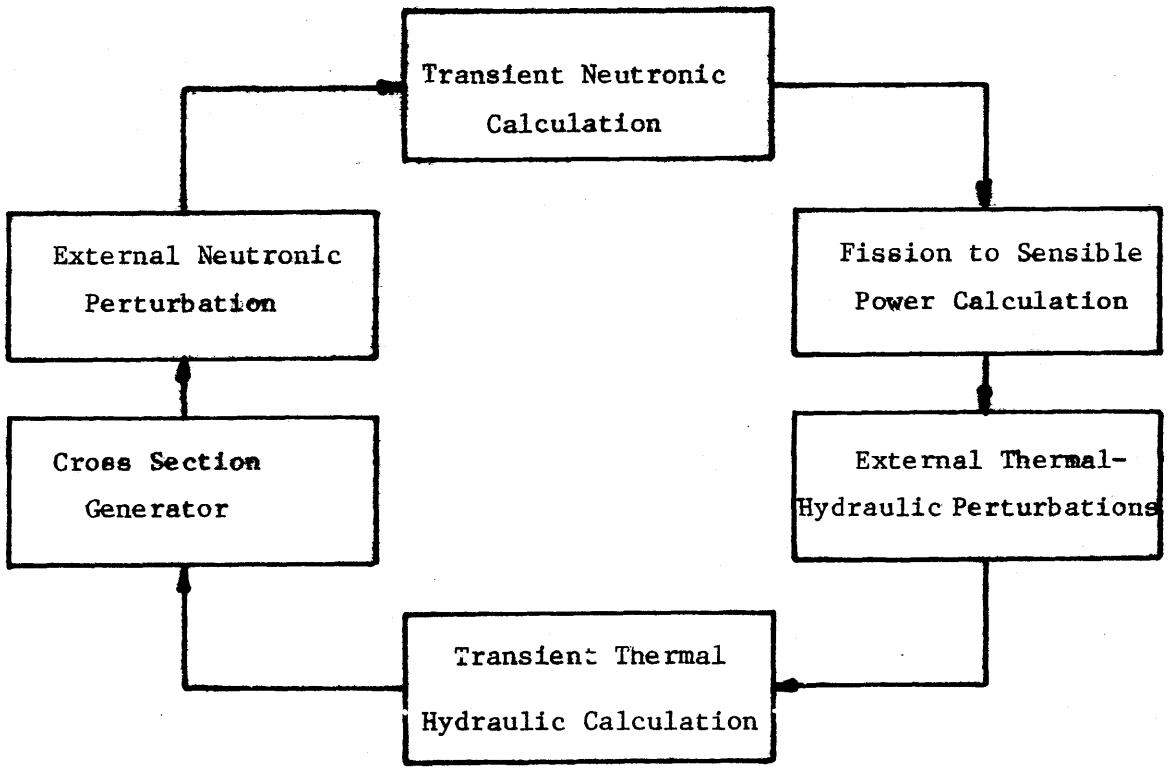

FIG. 2.4: TRANSIENT CALCULATION [2].

2.3 INPUT PREPARATION

Several of the user input parameters of MEKIN warrant special attention, and preliminary calculations may be necessary. A few examples of such neutronic parameters are discussed below.

Homogenized, macroscopic cross sections represent a user input in MEKIN, but separate codes must be employed to obtain these constants. Consequently, care must be taken to insure that generated cross sections are in the proper form for use in MEKIN. In addition, gathering the data may be a formidable task due to the large number of reactor regions for a full-scale problem. This is particularly true for an end-of-cycle core, where burnup causes region-to-region cross section variation in the axial as well as radial direction. In fact, a reactor-specific computer program may be the most efficient procedure for gathering, altering, and punching the data. Due to the nature of the data base for the test problems of this thesis, the macroscopic cross sections required both an alteration of form (see Appendix A for details) and a custom-made computer program. Keep in mind that Appendix A applies to a specific case, and the material may or may not be relevant to another user. The key point to remember is that inputting the macroscopic cross-sections to MEKIN may require a careful, tedious effort.

The MEKIN user has the option of specifying albedo boundary conditions at the core-reflector interface. A set of albedoes can be determined by either of two methods: nomalization of the power distribution or direct calculation. A normaliza-

tion procedure would involve iteratively varying the albedoes until the MEKIN power distribution approximates an accurately calculated distribution. However, the effort would probably outweigh the benefits in terms of expense and time relative to a questionable gain in accuracy. Direct calculation of the albedoes is the alternative, but an understanding of the use of the albedo boundary conditions in the MEKIN code is essential because albedoes do not have a standard definition. One method of calculating an appropriate set is the procedure developed by P. Kalambokas (10). Although his definition of albedoes does not match that in MEKIN, his procedure is still applicable. Details are set forth in Appendix A.

The cross section feedback parameters comprise another set of inputs which require extra calculations. Chapter 6 gives a discussion of these parameters in detail.

CHAPTER 3

NEUTRONIC CONVERGENCE CRITERIA SENSITIVITY

In the steady state, MEKIN solves the neutronics finite difference equations by accelerated iterative methods, and the computation proceeds until the convergence criteria has been satisfied. Because this criteria is among the input, the user can control the degree to which the solution is converged. The purpose of this chapter is to address the sensitivity of the "neutronics-only" steady state solution to the neutronic convergence criteria (Neutronics-only implies no thermal-hydraulic calculations.).

The input convergence criteria to MEKIN are EPSSPR, EPPSK, and DIFMAX. As defined in Volume 1, Part II, page 27 of the manual, EPSSPR is the convergence criteria on region power for reactor iterations at steady state. The maximum change in reactor power, over all regions, must be less than this value. EPSSK is the neutronic eigenvalue (K-effective) convergence criteria for the reactor solution at steady state. DIFMAX is the pointwise neutron flux convergence criteria for the neutronic steady state caluculation. When thermal-hydraulic feedback and xenon are not included, only one neutronic calculation is performed (i.e., one set of outer iterations). In this situation, EPSSPR and EPPSK are ignored; DIFMAX and criteria built into MEKIN monitor the convergence.

In order to determine the sensitivity of solution to DIFMAX, several cases were selected and DIFMAX was varied for

each case. Model 1 of Appendix B was the primary reactor used for this sensitivity. The first case involved this model with the following additional features: 10.4 cm. horizontal neutronic mesh spacing, identical material compositions for all regions, neutronics-only. The behavior of the steady state flux solution as a function of DIFMAX is well behaved, as illustrated in Fig. 3.1. The fact that the solutions are identical when DIFMAX is 10^{-1} and 10^{-2} indicates that the additional covergence criteria built into MEKIN controls the convergence when -log (DIFMAX) is sufficiently small.

The second case involved the same model with one exception: the material compositions were different from region to region. Results almost duplicate those from the initial case, as shown by Fig. 3.2.

To summarize the results of both cases, a value of 10^{-5} for DIFMAX appears to be a dependable value for accurate steady state power distributions. Less rigorous tests were performed on the same model with a smaller neutronic mesh spacing and on a different reactor (Model 3 of Appendix A). 10^{-5} was again shown to be an adequate value for DIFMAX.

The above results apply to steady state neutronics-only solutions. Two areas left open for future work are the effect of the steady state convergence criteria on the transient solution and the sensitivity of coupled (i.e., neutronic and thermal hydraulic) solutions to the convergence criteria. Concerning the latter, a combination of EPSSPR as 10^{-3}, EPSSK as 10^{-5}, and DIFMAX as 10^{-5} appears to give reliable and fairly economical

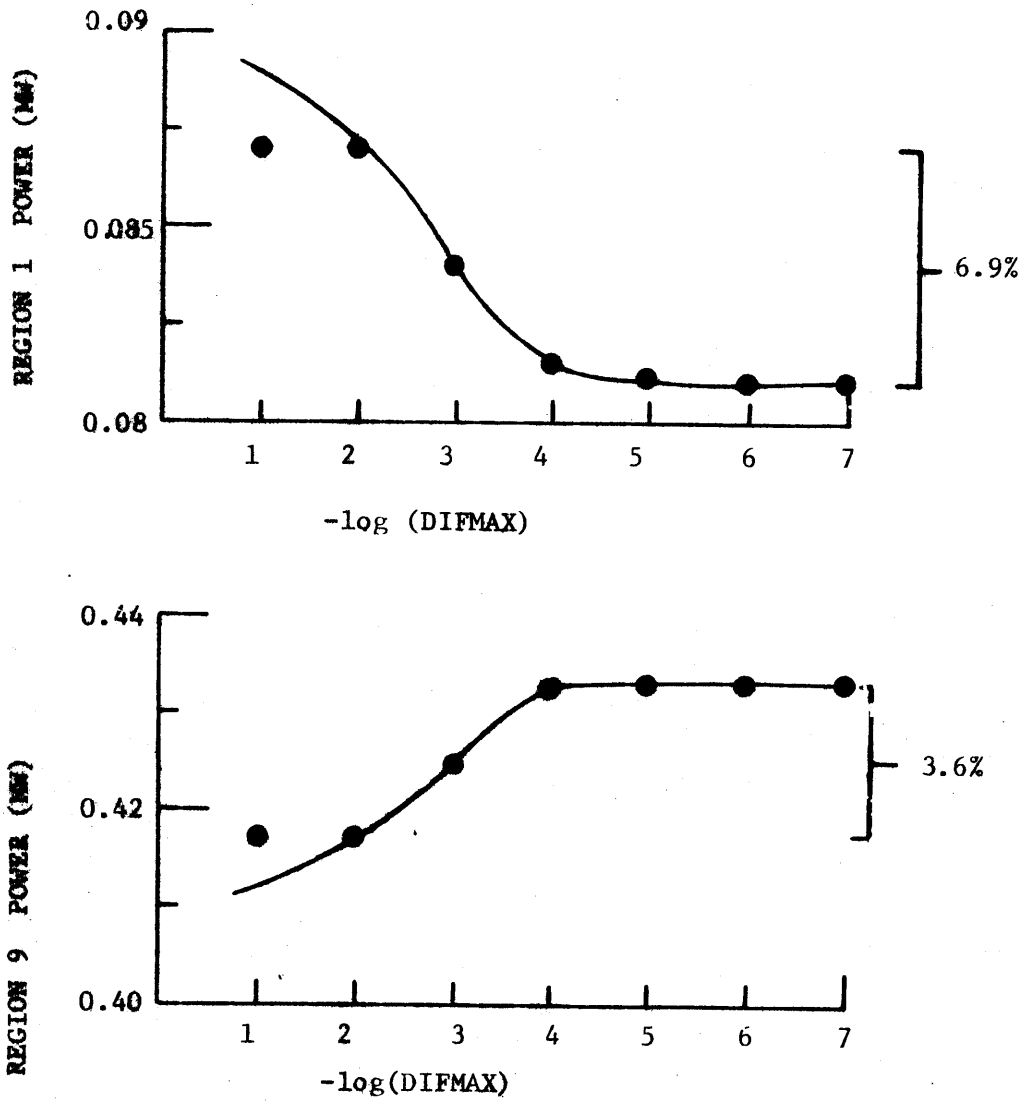

FIG. 3.1: DIFMAX SENSITIVITY: HOMOGENEOUS CORE.

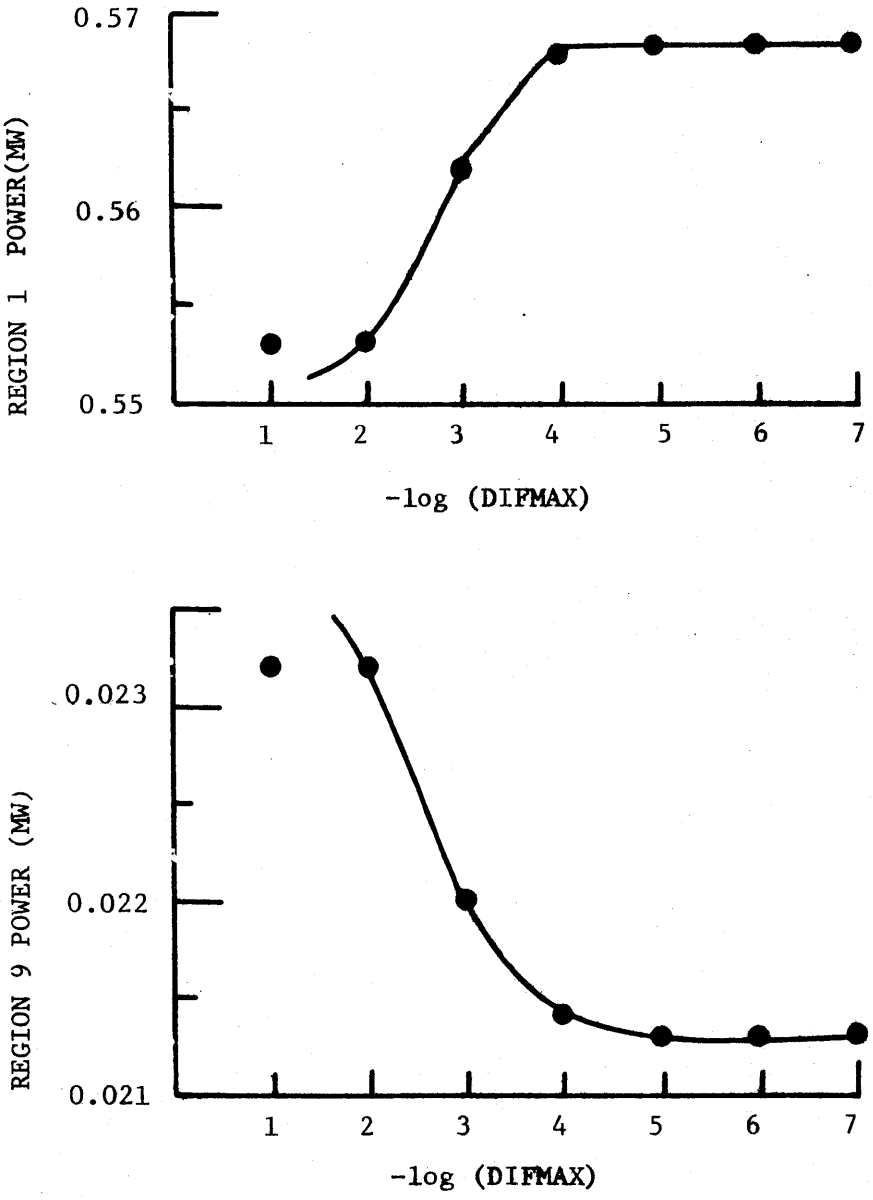

FIG. 3.2: DIFMAX SENSITIVITY: INHOMOGENEOUS CORE.

answers, so this set of convergence criteria was used for all coupled calculations discussed elsewhere in this thesis. However, a complete sensitivity study has not yet been performed.

CHAPTER 4

NEUTRONIC SPATIAL MESH SIZE SENSITIVITY

The transient neutron diffusion equations are solved in the MEKIN code by using numerical approximations such that values of neutron flux are generated at discrete points throughout the reactor. The distance between these points is specified by the user through two input parameters: the horizontal neutronic mesh spacing and the axial mesh spacing, as discussed in Section 2.1 of this thesis. Both inputs are restricted to being constant everywhere in the core, but the two may differ from one another. In addition, the mesh size cannot be changed during a MEKIN transient calculation. The purpose of this chapter is to give a description of the sensitivity of solution to the distance between neutronic mesh points.

Research work was divided into three areas: a steady state study of the horizontal mesh, a steady state investigation of the axial mesh, and a transient mesh study. This chapter is broken down in the same manner. Prior to describing the calculations and results, the neutronic solution techniques in MEKIN are briefly discussed.

4.1 NEUTRONIC SOLUTION TECHNIQUES IN MEKIN

In the steady state, the neutron diffusion equations are approximated in MEKIN by second-order three-dimensional finite differencing. A point-by-point flux solution is generated by accelerated iterative methods. In the transient, the user has

the option of one-dimensional synthesis, point kinetics, or three dimensional neutronics, where the solution technique is the non-symmetric-alternating-difference-explicit (NSADE) method. All transients discussed in this thesis involve three-dimensional neutronics.

The difference equations in MEKIN are of the mesh-centered type; the discrete flux points lie entirely within the boundaries of the bordering homogenized material compositions. This mesh scheme is employed in the CITATION codes. The widely used PDQ series of codes uses interface-centered, where all boundaries between material compositions contain at least one mesh point.

From a physical standpoint, finite differencing forces two compromises on the continuous three-dimensional diffusion equations. First, the value of the neutron flux at all continuous locations within an incremental volume is approximated as the value of the flux at the central point of that volume. Second, the spatial flux gradients are approximated as straight lines. Both of these compromises depend on the size of the neutronic mesh interval, and it can be proven that the solution of the difference equations converges to a unique limit as the mesh interval is reduced (9).

From a numerical standpoint, the approximations discussed above cause truncation error, where truncation error is a measure of how well a difference equation models the differential equation. This generalized error induces an error in neutron flux at each mesh point. For the case of a bare, one-dimensional homogeneous system with a uniform mesh, both the truncation error

and the pointwise errors can be shown to be bounded by the square of the mesh spacing (h^2) (19). For example, decreasing the mesh interval by a factor of two will decrease the local error by nearly a factor of four. Realistic problems have non-uniform material properties, and development of exact expressions for truncation error and pointwise error has never been achieved. However, error is expected to be proportional to h for a pattern of material discontinuities between every mesh point in a one-dimensional system with constant mesh size (19). In dealing with MEKIN, the situation is even more complex: three dimensions, two neutron energy groups, two-group albedo boundary conditions, and material discontinuities between some, but not all, mesh points. Development of exact analytical expressions for pointwise error appears impossible and other types of theoretical analysis are not well understood, so code experimentation is the logical alternative. The next three sections of this chapter include the calculations and results of such experimentation performed with MEKIN.

4.2 STEADY STATE HORIZONTAL MESH SENSITIVITY

For an adequate horizontal mesh sensitivity study, a reactor must be large enough to allow for spatial effects. On the other hand, economics can become a problem as the number of mesh points is increased. Models 1 and 2 of Appendix B appear to accomodate both constraints, so all of this section's calculations and results apply to these models. They represent a complete traverse of a pressurized water reactor core and each horizontal box has

the planer dimensions of one assembly.

The test cases are discussed in the following order:

Case 1: Model 1 of Appendix B, neutronics-only, material compositions identical for all regions.

Case 2: Model 1, neutronics-only, all regions identical except #3 (rod withdrawn).

Case 3: Model 1, neutronics-only, material compositions vary from region to region.

Case 4: Model 2 of Appendix B, thermal-hydraulic feedback included, all regions identical.

Case 5: Model 2, thermal-hydraulic feedback included, same material compositions as Case 3.

For each case, the test procedure was the same; the number of neutronic mesh points was varied with all other parameters held constant.

Case 1 is a homogeneous problem except at the ends, where albedo boundary conditions are used. These albedoes are derived from the material properties of a reflector region. As expected, this case displayed very little sensitivity to the solution. When comparing the 2.54 cm mesh to the 10.4 cm mesh, the largest region power difference was 2.6%. Comparing the 2.6 cm mesh to the 5.2 cm mesh , the maximum relative error was only 1%. Location of the maximum relative error was always in the end region. For this reason, the sensitivity is attributed to the albedo boundary conditions. Further details are given on Fig. 4.1 and Table C.1 of Appendix C.

Case 2 had the ejecting rod fully withdrawn. This single inhomogeneity caused the model to be slightly more sensitive to the number of mesh points. As before, the location of maximum relative error was the end region. The largest region power

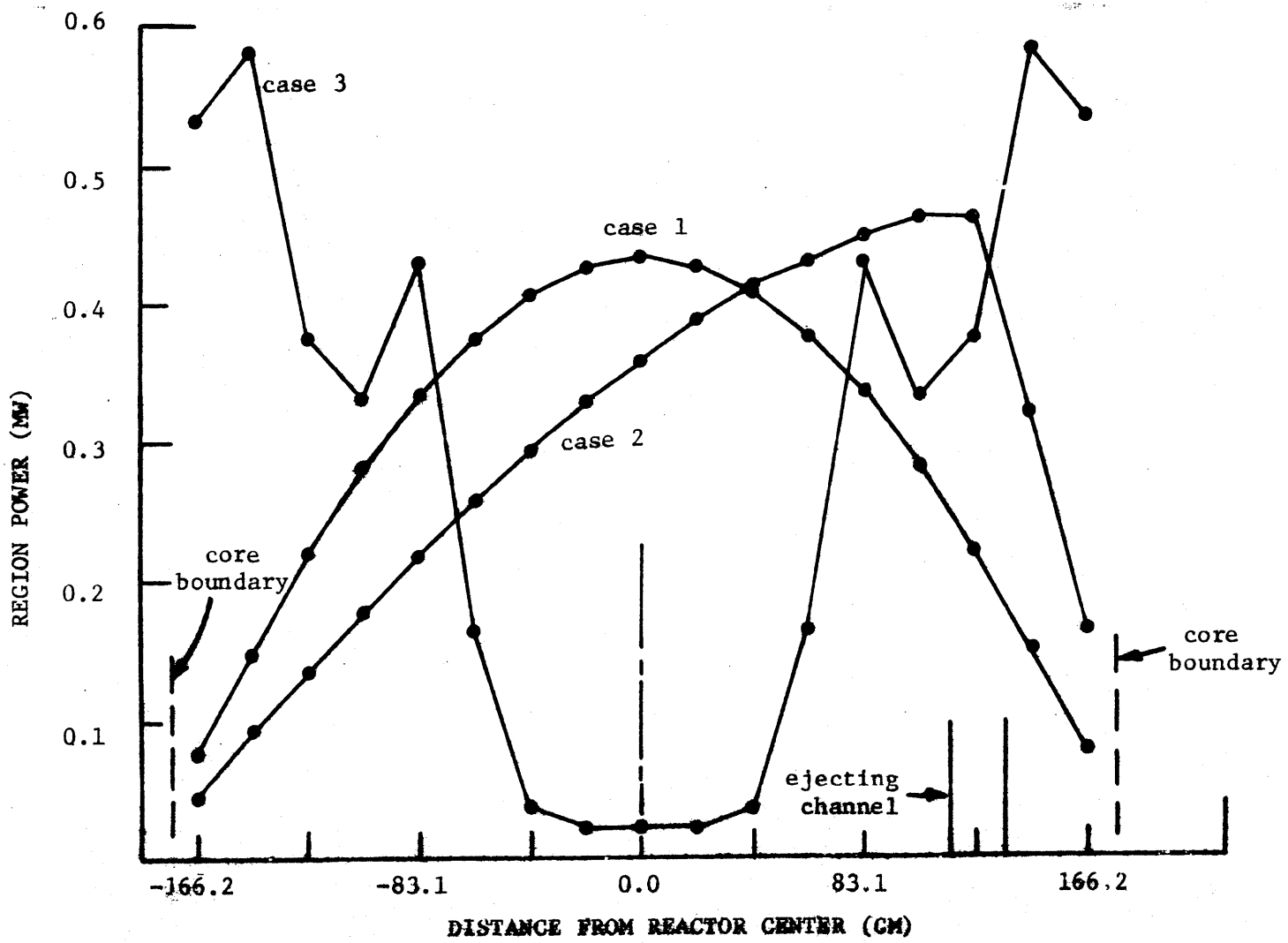

FIG. 4.1: POWER DISTRIBUTIONS FOR HORIZONTAL MESH SENSITIVITY CASES.

difference between the 2.6 cm mesh and the 10.4 cm mesh was 4%. Comparing the 5.2 cm mesh to the 2.6 cm mesh, 1.4% was the maximum relative error. The peak power region (the ejecting region in this case) was almost as sensitive as the end region. Fig. 4.1 and Table C.2 of Appendix C give more details.

Again using Model 1 of Appendix B, the material compositions were varied from region to region based on a reactor at the end of a cycle and in the hot-zero-power mode (Case 3). Due to the various burnups and the presence of control rods, the power distribution was very uneven (see Fig. 4.1). For this case, the power distribution is markedly sensitive to mesh spacing. The maximum relative error is over 10% when comparing the 10.4 cm mesh to the 1.3 cm mesh. The 5.2 cm mesh is somewhat better as the largest difference in region power is ≈5% matched against the 1.3 cm mesh. As with Case 1, increasing the number of mesh points tilts the power toward the center of the core. More detail is given on Table C.3 of Appendix C. The region material discontinuities appear to be chiefly responsible for the solution's sensitivity to mesh size. Indeed the most sensitive regions are those having a bordering region of significantly different composition and/or a large flux gradient (i.e. edge region, rodded-unrodded neighboring regions, etc.). This is consistent with theory (8).

Fig. 4.2 gives another view of the results. For two of the regions, power is plotted against mesh spacing. The curves are converging to better answers in a somewhat linear fashion.

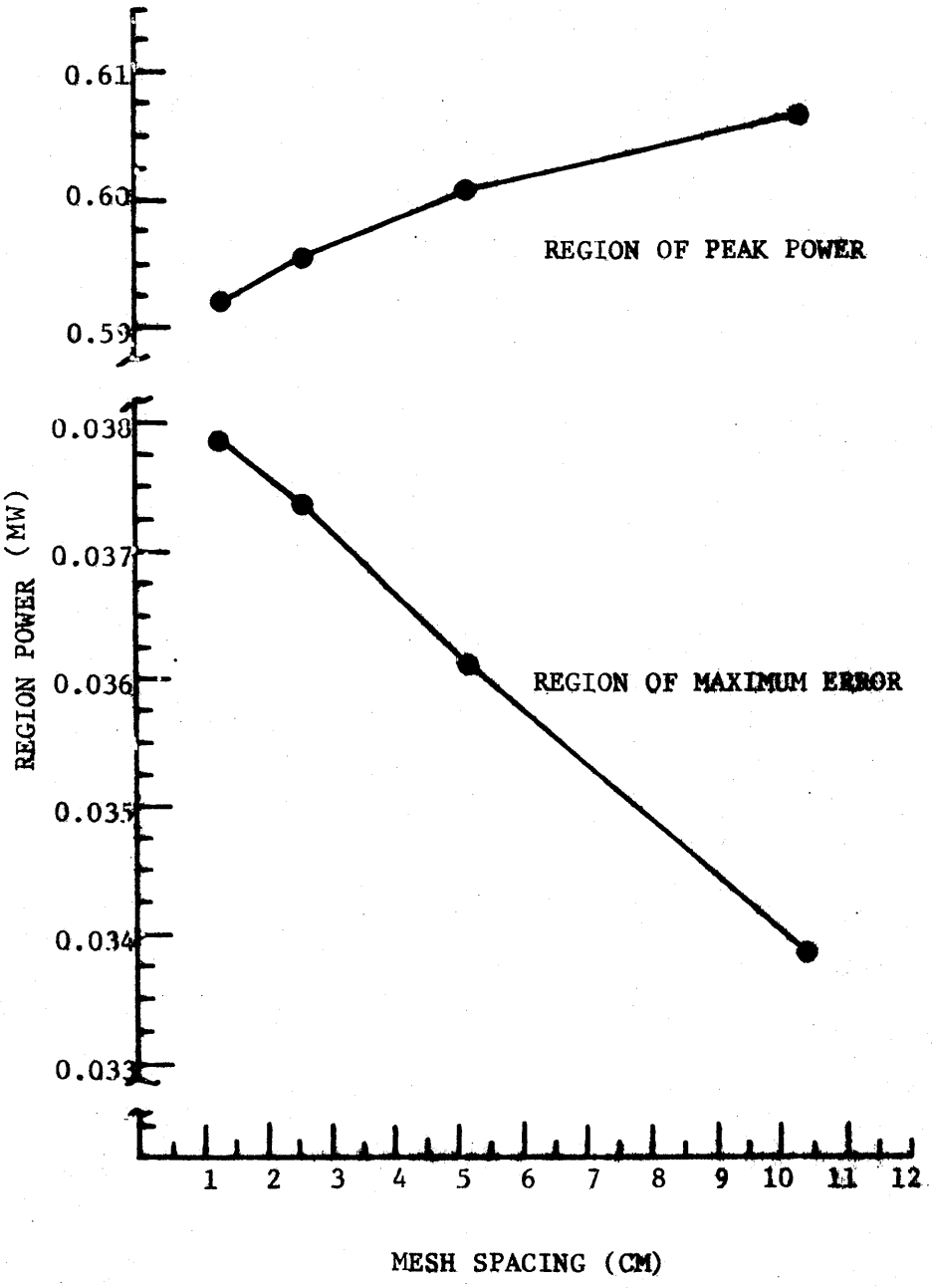

FIG. 4.2: HORIZONTAL MESH SPACING VS. REGION POWER: CASE 3.

Up to this point, just neutronics-only calculations have been considered. Cases 4 and 5 involve a similar model (2 of Appendix B) with thermal-hydraulic feedback. The amount of feedback per volume resembles the level achieved when a typical pressurized water reactor is operating at full power. The extra axial level was included to accomodate the thermal-hydraulic portion of the code. It has a negligible effect on horizontal power distribution because the two levels have identical initial cross sections. When all regions had identical compositions (Case 4), the results almost duplicated Case 1 (see Table C.4 of Appendix C).

When the material compositions were varied from region to region (Case 5), the results were again similar to the neutronics only data (Case 3). The only apparent difference was a slight dampening of the relative errors. For example, the maximum relative error between the 10.4 cm mesh and the 2.6 cm mesh is 7%. Details are given on Fig. 4.4 and Table C.5 of Appendix C. Fig. 4.5 plots region power against mesh spacing; again, convergence is close to being linear.

Several areas of these horizontal mesh studies deserve repetition or clarification. First, marked changes in material compositions from one region to another cause MEKIN to be very sensitive to the horizontal mesh interval. Second, convergence to better answers is close to being linear. Third, feedback does not have much effect on steady state sensitivity. Finally, the errors which should cause the most concern are those near power peaks and those near potential peaks (i.e., areas close

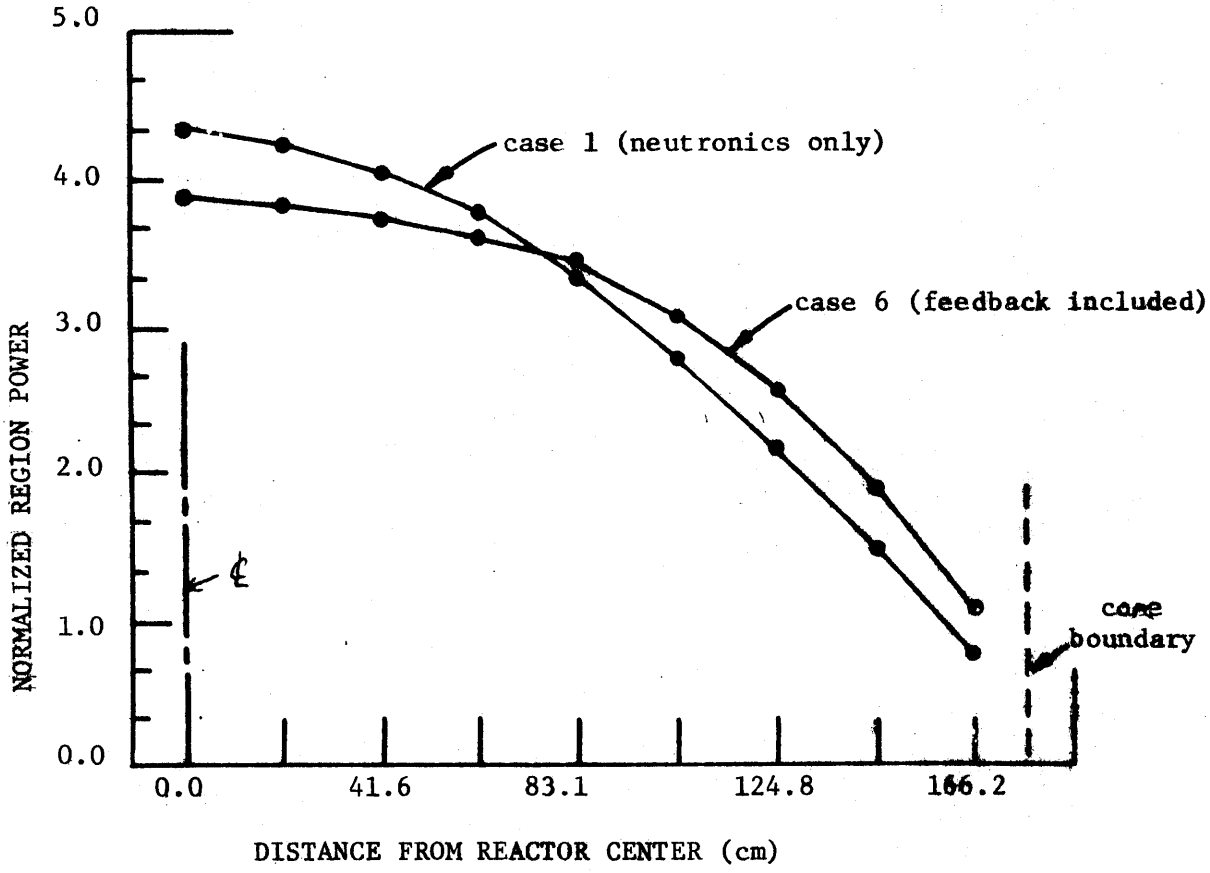

FIG. 4.3: EFFECT OF FEEDBACK: HOMOGENEOUS CORE.

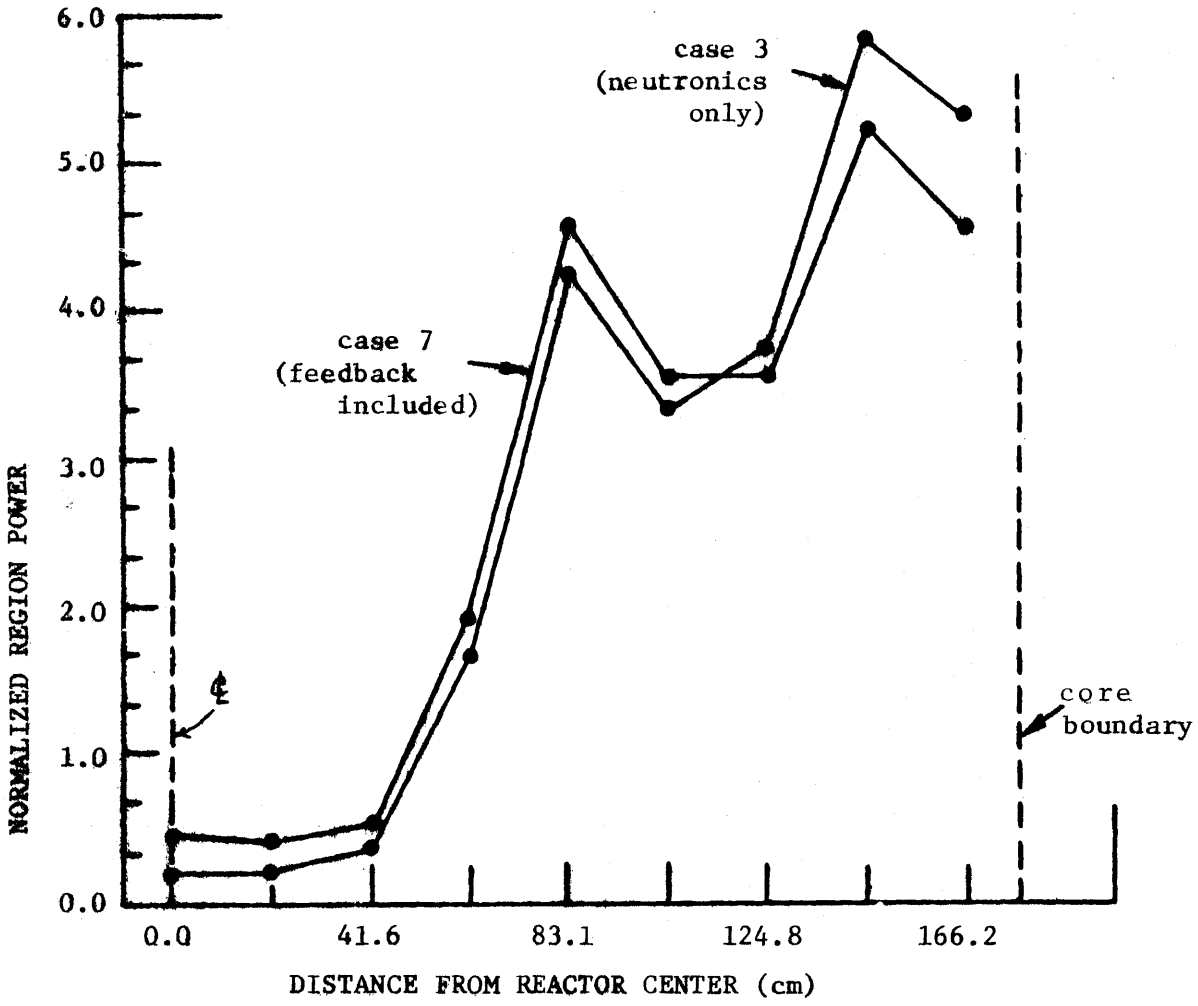

FIG. 4.4: EFFECT OF FEEDBACK: INHOMOGENEOUS CORE.

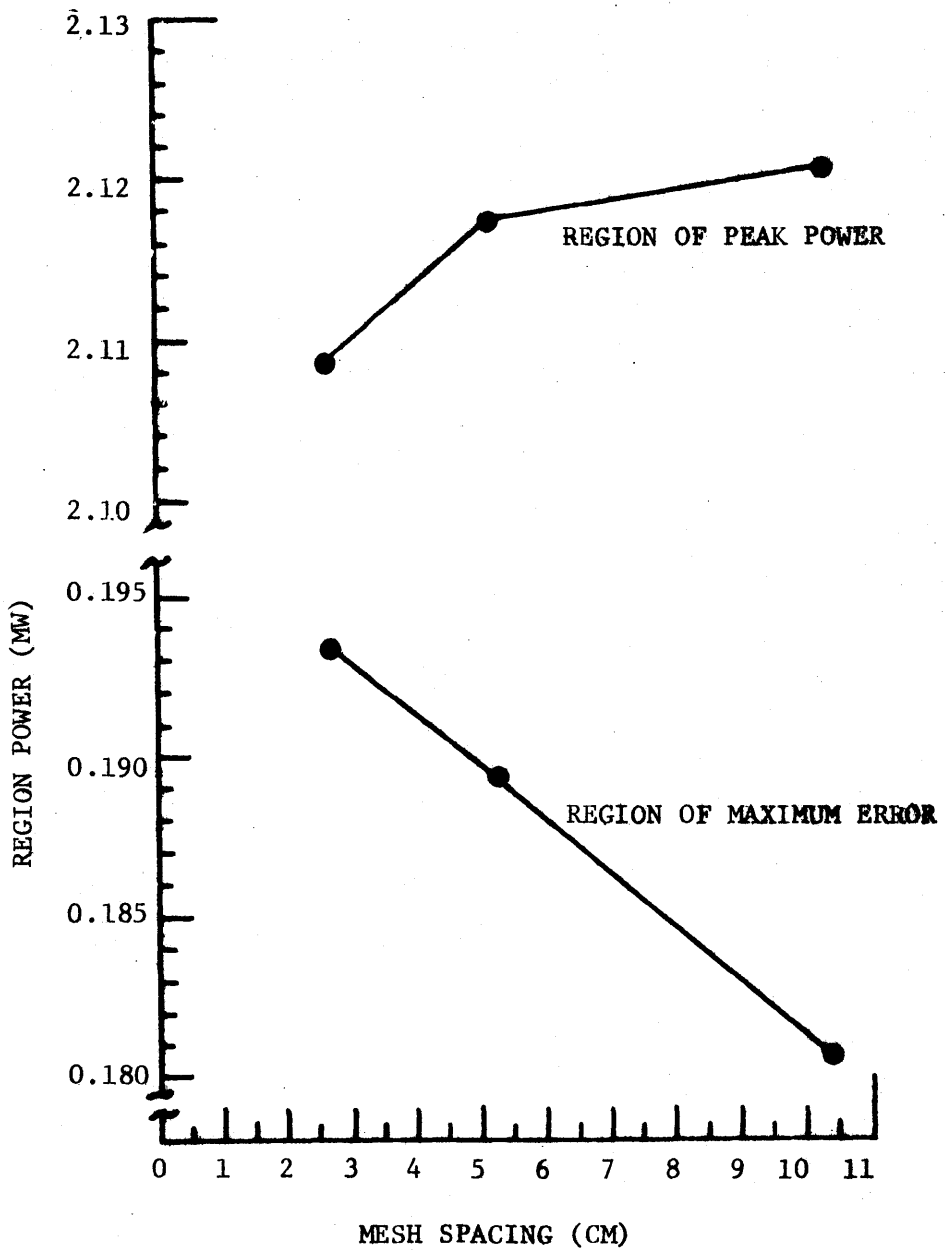

FIG. 4.5: HORIZONTAL MESH SPACING VS. REGION POWER: CASE 5.

to the perturbation of a transient).

4.3 STEADY STATE AXIAL MESH SENSITIVITY

The primary reactor for this investigation was Model 3 of Appendix B. This represents four identical full-length channels in a typical pressurized water reactor. The areas above and below the core have different material properties and different sets of albedoes were therefore used at the top and bottom. The material compositions were varied from region to region in order to represent channels corresponding to 8000 MWD/MT of burnup.

The solution exhibited significant sensitivity as the axial mesh was varied. The maximum relative error between the 29 cm mesh and the 7.2 cm mesh was nearly 10%. More detail is given on Fig. 4.6 and Table C.6 of Appendix C. Another view of the results is presented on Fig. 4.7, where region power is plotted against mesh spacing for three of the ten different regions. The data points for the 29 cm mesh do not fit the curves well. The probable cause is the fact that each mesh point sees different material compositions in both axial directions. From the shapes of the curves, the true solution in each region still has not been closely approximated. Unfortunately, this model cannot be input to MEKIN with more than four mesh points per region due to current storage limitations in the code.

In order to tighten the mesh further, keep within storage limitations, and hopefully converge to a better answer, a study was carried out on Model 4 of Appendix B. Region compositions

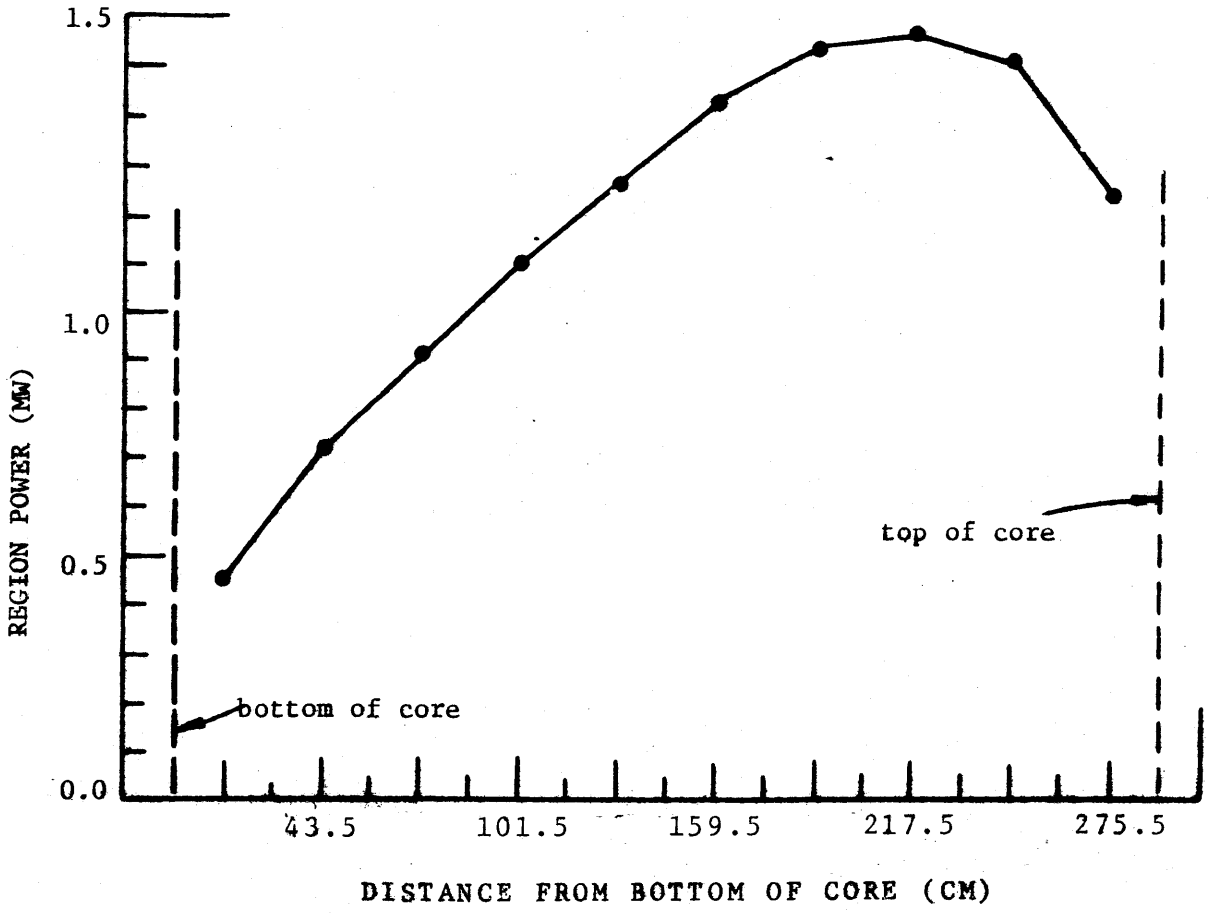

FIG. 4.6: AXIAL POWER DISTRIBUTION.

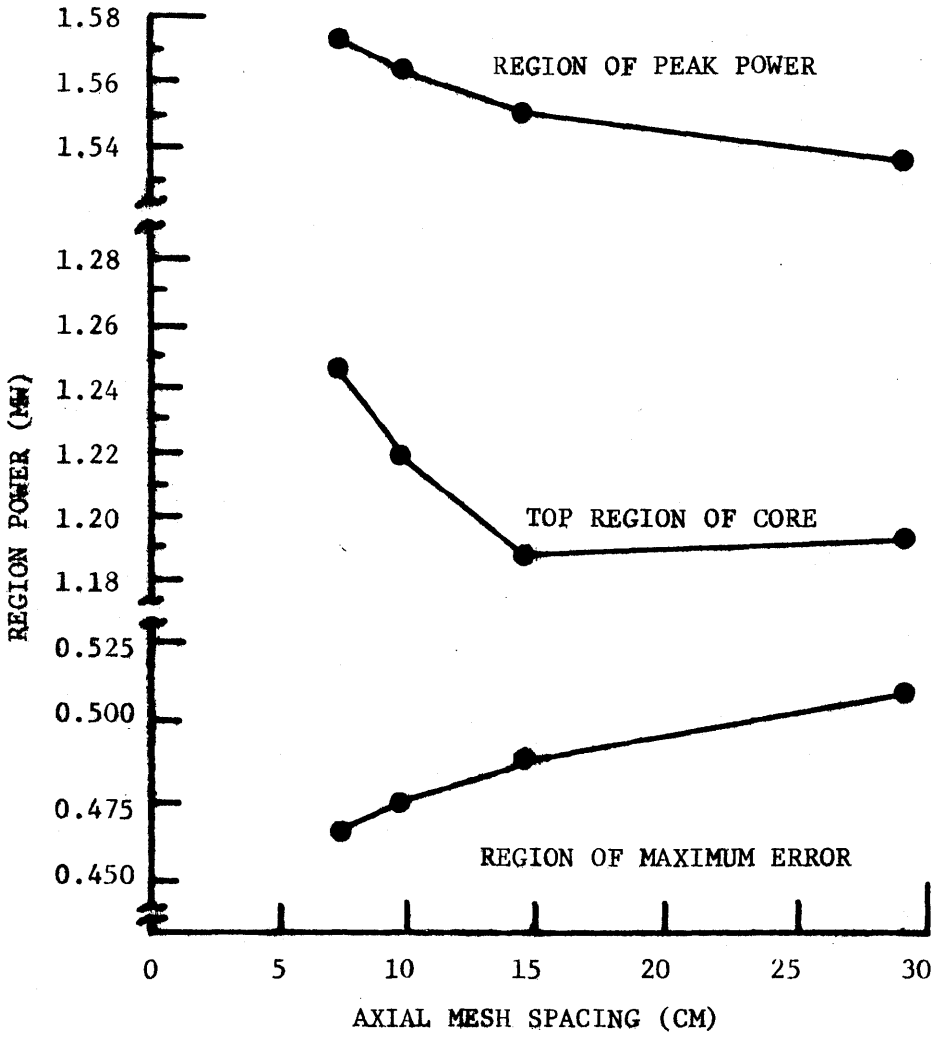

FIG. 4.7: AXIAL MESH SPACING VS. REGION POWER: 10 REGION CASE.

are identical to the bottom five regions of the previous case. Judging from Fig. 4.8 and Table C.7 of Appendix C., power solution appears to be fairly well converged for the 4.1 cm mesh. In addition, the relative error is almost exactly linear with axial mesh spacing (see Fig. 4.8).

In summary, the power solution error for both models is proportional to h^q, where h is the mesh spacing. "q" is approximately 1.0 for the five-region case. However, q appears to be slightly less than unity for the ten-region case, indicating greater sensitivity to axial mesh. This discrepancy can be attributed to the relative complexities of the problems. The 10-region case represents an extreme for a pressurized water reactor: full core height, different albedoes on top and bottom, different material compositions at every level. However, boiling water reactors may show a greater mesh sensitivity near the top of the core due to the drastic cross section changes induced by boiling.

No further axial mesh sensitivity studies were performed. The reasons were two-fold: results were very similar to those obtained with the horizontal models and the axial models are relatively more expensive due to computer storage.

4.4 TRANSIENT MESH SENSITIVITY

The transient mesh size studies employed Model 1 of Appendix B with material compostiions which varied from region to region (In the steady state, this reactor was identical to the one used in Case 3 of Section 3.2). An off-center control

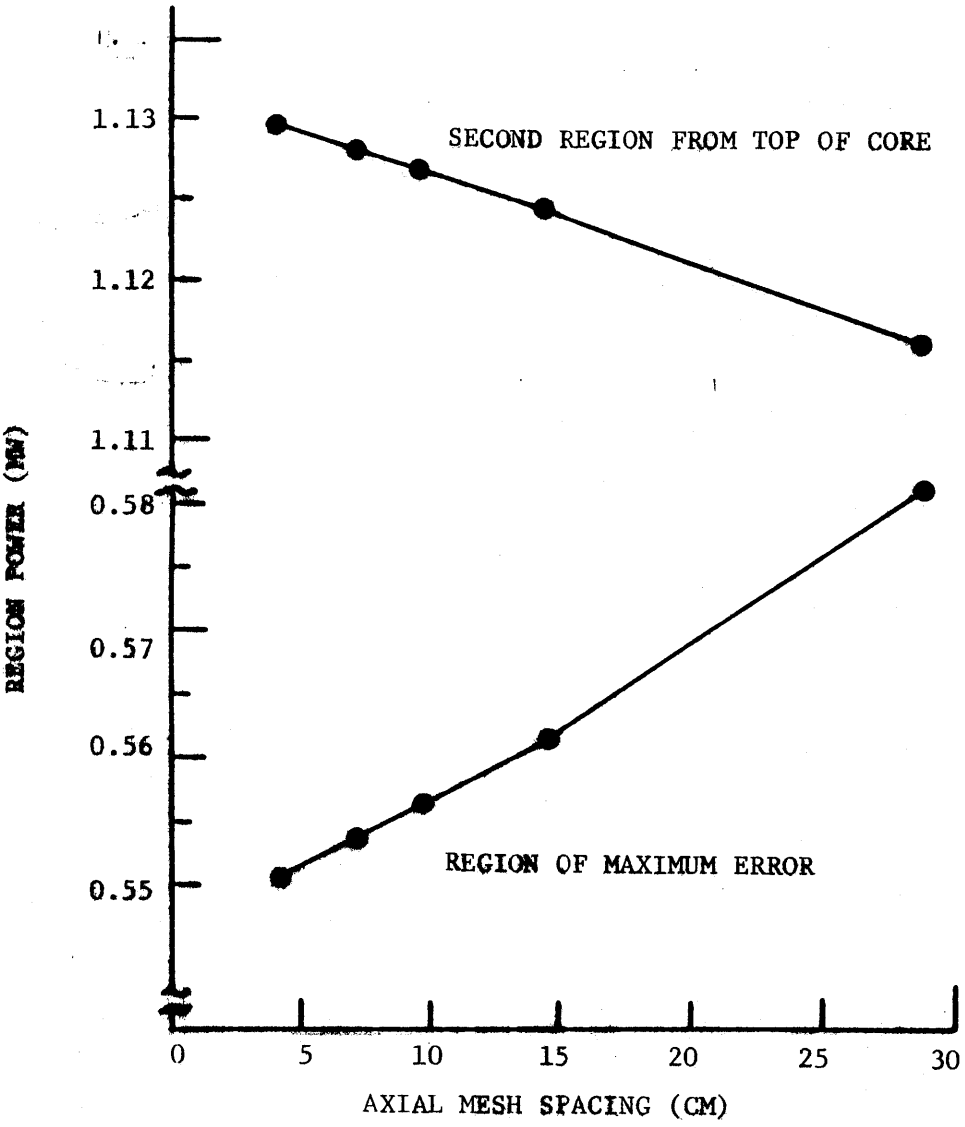

FIG. 4.8: AXIAL MESH SPACING VS REGION POWER: 5 REGION CASE.

rod ejection was the reactivity force that was used to drive the transient.

For neutronic mesh intervals of 2.6 cm, 5.2 cm, and 10.4 cm, the transient was carried out to 0.03 seconds. Despite this relatively short time period, the solutions show significant divergences (see Fig. 4.9 and Table C.8 of Appendix C). Total reactor power for the 10.4 cm mesh differed from the power for the 2.6 cm mesh by over 10% after 0.03 seconds. Better agreement occurred in the 5.2 cm - 2.6 cm mesh comparison, but reactor power still varied by ≈3%. To make matters worse, the 10.4 cm mesh underpredicted the power, indicating a non-conservative trend for less accurate calculations. With respect to individual regions, power variation as a function of mesh was even more accented. When comparing the 10.4 cm mesh to the 2.6 cm mesh, the ejecting channel power varied by 18% while the region of peak power had a power difference of 13%. Error as a function of neutronic mesh appears to be fairly linear, as indicated by Fig. 4.10. (The data point for the 2.6 cm mesh should be interpreted as the best reference rather than the exact answer.)

A separate study on the time step size assures that any differences reflect only the spatial mesh size. The time step size for the reported results was 0.0002 seconds and the error from using this value is small compared to the error induced by varying the mesh spacing. For example, with a 2.6 cm mesh at 0.25 seconds, the powers were 0.00906 and 0.00899 MW for time steps of 0.0002 and 0.0001 seconds. For the 10.4 cm mesh

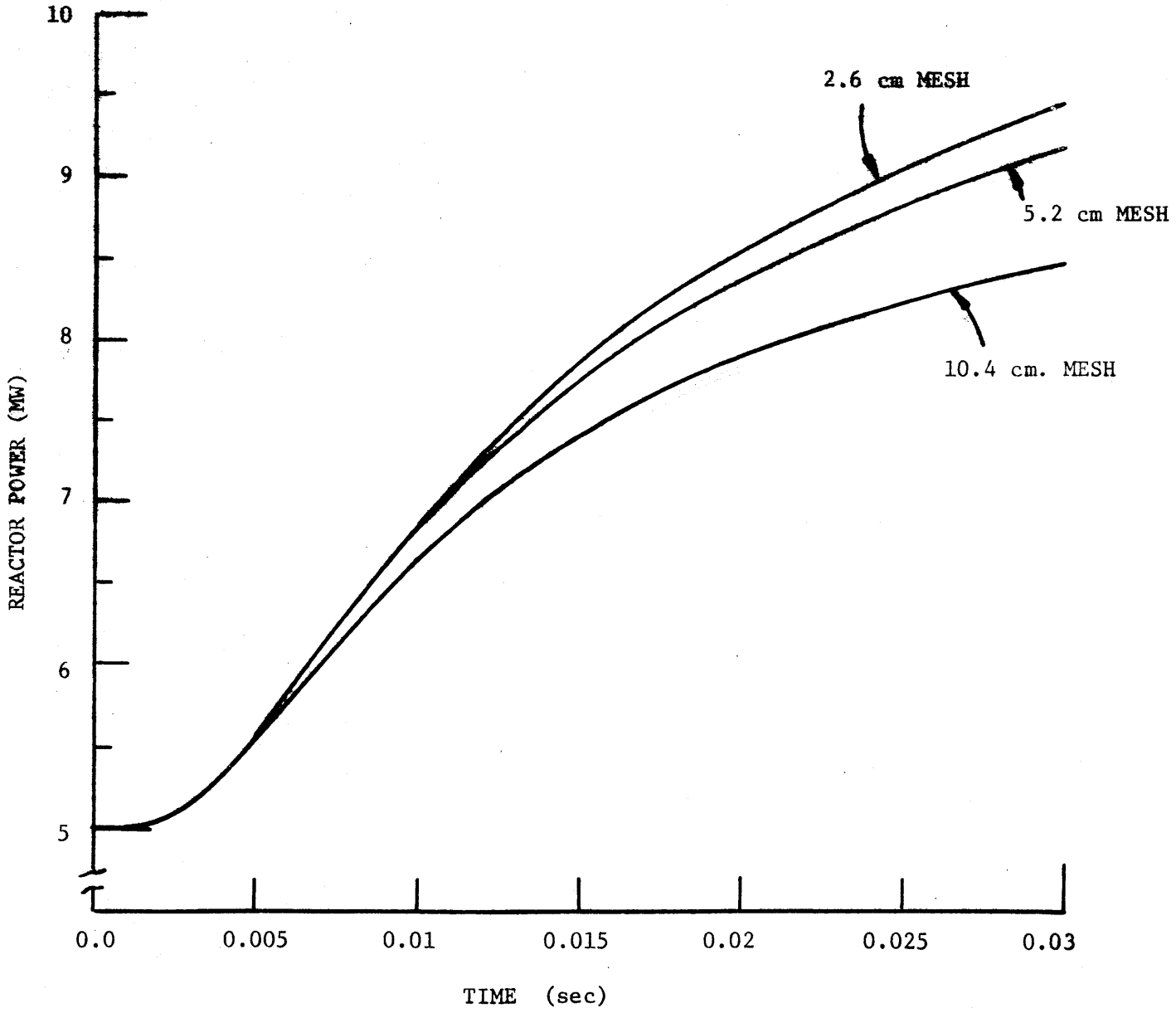

FIG. 4.9: REACTOR POWER VS TIME: HORIZONTAL MESH SENSITIVITY.

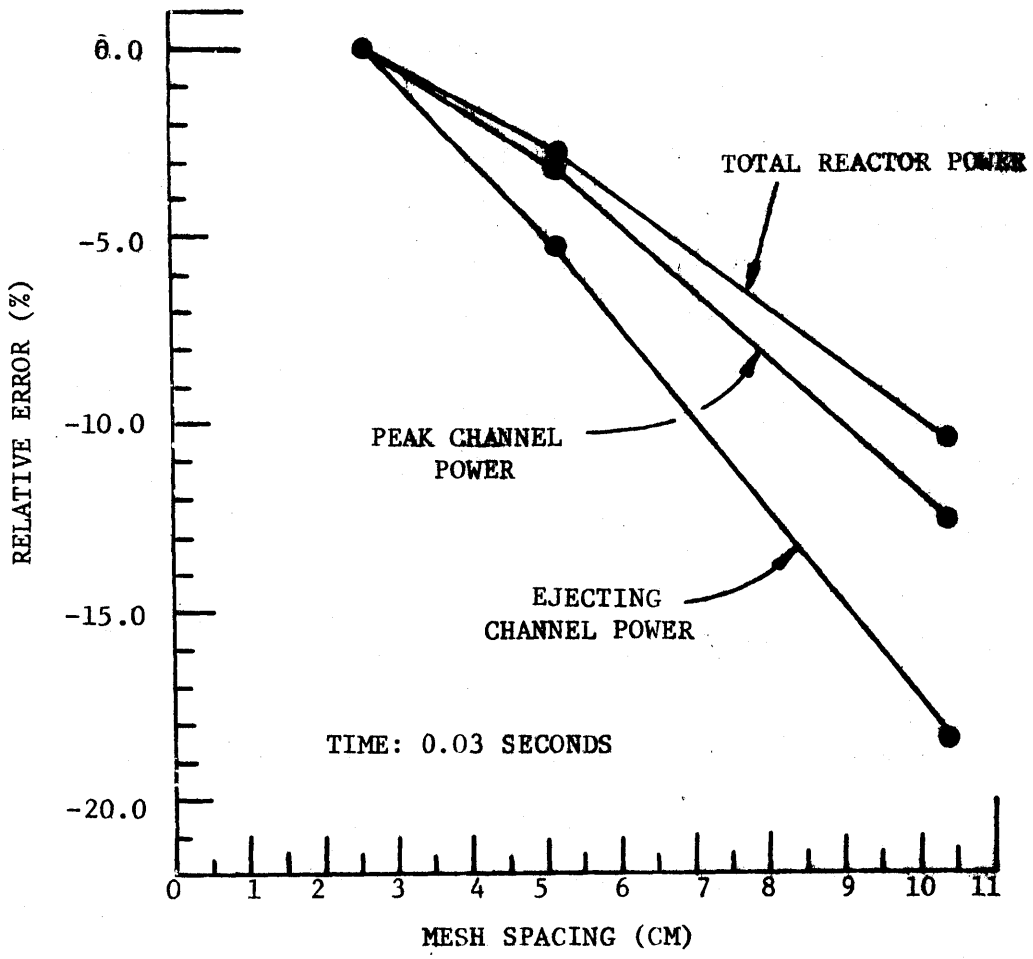

FIG. 4.10: HORIZONTAL MESH SPACING VS. RELATIVE ERROR: TRANSIENT CASE.

at 0.025 seconds, the powers were 0.00823 and 0.00819 for time steps of 0.0002 and 0.0001 seconds.

The above results indicate that errors grow as the transient evolves. Next, the probable cause and a simple formula for predicting such behavior will be investigated.

Since K-effective is sensitive to mesh spacing, rod worth is also affected. Therefore, an identical rod ejection for different mesh sizes will result in different periods. For the case at hand, different periods resulted and the rod worths differ, but the two phenomena still must be linked together in a quantitative manner.

The height of the prompt jump can easily be calculated by: (12)

$$\frac{P_1}{P_0} = \frac{\beta(1-\rho)}{\beta-\rho}, \qquad (4.1)$$

where

P_1 = reactor power level after prompt jump,

P_0 = initial reactor power level,

β = delayed neutron fraction,

ρ = reactivity insertion (rod worth in this case).

In words, the power jumps by the factor $\frac{\beta(1-\rho)}{\beta-\rho}$ very soon after reactivity ρ has been introduced to the system. This formula was developed under the following conditions: system originally at steady state, step change in reactivity, concentrations of precursers remain constant during prompt jump, homogeneous slab reactor, reactivity, ρ, is less than the delayed neutron fraction, β.

Unfortunately, with the exception of the final condition, the other criteria differ for the case at hand. Despite these differences, when this formula was tested against the MEKIN calculations, the results were encouraging (see Table 4.1). This table may be misleading because the calculated power ratio does not match the MEKIN power ratio. However, the percentage differences between the two mesh sizes are fairly close: 7.64 to 7.63 and 7.64 to 9.00, depending on the value of the delayed neutron fraction. The exact reactor-averaged delayed neutron fraction is not known because the input values vary from region to region. The best value for the given formula would have to be determined by weighting the region values by the regions' importances.

Consequently the MEKIN user has a method of predicting the error in power-time behavior which is induced by a coarse mesh interval. Required information includes the coarse mesh rod worth from two MEKIN steady state calculations and a fine mesh rod worth from two more MEKIN steady state calculations. The fine mesh result acts as an accurate reference when the two worths are used in Eq. (4.1). The two calculations will yield different power ratios, and the percentage difference in power ratios is then an indication of the error in the true power ratio between a fine mesh transient and a coarse mesh transient. This procedure is only valid for reactivity insertions less than the delayed neutron fraction.

TABLE 4.1.

Prediction of Transient Error.

	10.4 cm mesh	5.2 cm mesh	Percentage Difference
K-Effective (Rod Out)	.9713007	.9691710	
K-Effective (Rod In)	.9683575	.9651820	
Rod Worth ($\Delta K/K$)	.003093	.0031890	
P_1/P_0* (β = .005)	2.542	2.752	-7.63
P/P_0* (β = .0047)	2.822	3.101	-9.00
Reactor Power (t=.03sec)	.008466(MW)	.009165(MW)	
Reactor Power (t=0)	.005000(MW)	.005000(MW)	
P/P_0 (MEKIN)	1.693	1.833	-7.64

$$*\frac{P_1}{P_0} = \frac{\beta(1-\rho)}{(\beta-\rho)} ,$$

where β = delayed neutron fraction x.005 ,

ρ = Rod Worth.

4.5 USER APPLICATIONS OF THE MESH SENSITIVITY

Prior to using the results of this study as an aid to mesh size selection, several concluding remarks deserve consideration. For one thing, the steady state magnitudes of error refer to the horizontal and axial directions separately. When MEKIN is used in three dimensions, the error in region power will be a function of both the horizontal and axial uncertainty. As a first approximation to this combined error and with the exact solution normalized to unity:

$$\varepsilon_i = (1+\alpha_i)(1+\gamma_i)-1, \qquad (4.2)$$

where ε_i = fractional error in steady state power for region i,

α_i = fractional error in region i due to the horizontal mesh spacing,

γ_i = fractional error in region i due to the axial mesh spacing.

The steady state results can provide a users' guide for bracketing undertainties as a function of mesh size. Both extremes (i.e., a homogeneous reactor and very inhomogeneous reactors) have been studied, and a typical problem should fall somewhere within these bounds. In the case of a delayed-critical reactivity insertion transient, a simple method for predicting mesh size induced errors has been provided.

4.6 IMPLICATIONS OF THE MESH SENSITIVITY

Concerning solution behavior, better answers appear to be approached in a somewhat linear fashion as the mesh size is reduced. Unfortunately, a high degree of accuracy may be too

costly for large problems. Consider the case of a full core problem with a 2.6 cm horizontal mesh and a 10 cm axial mesh. These values are not unreasonable based on the results presented here and they correspond to ≈400,000 neutronic mesh points for the full core. On the IBM 370/168 computer at MIT, such a problem is estimated to require anywhere from 20 to 50 hours of CPU time. Now remember, this is only a steady state neutronics-only calculation. In view of this excessive computational time, alternative solution techniques to the finite difference method are under consideration. Two techniques which show promise have been developed by R. Sims (16) and T. Shober (17) at M.I.T. Both methods involve nodal codes based on response matrices.

CHAPTER 5

NEUTRONIC TIME STEP SIZE SENSITIVITY

When transient conditions are represented by MEKIN, the neutronic power distribution is computed at successive times, and the interval between calculations (i.e., neutronic time step size) is user specified. This input is somewhat more flexible than spatial mesh size because the user can vary the time interval as desired. Currently, the code has no means of automatic time step size selection.

The purpose of this chapter is to give a description of the sensitivity of solution to the neutronic time step size. As mentioned, the three-dimensional transient solution technique is the NSADE method, and its theory is breifly presented in Section 5.1. The remaining sections of this chapter include the test cases and results, data correlation, user applications, and implications of this particular sensitivity study.

5.1 THE NSADE METHOD IN MEKIN

The non-symmetric alternating-direction explicit (NSADE) method is the solution technique used to solve the transient three-dimensional neutronic finite difference equations in MEKIN. In matrix form, these equations can be expressed as

$$\nu^{-1}\frac{\partial}{\partial t}\,T(t) = A\,T(t), \tag{5.1}$$

where the solution vector is

$$T = [\underline{\phi}^1\ \underline{\phi}^2\ \underline{C}^1\ ---\ C^L]^T. \tag{5.2}$$

$\underline{\phi}^g$ is the vector of all point fluxes in group g and $\underline{C}^\ell$ is the vector of all point precursers in family ℓ. ν^{-1} is a diagonal matrix of inverse group velocities, while A is the net production matrix.

Under transient conditions, the power distribution is computed at successive times. Between any two such times, the NSADE method performs a two-step semi-implicit calculation. Matrix A of Eq. (5.1) is split into four triangular matrices to allow the inversions to be obtained simply by forward substitution and backward substitution. The forward-back substitutions are in fact a sweeping of the mesh points starting in the lower left corner and solving points successively while advancing to the upper right, and then reversing direction and sweeping back. The details of this procedure are set forth in Volume 1, Part 1 of the MEKIN manual.

A special feature of this technique in MEKIN is the exponential frequency transform of the group fluxes. The fluxes are transformed by

$$\hat{\phi}_m^{g,n} = e^{\Omega_m h}\, \phi_m^{g,n}, \text{ all g, m,} \qquad (5.3)$$

where Ω_m = frequency at point m,

h = time step size,

$\phi_m^{g,n}$ = the group g flux at time n at mesh point m.

The precursers are not transformed and a frequency is calculated for each mesh point after each time step. The frequencies at point m used during the time step from t_n to t_{n+1} are computed by

$$\Omega_m = \frac{1}{t_n - t_{n-1}} \ln[\phi_m^{g=2,n} / \phi_m^{g=2,n-1}] . \qquad (5.4)$$

This transform was originally implemented because "exponential growths are characteristic of neutron kinetics." (11) Unfortunately, such growths should not always be anticipated in transient conditions. The "knee" of the prompt jump and the turnaround in power due to thermal-hydraulic feedback are two examples.

The main advantage of the NSADE method is the fact that each time step is a direct calculation rather than an iterative process. This results in a large savings in CPU time per time step. Past studies (11) indicate that the main disadvantage is the need for small time steps. Exactly how small will be discussed in the next section.

5.2 TEST CASES AND NUMERICAL RESULTS

The functional form of the power-time behavior is largely dependent on the transient and the point in time within a particular transient. For this reason, a wide variety of test cases were studied. The procedure involved varying the time step size over a fixed time interval with the initial conditions and all other parameters held constant. This methodology was made possible by the restart option in MEKIN. This restart option allows the user to store the solution on disk at a discrete time and , subsequently, to continue the calculation from that point as often as desired.

The test cases include:

Case A: Model 6 of Appendix B, neutronics-only, super-prompt critical transient, constant reactor frequency (Fig. 5.1),

Case B: Model 1 of Appendix B, neutronics-only, prompt jump (Fig. 5.2),

Case C: Model 1 of Appendix B, neutronics-only, after the prompt jump (Fig. 5.3),

Case D: Model 1 of Appendix B, neutronics-only, knee of prompt jump (Fig. 5.2),

Case E: Model 3 of Appendix B, neutronics-only, beginning of transient (Fig. 5.4),

Case F: Model 6 of Appendix B, feedback included, turn-around in power (Fig. 5.5).

Results are tabulated on Table 5.1. Error was measured by the average reactor period over the time range under study. The periods given on the figure were calculated by

$$T = \frac{(t_f - t_o)}{\ln(P_f/P_o)} \quad , \tag{5.5}$$

where

t_f = the final time of the range,

t_o = the initial time of the range,

P_f = the final reactor power level,

P_o = the intial reactor power level.

Time step size as a function of error is plotted on Fig. 5.9.

Several observations deserve emphasis. Cases A, B, and C are sensitive to time step size, but the general shapes of the power-time curves show nothing surprising. On the other hand, Cases D, E, and F involve more dramatic variation, as illustrated by Figs. 5.6, 5.7, and 5.8. For all but Case C, the required

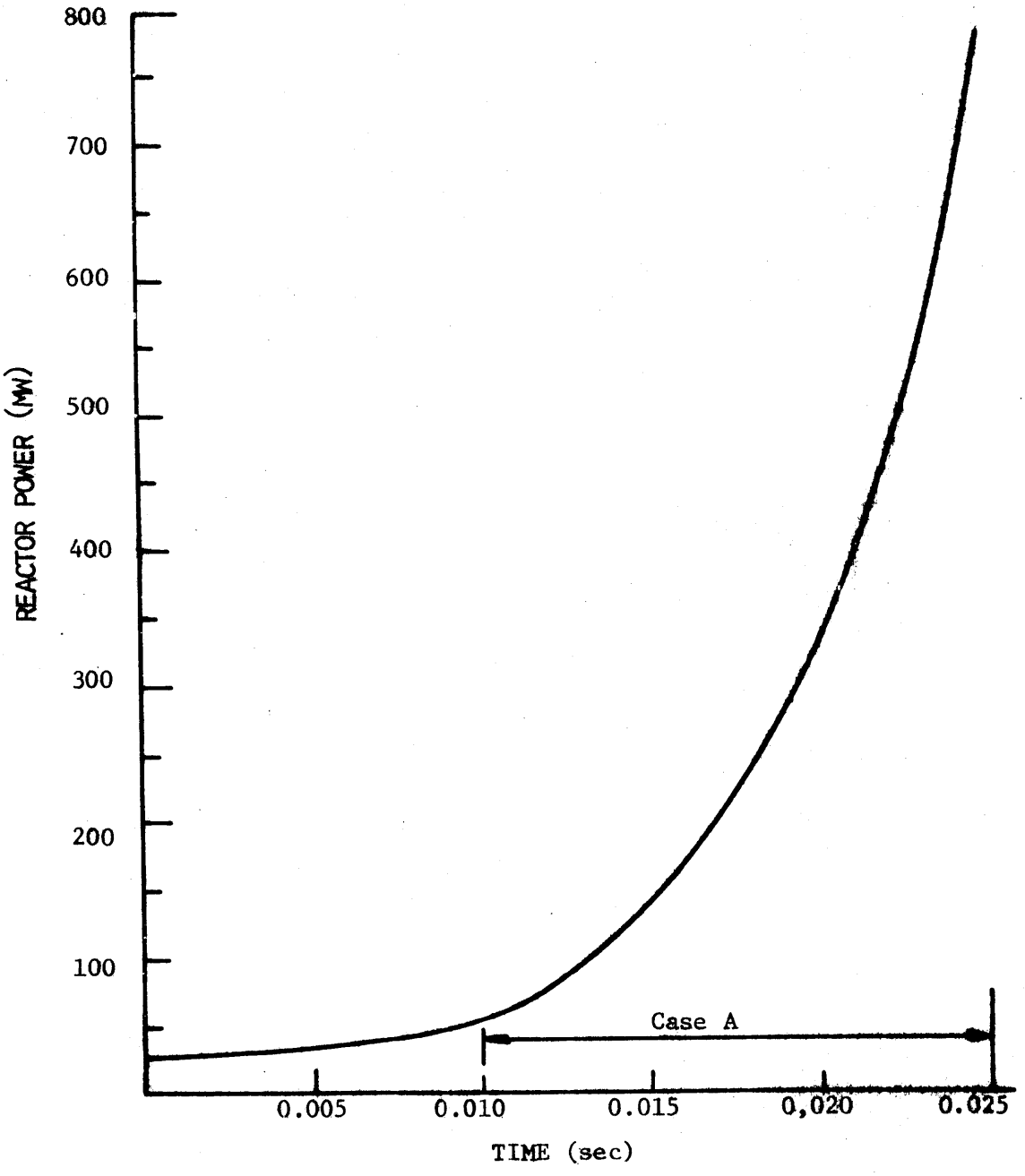

FIG. 5.1: POWER VS TIME: CASE A.

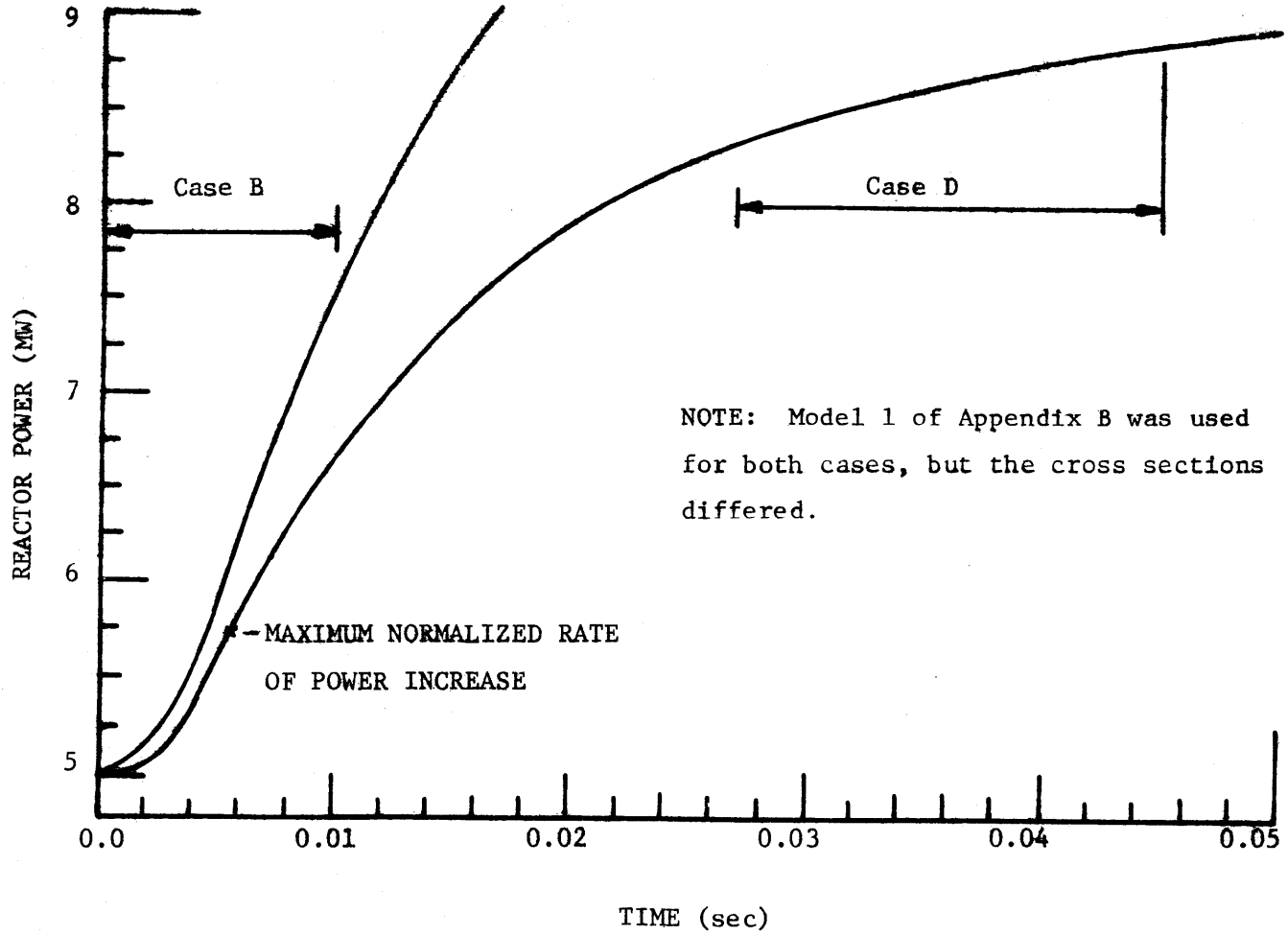

FIG. 5.2: POWER VS. TIME: CASES B AND D.

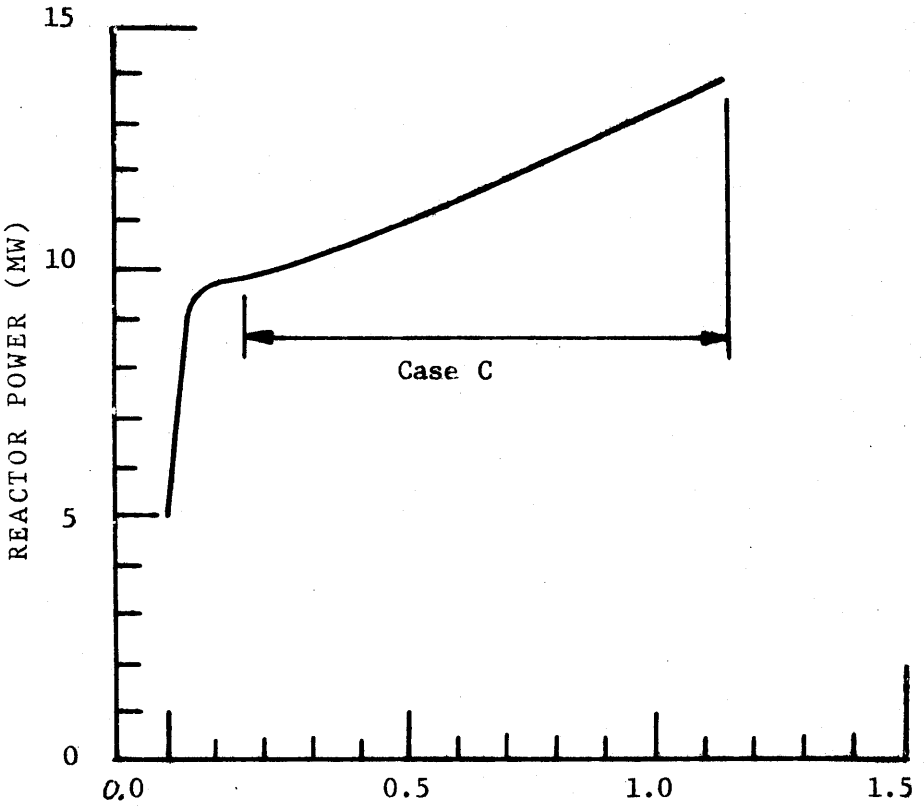

FIG. 5.3: POWER VS. TIME: CASE C.

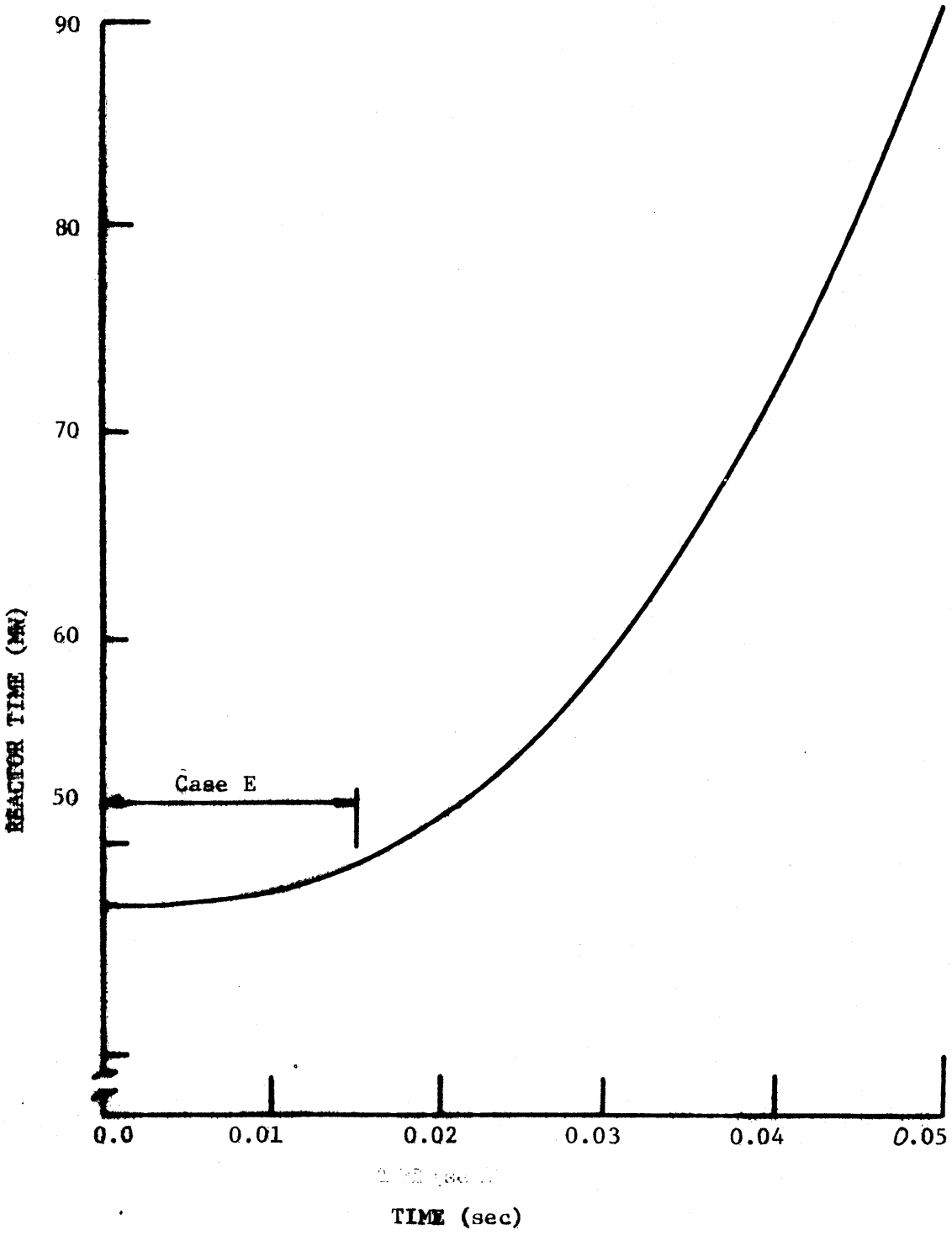

FIG. 5.4: POWER VS. TIME: CASE E.

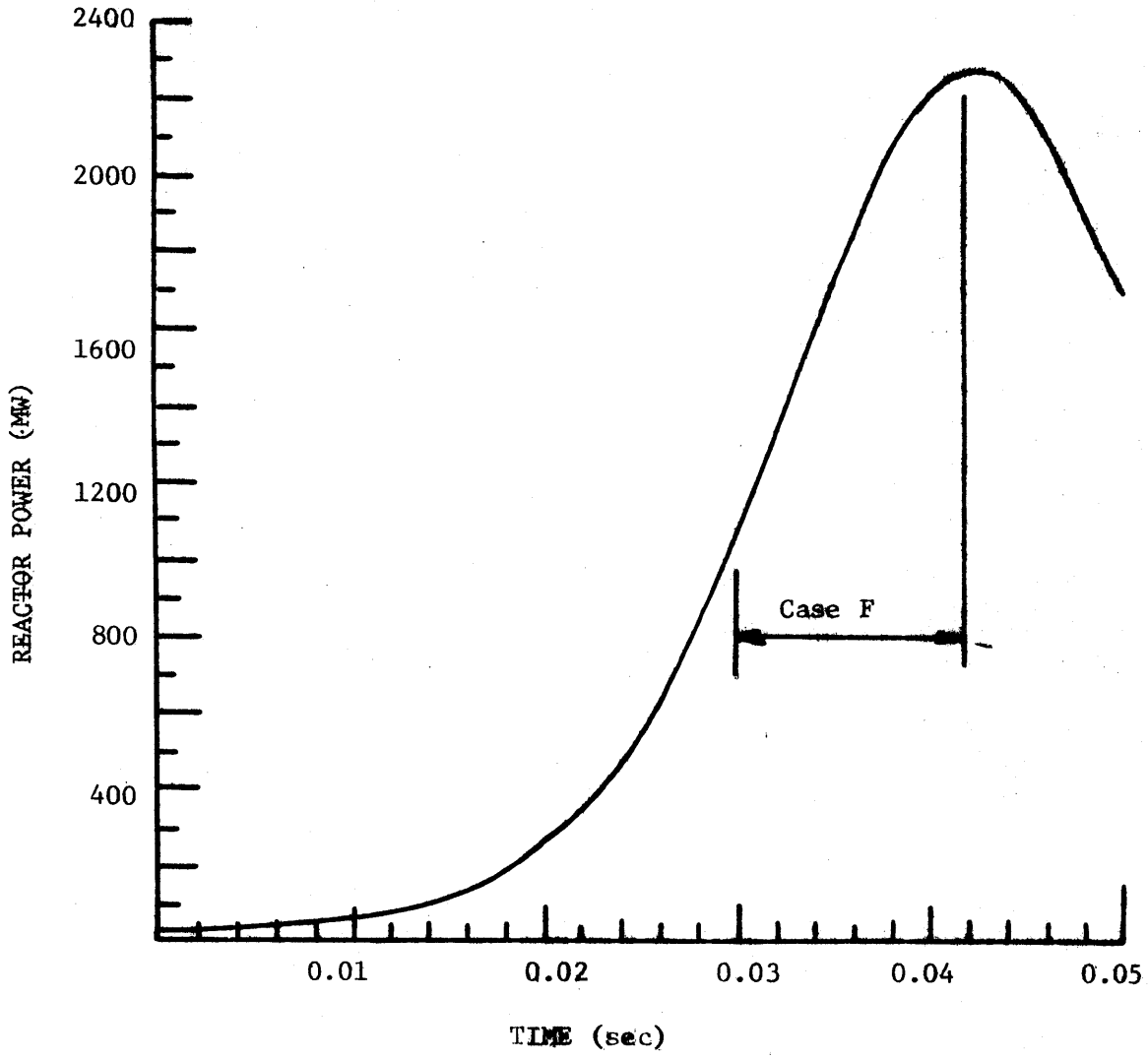

FIG. 5.5: POWER VS. TIME: CASE F.

TABLE 5.1.

Time Step Size Sensitivity by Case.

Case (Initial Power: P_o - MW)	Time Step Size: Δt (sec)	Final Power: P_f (MW)	Average Period: $\bar{T}$ (sec)	% Error in Period (%)
A	0.000025	141.297	0.005606	
	0.00005	141.380	0.005602	-0.07
(57.912)	0.0001	141.788	0.005584	-0.39
	0.0002	143.272	0.005520	-1.53
	0.0005	148.112	0.005320	-5.10
	0.005	150.804	0.005220	-6.89
B	0.000066	7.5585	0.02420	
	0.0001	7.5684	0.02412	-0.33
(5.0000)	0.00025	7.5994	0.02389	-1.28
	0.001	6.0065	0.05452	125.0
C	0.01	13.9040	2.557	
	0.014	13.9296	2.545	-0.47
(9.4036)	0.0179	14.1498	2.447	-4.30
	0.02	14.3071	2.383	-6.80
	0.033	15.0396	2.129	-16.74
	0.1	15.7377	1.942	-24.05
D	0.0001	8.8055	0.277	
	0.0002	8.8151	0.272	-1.81
(8.1912)	0.00033	8.8394	0.263	-5.05
	0.0005	8.8958	0.243	-12.27
	0.00067	8.9756	0.219	-20.94
	0.00083	9.0573	0.199	-28.16
	0.00091	9.0906	0.192	-30.69
	0.0014	9.2475	0.165	-40.43
E	0.00021	49.5739	0.281	
	0.00031	49.4774	0.292	3.91
(47.0000)	0.0005	49.1941	0.329	17.08
	0.00083	48.6104	0.445	58.36
	0.00125	48.0989	0.649	130.96
F	0.00005	2321.6	0.01518	
(1053.0)	0.0001	2345.2	0.01499	-1.26
	0.0002	2442.2	0.01427	-6.02
	0.0004	2804.5	0.01225	-19.30

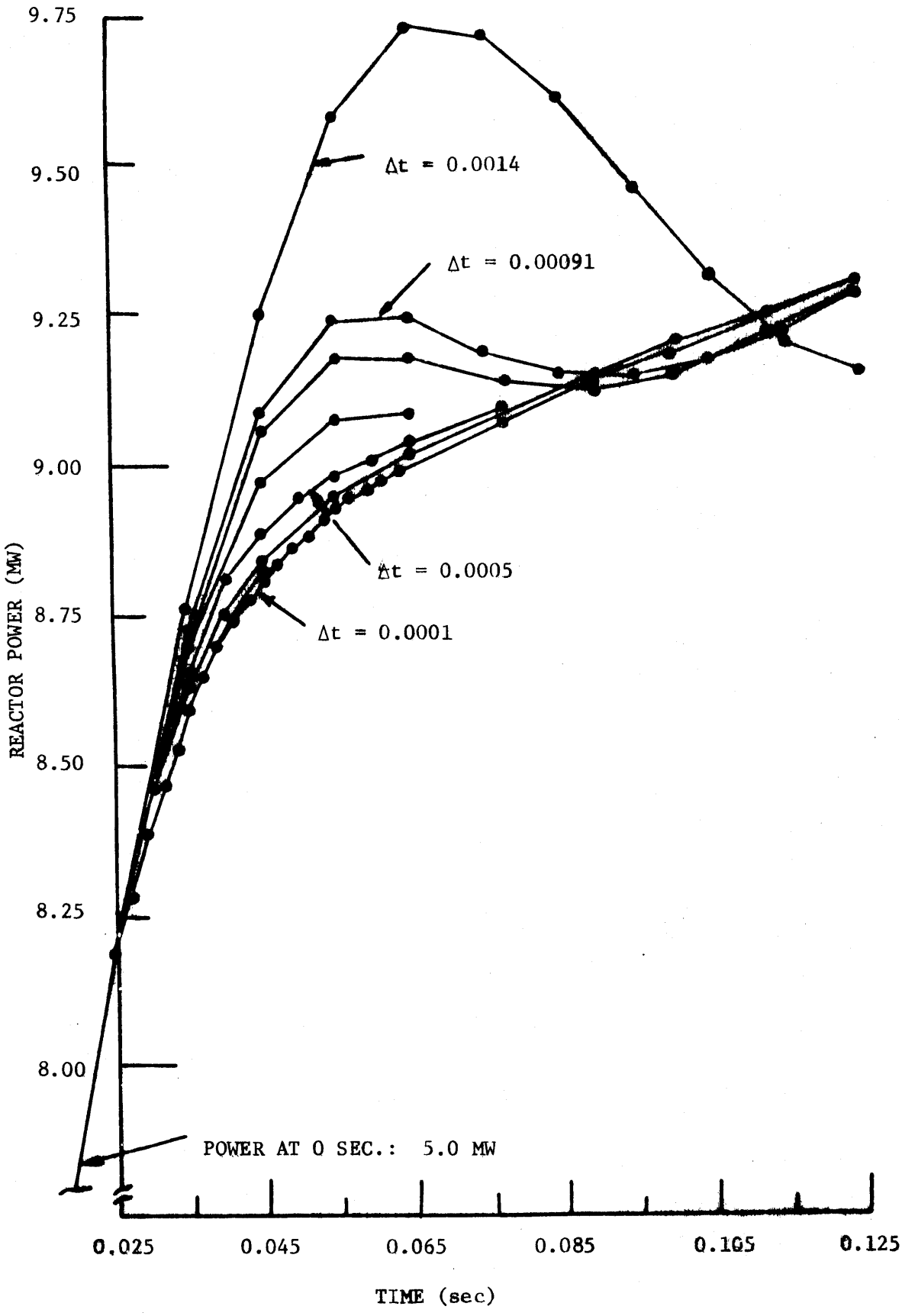

FIG. 5.6: TIME STEP SENSITIVITY: CASE D.

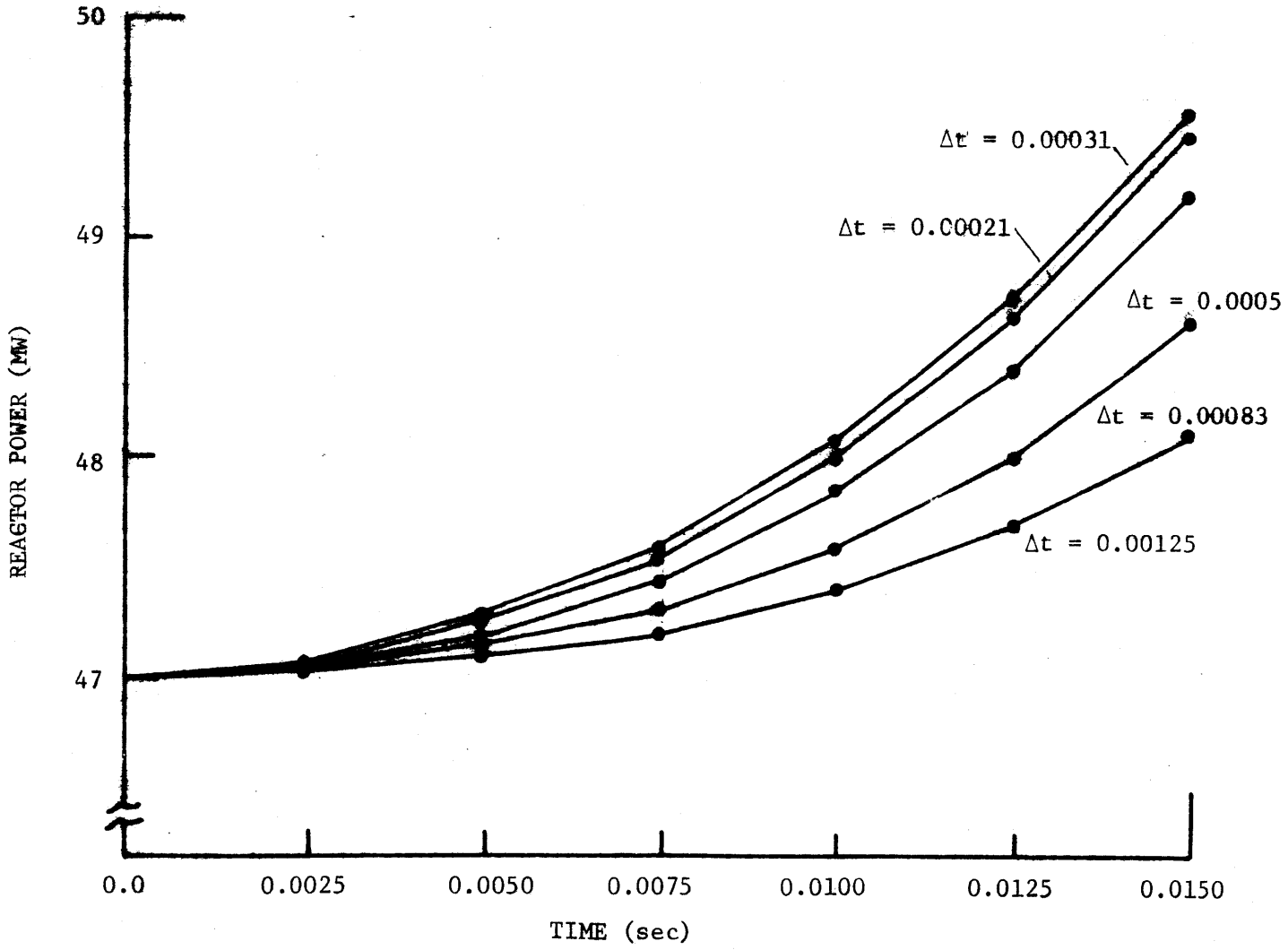

FIG. 5.7: TIME STEP SENSITIVITY: CASE E,

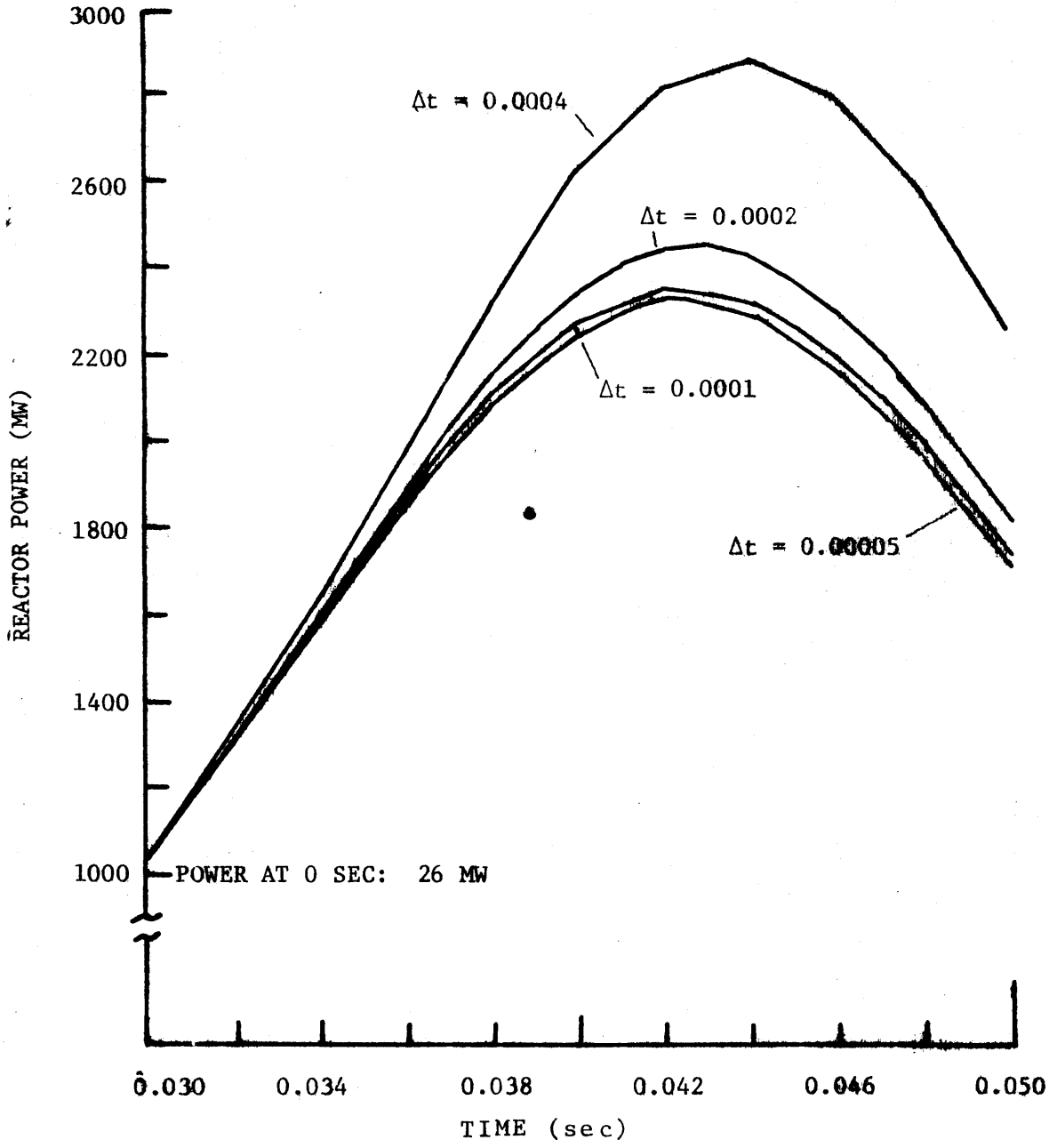

FIG. 5.8: TIME STEP SENSITIVITY: CASE F.

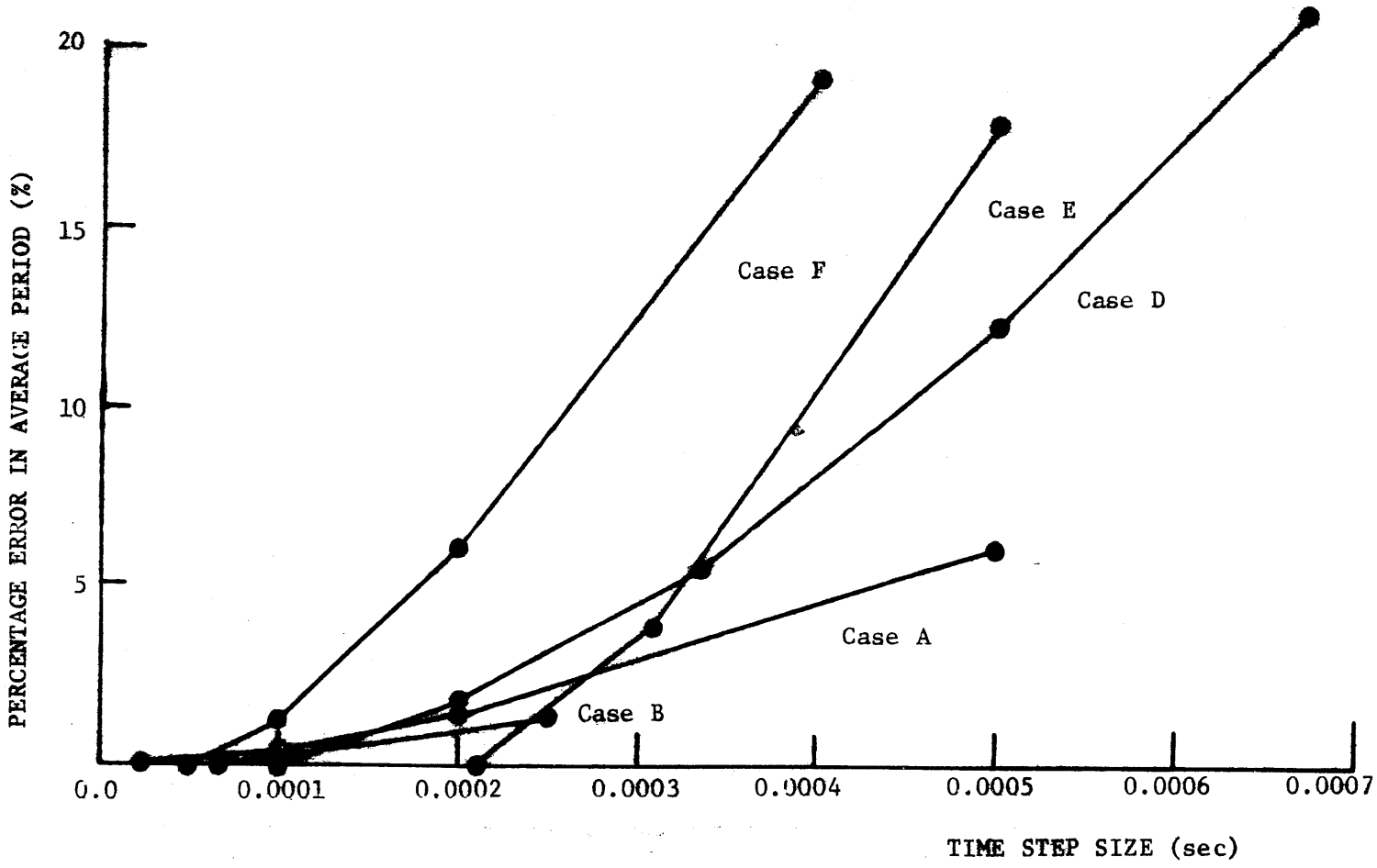

FIG. 5.9: ERROR VS. NEUTRONIC TIME STEP SIZE.

time step size for accurate answers was very small.

In order to interpret the results presented above, a close look at the NSADE method is required. Past studies indicate that excellent results were achieved for super-prompt critical neutronics-only transients which were induced by a step change in reactivity (6) (11) (13). These characteristics mean a constant A matrix in Eq. (5.1), an exponential power increase, and a constant frequency. The last two characteristics match perfectly with the exponential transform and the method of frequency selection (i.e., Eqs. (5.3) and (5.4)). Consequently, good results should be expected for such conditions. The results from Case A confirm such expectations.

Results are not as encouraging when the frequency is changing rapidly such as at the beginning of a transient (Case E), at the knee (Case D), and at the point of power turnaround due to feedback (Case F). At the beginning, large time steps retard the power rise (Fig. 5.8). At the knee, non-physical oscillations result (Fig. 5.9). At turnaround, the peak power level is overestimated (Fig. 5.9), and oscillations will probably follow. The oscillations are particularly disturbing because the thermal-hydraulics calculations in MEKIN rely on the power levels. The cause of these problems is the frequency transform used in the NSADE method. As implied by Eq. (5.4), this method predicts the point fluxes at the next time step based on the frequencies of the previous time step. For this reason, inertia is built into the system. This inertia is particularly well illustrated in Fig. 5.7, where large time steps coax the curves to proceed

in their current directions rather than follow the bend of the exact solution. From a numerical standpoint, addition of the frequency transformation changes the solution technique from a first order system to a second order system:

$$\begin{aligned} \phi^{n+1} &= f_1(\phi^n, \omega^n), \\ \text{but} \quad \omega^n &= f_2(\phi^{n-1}, \phi^n), \\ \text{so} \quad \phi^{n+1} &= f_3(\phi^n, \phi^{n-1}), \end{aligned} \tag{5.6}$$

where ϕ^n = flux at time n ,

ω^n = flux frequency at time n .

5.3 DATA CORRELATION

Previous studies (6) (13) recommend choosing a time step size based on one hundred time steps per doubling of reactor power for accuracies in reactor period within one percent. Such criteria appears to work very well when the reactor period is constant. However, this number is far too small when examining a portion of a transient where the period is changing rapidly. Therefore, a generalized expression for the number of time steps per doubling of reactor power must account for the rate of change of the frequency. A rough correlation of the data in this study yielded:

$$N_n = C_1 + C_2 \left(\frac{1}{\omega_n^2} \frac{\partial \omega_n}{\partial t}\right), \tag{5.7}$$

where N_n = the number of time steps per doubling of reactor power for errors in frequency of less than one percent at time n,

C_1 = the number of time steps per doubling of reactor power when $\frac{\partial \omega_n}{\partial t}$ is zero,

$C_2 \left(\frac{1}{\omega_n^2} \frac{\partial \omega_n}{\partial t}\right)$ = the number of additional time steps per

doubling of reactor power needed to compensate for the changing period.

From the results of this study, $C_1 \simeq 80$, $C_2 \simeq -100$ when $\frac{\partial \omega_n}{\partial t} < 0$ and $C_2 \simeq 25$ when $\frac{\partial \omega_n}{\partial t} > 0$. The fact that C_2 was found to be greater for $\frac{\partial \omega_n}{\partial t} < 0$ is not surprising; all derivatives of an exponential are positive, and when $\frac{\partial \omega_n}{\partial t} > 0$, all derivatives of the power time function are probably also positive. Therefore, an exponential is more closely matched when $\frac{\partial \omega_n}{\partial t} > 0$ than when $\frac{\partial \omega}{\partial t} < 0$.

The form of Eq. (5.7) was chosen to fit the available calculated data and to be dimensionally correct. Complete theoretical justification has not been established, and such a task appears non-trivial. The analysis done here is based on errors in reactor frequency over many time steps. Therefore, each time step is assumed to contribute equally to the integrated error over the range. In addition, the data base involved only three cases where the second term of Eq. (5.7) dominated.

In summary, due to the lack of experimental and theoretical evidence, the correlation presented above should not be taken as a reliable quantitative guide for choosing the best time step size. However, the correlation serves as a first attempt in developing an automatic time step selector. In addition, it shows that the NSADE method is often more sensitive to the rate of change of frequency as opposed to the rate of change of power. Indeed, a previous study noted that the NSADE method's limiting factor is the "ability of the frequencies to follow a

bend in solution rather than just a large change in power."(11)

5.4 USER APPLICATIONS OF THE TIME STEP SIZE SENSITIVITY

The most obvious application of this work is choice of time step size based on the results of Section 5.2. However, time step size is very dependent on the problem and desired accuracy, so more universal guidelines are necessary.

As with any kinetics code where the time step is user specified, a chief drawback is the fact that the user must have some idea of what the answer will be before it is calculated. With MEKIN, several options exist for estimating the power-time behavior prior to an accurate calculation. First a simple point kinetics formula can crudely predict the frequency of the prompt jump:

$$\omega = \frac{\rho}{\ell}, \tag{5.9}$$

where ω = the reactor frequency,

ℓ = prompt neutron lifetime ($\simeq 10^{-4}$ for light water reactors),

ρ = reactivity insertion (rod worth in the case of a rod ejection).

Second, a crude scoping calculation could be performed with MEKIN with the time step size kept relatively large. Unfortunately, this approach has a serious drawback. If the time step size is too large, the power-time oscillations may be so bad that no useful information is gained from the run. Third, the user may choose to take advantage of the MEKIN transient restart option, which allows storing the solution on disk at a discrete

time and subsequently continuing the calculation from this point as often as desired. Such action permits a way of monitoring the transient as it evolves, an economic method of recalculating suspicious portions of the transient, and a means of catching errors before they propagate. This approach may require more time and effort in the short run, but it may turn out to be the most efficient procedure over the long run.

After estimating the power-time behavior, the user must choose a time step size such that results fall within the desired accuracy. From the experience in this study, two general rules have evolved. Each rule is intended to govern the selection of the maximum time step size for less than one or two percent error in reactor frequency.

For transients of constant frequency, eighty time steps per doubling of reactor power appears adequate. An example of such a situation is a super-prmpt critical transient which is induced by a step change in reactivity and does not have feedback effects (i.e., similar to Case A of Section 5.2). This rule also applies for long intervals of constant frequency within any transient, such as the asymptotic portion (after the knee) of a "neutronics - only" delayed critical transient. When thermal-hydraulic feedback is included, a perfectly constant frequency is almost never seen. However, many portions of such transients have frequencies which are changing slowly enough to accomodate the rule given above.

For transients which include portions of rapidly changing frequency, an adequate time step size corresponds to one hundred

time steps per doubling of reactor power, based on the "maximum normalized" rate of power increase within the transient. Maximum normalized rate of power increase can be defined as

$$R = \frac{1}{P_x} \frac{\partial P_x}{\partial t} , \tag{5.9}$$

where P_x = reactor power at time x,

$\frac{\partial P_x}{\partial t}$ = the slope of the curve at time x, "x" corresponds to the time of maximum normalized rate of power increase.

The time step size can then be determined by

$$\Delta t = \frac{1}{RN} , \tag{5.10}$$

where Δt = time step size,

N = the number of time steps per doubling of reactor power (= 100, if the criteria given above is followed).

This rule is meant to be applied to transients similar to Fig. 5.2, a "neutronics-only" delayed critical transient induced by a fast rod ejection. For the particular conditions of Fig. 5.2, the time step size would be based on the normalized rate of power increase at the indicated location. However, once the asymptotic portion after the knee is reached, the time step size can be drastically increased. A second application of this rule is a super-prompt critical rod ejection with thermal-hydraulic feedback (i.e., Fig. 5.5). If the rod is out before significant changes in temperature, the power will rise via a constant frequency. As the negative doppler feedback becomes important,

the rate of power increase will decline and eventually turn around. The maximum normalized rate of power increase should be based on the frequency before feedback becomes important.

5.5 IMPLICATIONS OF THE TIME STEP SIZE SENSITIVITY

The transient solution appears to be very sensitive to neutronic time step size. For this reason, an automatic time step selector may be among future modifications of the MEKIN code. In order to comply with data storage limitations in MEKIN, the selector will probably need to be based on total reactor parameters (i.e., powers and frequencies) rather than point fluxes and frequencies.

In most of the situations tested here, the required time step size has been significantly smaller than originally anticipated. This makes the NSADE method less attractive from an economic point of view. Even a finely tuned time step selector will not erase this drawback.

The test cases discussed in this chapter were either "neutronics-only" or fast coupled transients. Slow transients with thermal-hydraulic feedback also constitute an important application of MEKIN. Unfortunately, attempts to represent such conditions with MEKIN resulted in difficulties with respect to time step size and power-time behavior (see Section 6.3).

If the NSADE method is to be modified, the frequency transform or perhaps just the choice of frequencies may be the place to start. Although the method works well under certain conditions, results of this study indicate problems arise as the

power-time behavior deviates from an exponential form. This conclusion agrees with the recommendations of at least one previous study (11).

CHAPTER 6

CROSS SECTION FEEDBACK PARAMETER SENSITIVITY

As explained in Chapter 2, feedback between neutronics and thermal-hydraulics is one of the main features of the MEKIN code. With respect to neutronics, the cross sections are represented as linear functions of coolant density, coolant temperature, and metal temperature. In equation form, the cross sections are updated after each thermal-hydraulic calculation by

$$\Sigma_i (C_c, T_c, T_m) = \Sigma_i^* (C_c^*, T_c^*, T_m^*) + C_1(e_c - e_c^*) + C_2 (T_c - T_c^*) + C_3 (T_m - T_m^*), \quad (6.1)$$

where $C_1 = \partial \Sigma_i / \partial e_c$,

$C_2 = \partial \Sigma_i / \partial T_c$,

$C_3 = \partial \Sigma_i / \partial Tm$,

"*" indicates reference state,

"C" refers to the coolant,

"m" refers to metal (the fuel and clad).

C_1, C_2, C_3, e_c^*, T_c^*, T_m^*, and Σ_i^* are user inputs.

The purpose of this chapter is to give a description of the sensitivity of solution to the cross section feedback parameters (i.e., C_1, C_2, and C_3 of Eq. (6.1)). Research

involved three separate tasks: background work, fuel feedback sensitivity, and coolant feedback sensitivity. The chapter is divided accordingly, and it also includes sections on user applications and implications of this sensitivity study.

6.1 PRELIMINARY RESEARCH

Unlike the inputs of mesh size and time step size, the feedback parameters require preliminary calculations. Consequently, a significant amount of background work was done prior to transient studies with the MEKIN code.

When calculating cross section feedback parameters, a computer code is needed to help generate homogenized cross sections at different fuel temperatures, coolant temperatures, and coolant densities. Once the cross section-temperature and cross section-density behaviors are known, the data must be linearly approximated. Units and cross section definitions must be carefully monitored when converting output from a cross section code to input for the MEKIN code. All feedback parameters employed in this research project were obtained by using the LEOPARD code (1). Appendix D explains the manner in which LEOPARD has been and can be applied to input preparation for MEKIN.

The cross section feedback parameters used in MEKIN are a function of the initial composition of the reactor region, the burnup, metal temperature, coolant temperature, and coolant density. Only the temperatures and density are

coupled to the MEKIN calculational strategy. For this reason, the burnup and initial composition were held constant when the feedback parameters were calculated for the test cases of Sections 6.2 and 6.3. However, the MEKIN user cannot ignore these variables when preparing input, and further discussion is provided in Section 6.4.

Prior to running expensive transient calculations with MEKIN, efforts were made to determine the most important feedback parameters with respect to sensitivity of solution. This task was approached from three directions: 1) a steady state cross section sensitivity; 2) a prediction of actual cross section changes during a transient; and 3) a measure of the uncertainty of the linear feedback approximation.

The cross section sensitivity study was done by using Model 5 of Appendix B. Each cross section was varied individually in one of the regions and samples of the results are given on Tables 6.1 and 6.2. These tables show the sensitivity of the results to variation in one cross section relative to the same variations in another. Altered boundary conditions and different reference cross sections were also considered, but these changes did not significantly influence the results.

The next step involved estimating the amount by which the cross sections would actually change during a transient. This was done by multiplying the calculated feedback parameters by anticipated temperature changes and then normalizing

TABLE 6.1,

CROSS SECTION SENSITIVITY - PART I.

PROBLEM: MODEL 5 OF APPENDIX B, REFLECTING BOUNDARY CONDITIONS, CROSS SECTIONS AT SUBCOOLED CONDITIONS

Cross Section	Reference Value (cm^{-1})	% Variation From Reference[3]		
		Cross Section	K-effective[1]	Region Power[2]
D_1^{-1}	0.6808	1.0	0.00	0.00
Σ_{f1}	0.001860	1.0	0.05	0.21
Σ_{c1}	0.007351	1.0	-0.14	-0.37
D_2^{-1}	2.855	1.0	0.00	0.00
Σ_{f2}	0.04462	1.0	0.18	0.68
Σ_{c2}	0.03398	1.0	-0.18	-0.64
$\Sigma_{s1\to2}$	0.01687	1.0	0.09	0.62
D_1^{-1}	0.6808	10.0	0.00	0.00
Σ_{f1}	0.001860	10.0	0.48	2.04
Σ_{c1}	0.007351	10.0	-1.33	-3.71
D_2^{-1}	2.855	10.0	0.00	0.00
Σ_{f2}	0.04462	10.0	1.78	6.34
Σ_{c2}	0.03398	10.0	-1.65	-6.22
$\Sigma_{s1\to2}$	0.01687	10.0	0.93	5.95

[1] Reference K-effective is 1.14797.

[2] Reference region power is 1.000.

[3] % variation = $\frac{\text{Case Value - Reference Value}}{\text{Reference Value}} \times 100.$

TABLE 6.2.

CROSS SECTION SENSITIVITY - PART II.

PROBLEM: MODEL 5 OF APPENDIX B, ALBEDO BOUNDARY CONDITIONS, REFERENCE CROSS SECTIONS AT BOILING CONDITIONS

Cross Section	Reference Value (cm^{-1})	% Variation From Reference[3]		
		Cross Section	K-Effective[1]	Region[2] Power
D_1^{-1}	0.5805	50.0	0.43	2.92
Σ_{f1}	0.001857	1.0	0.11	0.17
Σ_{c1}	0.007262	1.0	-0.25	-0.17
D_2^{-1}	2.186	50.0	0.02	0.21
Σ_{f2}	0.04459	1.0	0.23	0.30
Σ_{c2}	0.03136	1.0	-0.22	-0.26
$\Sigma_{s1\to2}$	0.01027	1.0	0.19	0.37
D_1^{-1}	0.5805	-50.0	- .47	-3.15
Σ_{f1}	0.001857	10.0	1.11	1.61
Σ_{c1}	0.007262	10.0	-2.42	-1.75
D_{2-1}	2.186	-50.0	-0.04	-0.37
Σ_{f2}	0.04459	10.0	2.19	2.72
Σ_{c2}	0.03136	10.0	-2.16	-2.57
$\Sigma_{s1\to2}$	0.01027	10.0	1.92	3.64

[1] Reference K-effective is 0.979413.

[2] Reference region power is 1.2538.

[3] % variation = $\frac{\text{Case Value - Reference Value}}{\text{Reference Value}} \times 100.$

to a percentage. In equation form,

$$X_{1M} = \frac{/\ \partial\Sigma i/\partial T_M \ x\Delta T_M\ /}{\Sigma_i} \quad x\ 100$$

and

$$X_{1C} = \frac{/\partial\Sigma i/\partial Tc\ x\Delta T_c\ /}{\Sigma i} \quad x\ 100, \qquad (6.3)$$

where $\partial\Sigma i/\partial T_c$ accounts for both subcooled density and temperature changes. ΔT_m and ΔT_c are anticipated changes in metal and coolant temperature for an arbitrary transient. T_m was taken as 1000° C while T_c was 40° C.

The final step consisted of evaluating the uncertainty of the linear feedback approximation. The method used here involved the calculations

$$X_{2M} = \frac{/\ (\partial\Sigma i/\partial T_M)_1 - (\partial\Sigma i/\partial T_M)_2 \ x\ \Delta T_m\ /}{\Sigma_i} \quad x\ 100,$$

and

$$X_{2C} = \frac{/\ (\partial\Sigma i/\partial T_c)_1 - (\partial\Sigma i/\partial T_c)_2 \ x\ \Delta T_c/}{\Sigma_i} \quad x\ 100, \qquad (6.4)$$

where "1" and "2" represent different ranges over which the feedback parameters were evaluated and the other terms are defined after Eq. (6.3). This calculation may seem redundant with that of Eq. (6.3), but both are included due to the uncertainty of the data.

The results of the cross section sensitivity study, the calculations with Eq. (6.3) and the computations with Eq. (6.4) are tabulated on Table 6.3. All values in columns A, B, C, and D are percentages. Column A and B indicate the effect on K and power distribution when a particular cross section is altered by 10%. Column C represents the expected percentage change in cross section value for an arbitrary transient (i.e., X_{1M} and X_{1C} of Eq. (6.3)). Column D measures the uncertainty of the linear cross section change (i.e, X_{2M} and X_{2C} of Eq. (6.4)). In order to predict which feedback parameters are the most important with respect to the calculational strategy in MEKIN, all four columns of this table must be considered together. With respect to metal temperatures, $\partial\Sigma c1/\partial T_M$, $\partial\Sigma f2/\partial T_M$, and, to a lesser extent, $\partial\Sigma_s^{1\to2}/\partial T_M$ appear to be the most important feedback parameters. Concerning the coolant, $\partial\Sigma s^{1\to2}/\partial T_c$ (or $\partial\Sigma_s^{1\to2}/\partial e_c$) can be expected to have a greater influence on the solution than the other feedback parameters.

In summary, these results point out the most important feedback parameters and indicate that some sensitivity of solution should be expected; this data does <u>not</u> describe the sensitivity of the MEKIN solution to feedback effects. The latter is addressed in the next two sections of this chapter.

TABLE 6.3.

ESTIMATION OF FEEDBACK PARAMETER SENSITIVITY

(SEE TEXT FOR COMPLETE EXPLANATION)

Cross Section	Value	$\frac{A'}{\%\ \text{Change}}$ $\Delta K/K$	$\frac{B'}{\%\ \text{Change}}$ Region Power	$\frac{C'^{2}}{\%\ \text{Change}}$ Fuel	(Coolant)	$\frac{D'^{3}}{\%\text{Change}}$ Fuel	(Coolant)
D_1^{-1}	0.68080	0.0	0.0	0.5	(6.0)	0.3	(0.6)
Σ_{f1}	0.00186	0.48	2.04	2.2	(1.3)	0.7	(0.3)
Σ_{c1}	0.00735	1.33	3.71	9.0	(1.6)	1.1	(0.3)
D_2^{-1}	2.85500	0.0	0.0	0.5	(15.3)	0.2	(0.8)
Σ_{f2}	0.04462	1.78	6.34	2.4	(1.4)	0.7	(0.5)
Σ_{c2}	0.03398	1.65	6.22	1.8	(0.7)	0.4	(0.4)
$\Sigma_{R1\to 2}$	0.01687	0.93	5.95	2.1	(14.1)	0.3	(1.7)

[1] See Fig. 6.1, 10% increase in cross section.

[2] See Eq. (6.3).

[3] See Eq. (6.4)

6.2 FUEL FEEDBACK SENSITIVITY

This section deals exclusively with the cross section feedback parameters associated with fuel temperature (i.e., $\partial\Sigma i/\partial T_M$ of Eq. (6.1)). All test cases were performed with Model 6 of Appendix B. Thermal-hydraulic feedback was included and an off-center rod ejection was the reactivity force driving the transient. Each calculation was carried out to 0.05 seconds, and peak power was always reached between 0.040 and 0.045 seconds. A time step sensitivity preceded the test cases, so the level of the power turnaround was due entirely to feedback effects rather than numerical instabilities. (As shown in Chapter 5, this will always be a concern with the NSADE technique in its current form.) In order to assure that all thermal-hydraulic feedback occurred in the fuel, the feedback parameters associated with the coolant were all set to zero. In addition, each calculation involved one set of feedback parameters for the entire reactor. All feedback parameters in this section are based on a pressurized water reactor assembly with a burnup of 6000 $^{MWD}/MT$ and an initial enrichment of 2.73% U-235.

Research was divided into three areas: individual variation of the linear feedback parameters, variation of the parameters as a group, and implementation of higher order fits to represent cross section changes as a function of temperature.

The feedback parameters were varied individually in the first set of test cases. Based on the results given in Section 6.1, attention was focused on $\partial\Sigma c1/\partial T_M$, $\partial\Sigma f2/\partial T_M$,

and $\partial\Sigma_s^{1\to2}/\partial T_M$. The range over which these inputs were varied and the reference set of feedback parameters are given on Table 6.4. These values were chosen from LEOPARD calculations over a wide fuel temperature range, and realistic upper and lower bounds are therefore represented. As an example, the group one capture cross section is plotted against fuel temperature in Fig. 6.1. The data points are assumed to be the benchmark temperature-cross section behavior, while the slopes of the three linear approximations yield the input value for $\partial\Sigma_{c1}/\partial T_M$. All lines intersect at the first point because the user inputs of reference cross section and reference temperature make this point a known starting condition. The input values of $\partial\Sigma_{f2}/\partial T_M$ and $\partial\Sigma_s^{1\to2}/\partial T_M$ were determined in the same manner.

When used as input to MEKIN, the different feedback parameters significantly affected both peak power level (i.e., power at "turnaround" time) and energy deposition. Energy deposition is inferred by the rise in the average fuel temperature from steady state to 0.05 seconds. Using the two extreme $\partial\Sigma_{c1}/\partial T_M$ cases as an example, the peak power levels differed by 32% and the hot channel fuel temperature changes disagreed by 27%. Similar results were obtained for the $\partial\Sigma_{f2}/\partial T_M$ cases, while the $\partial\Sigma_s^{1\to2}/\partial T_M$ cases were much less sensitive. Although the power level varied noticeably in all cases, the power shapes were almost identical at

TABLE 6.4.

INDIVIDUAL VARIATION OF FEEDBACK PARAMETERS - RESULTS.

Case ($cm^{-1}/°C$)	Peak Power (MW)	T_M (2) (°F)	$\partial\rho/\partial T_M$ (3) (/°F)
Reference:	2229.9	649.9	-1.25E-5
$\partial\Sigma_{c1}/\partial T_M$ = 0.630E-6			
$\partial\Sigma_{f2}/\partial T_M$ = 0.108E-5			
$\partial\Sigma_s^{1\to2}/\partial T_M$ = -0.353E-6			
$\partial\Sigma_{c1}/\partial T_M$ = 0.540E-6	2650.2	749.0	-1.07E-5
(% variation')	(18.9)	(15.3)	(-14.4)
$\partial\Sigma_{c1}/\partial T_M$ = 0.720E-6	1925.6	574.1	-1.44E-5
(% variation')	(-13.7)	(-11.7)	(15.2)
$\partial\Sigma_{f2}/\partial T_M$ = 0.132E-5	2470.9	702.5	-1.12E-5
(% variation')	(10.8)	(8.1)	(-10.4)
$\partial\Sigma_{f2}/\partial T_M$ = 0.0675E-5	1919.0	577.3	-1.48E-5
(% variation')	(-13.9)	(-11.2)	(18.4)
$\partial\Sigma_s^{1\to2}/\partial T_M$ = -0.312E-6	2300.1	667.2	-1.22E-5
(% variation')	(3.2)	(2.7)	(-2.4)
$\partial\Sigma_s^{1\to2}/T_M$ = -0.394E-6	2165.4	633.6	-1.28E-5
(% variation')	(2.9)	(-2.5)	(2.4)

[1] % variation = $\frac{\text{Case Value - Reference Value}}{\text{Reference Value}}$ x 100.

[2] Metal temperature rise in hot channel from 0.0 seconds to 0.05 seconds.

[3] Temperature coefficient of reactivity; calculated from steady state runs.

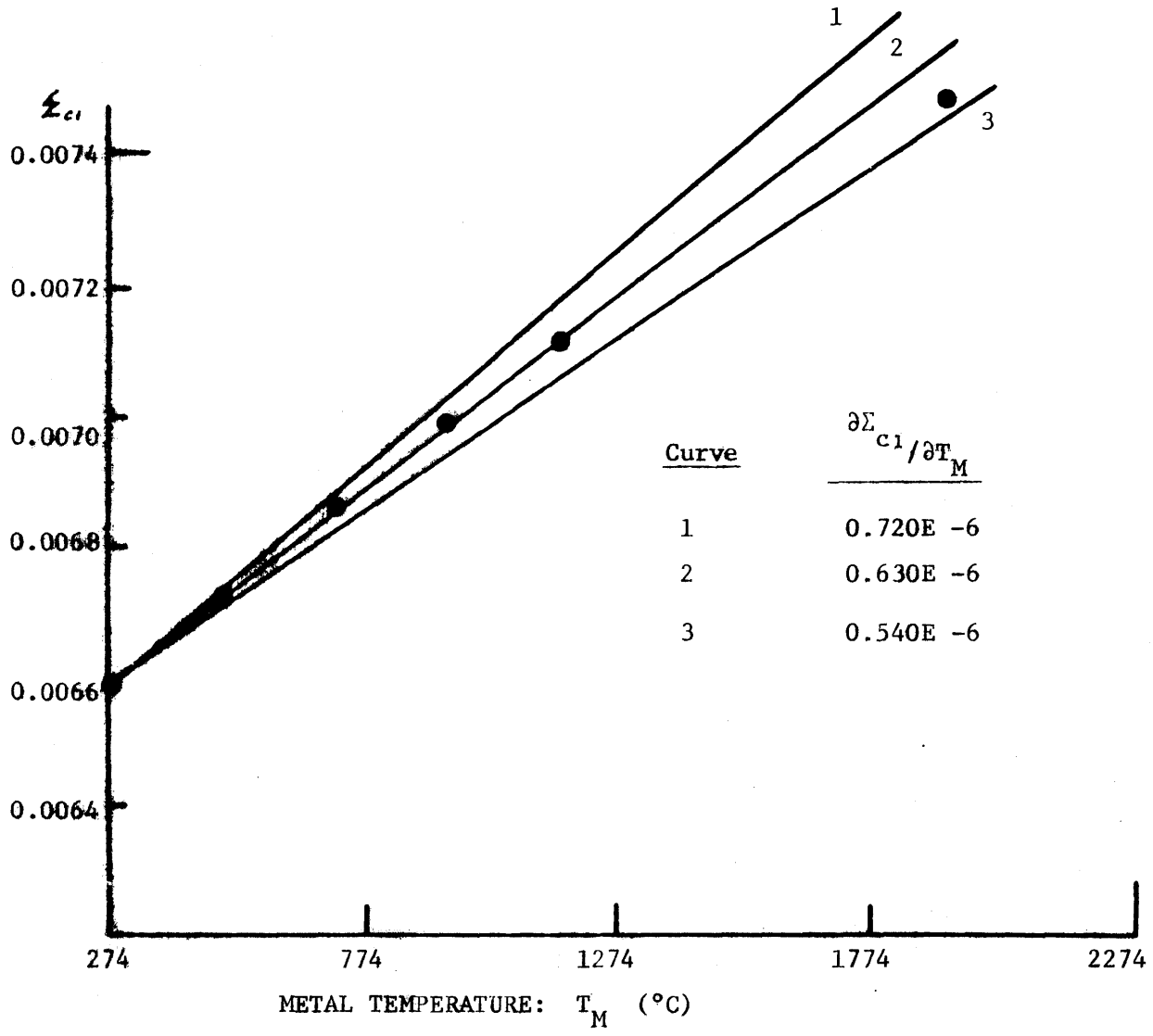

FIG. 6.1: Σ_{c_1} VS. METAL TEMPERATURE AND LINEAR APPROXIMATIONS.

turnaround time. Results are given in Table 6.4 and graphed on Figs. 6.2, 6.3, and 6.4.

In reference to Table 6.4, the temperature coefficients of reactivity serve as an attempt to predict the transient behavior from steady state data. For each case, these values were develcped from two steady state computer calculations with the following conditions: Model 6 of Appendix B, control rod fully inserted, reactor power of 26 MW for the first run, and reactor power at 36 MW for the second run. Results for the two power levels yielded two different values of K-effective (K) and two different average reactor fuel temperatures ($\bar{T}$). Thus, the temperature coefficient of reactivity is defined as

$$\partial\rho/\partial T_M = \frac{K_{36} - K_{26}}{\bar{T}_{36} - \bar{T}_{26}} \quad . \tag{6.5}$$

As indicated by Table 6.4, the percentage differences for $\partial\rho/\partial T_m$ give a crude estimate of the relative variations in peak power and energy deposition.

The results are depicted differently on Fig. 6.5, where the effect on power level is shown to be almost linear as the $\partial\Sigma_i/\partial T_M$ are varied. This figure also does an excellent job of indicating that variations in $\partial\Sigma_{f2}/\partial T_M$ and $\partial\Sigma_{c1}/\partial T_M$ have similar effects on the solution, both of which are much greater than the effect induced by changing $\partial\Sigma_s^{1\to 2}/\partial T_M$.

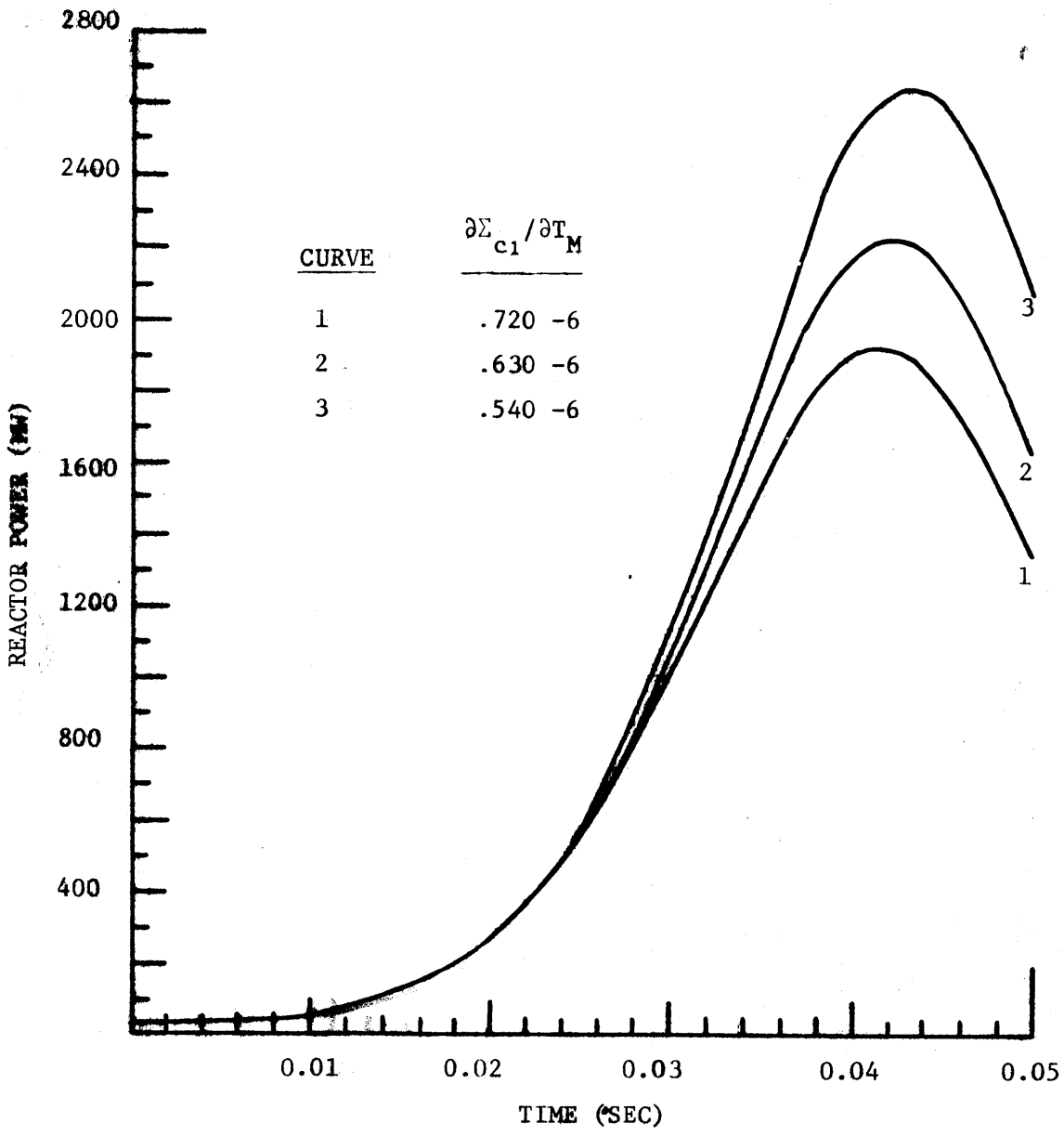

FIG. 6.2: METAL FEEDBACK SENSITIVITY: $\partial\Sigma_{c1}/\partial T_M$.

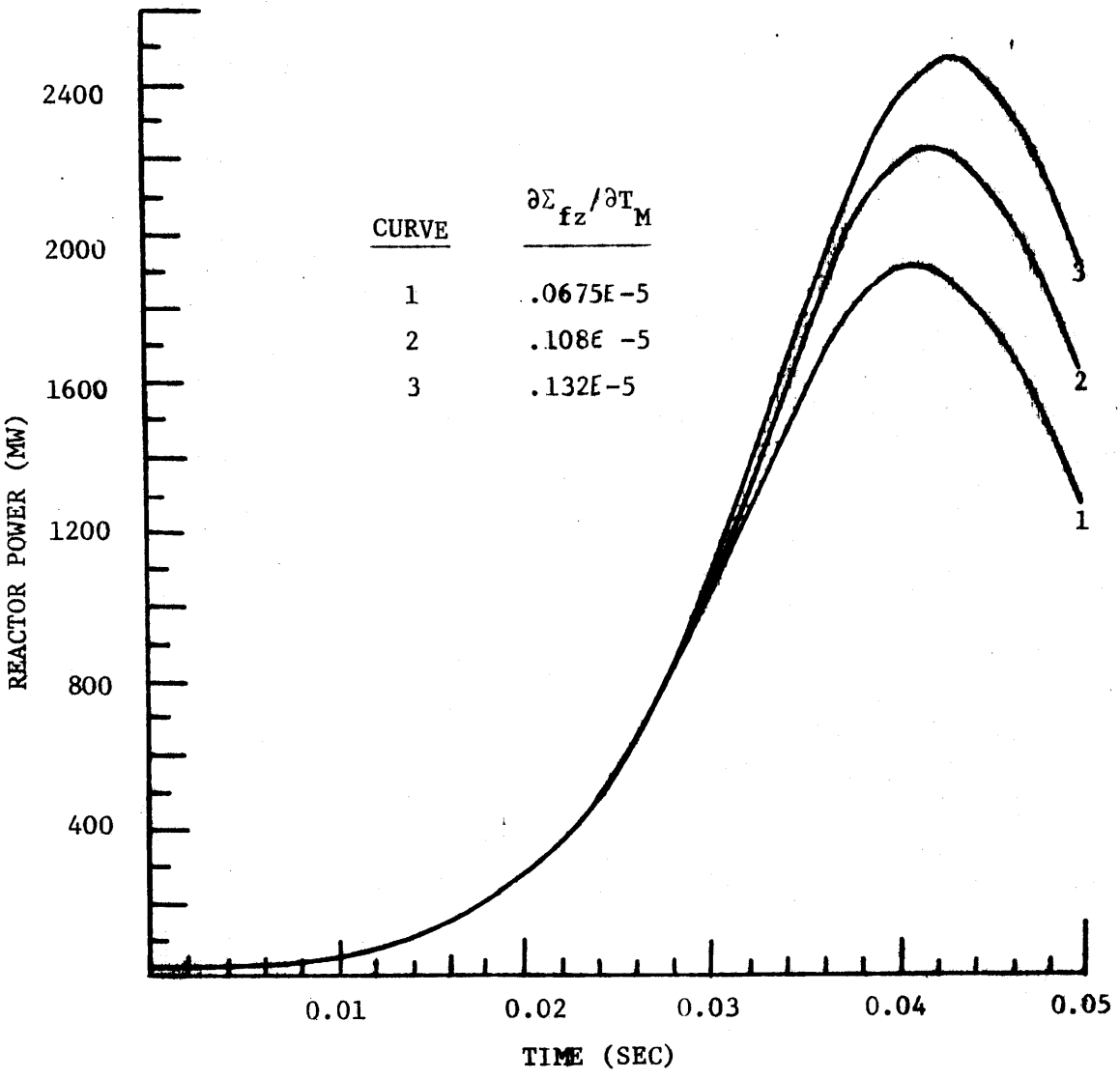

FIG. 6.3: METAL FEEDBACK SENSITIVITY: $\partial\Sigma_{f_2}/\partial T_M$..

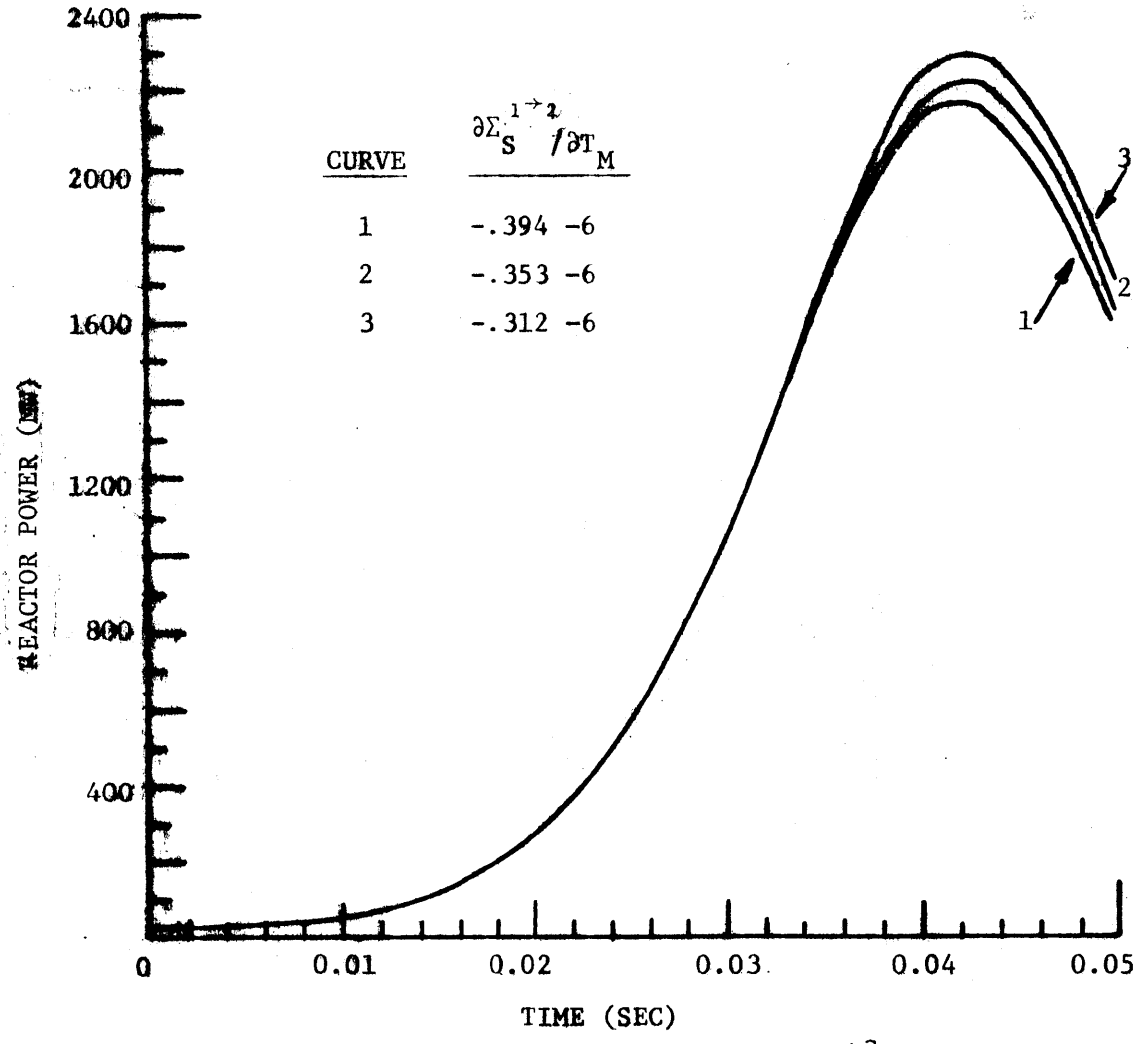

FIG. 6.4: METAL FEEDBACK SENSITIVITY: $\partial\Sigma_S^{1\to 2}/\partial T_M$

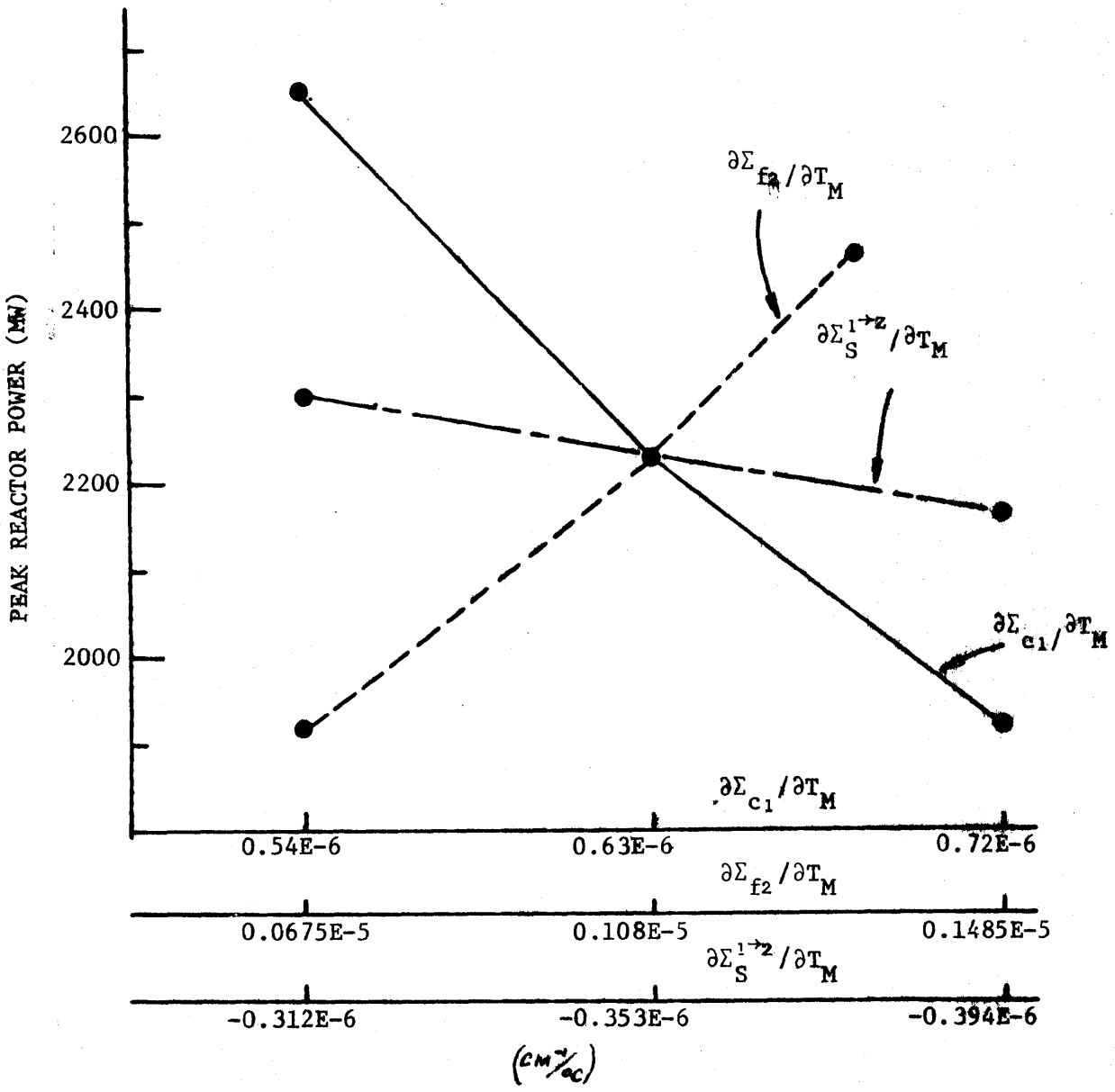

FIG. 6.5: PEAK POWER VS. FEEDBACK PARAMETER.

The above results point out that the solution of the MEKIN code is quite sensitive to individual variation of the most important feedback parameters associated with metal temperature. However, this data alone does not preclude the possibility of cancelling effects if the feedback parameters are varied as a group. To answer this question, three temperature ranges were selected and a set of feedback parameters was calculated for each range. In other words, the conditions were varied and each test case involved an entire set of $\partial\Sigma_i/\partial T_M$ corresponding to particular conditions. The actual cases input to MEKIN were:

Case A (reference): All $\partial\Sigma_i/\partial T_M$ linearly approximated from cross section differences at 525° F and 2125° F,

Case B: all $\partial\Sigma_i/\partial T_M$ linearly approximated from cross section differences at 525° F and 1325° F,

Case C: all $\partial\Sigma_i/\partial T_M$ linearly approximated from cross section differences at 525° F and 3500 ° F

The input values are tabulated on Table 6.5.

For the extreme cases (i.e., B and C), peak power level differed by 27% while fuel temperature rise varied by 24% in the hot channel. Results are given on Table 6.6 and Fig. 6.6, and the temperature coefficient of reactivity calculation is described elsewhere in this section. As before, the power shapes were nearly identical.

Another view of the results is presented on Fig. 6.7, where peak power level is plotted against the temperature

TABLE 6.5.

FEEDBACK PARAMETERS VARIED AS A GROUP.

$(cm^{-1}/^{\circ}C)$

Feedback Parameter	(Reference) Case A (525 to 2125° F)	Case B (525 to 1325° F)	Case C (525 to 3500° F)
$\partial D_1^{-1}/\partial T_M$	0.331E-5	0.149E-5	0.388E-5
$\partial \Sigma_{c1}/\partial T_M$	0.616E-6	0.643E-6	0.559E-6
$\partial \Sigma_{f1}/\partial T_M$	0.407E-7	0.304E-7	0.425E-7
$\partial D_2^{-1}/\partial T_M$	0.134E-4	0.099E-4	0.143E-4
$\partial \Sigma_{c2}/\partial T_M$	0.614E-6	0.475E-6	0.633E-6
$\partial \Sigma_{f_{I\to 2}}/\partial T_M$	0.108E-5	0.0835E-5	0.111E-5
$\partial \Sigma_s/\partial T_M$	-0.353E-6	-0.371E-6	-0.317E-6

TABLE 6.6.

FEEDBACK PARAMETERS VARIED AS A GROUP - RESULTS.

Case[1]	Peak Power (MW)	ΔT_M (3) (°F)	$\partial\rho/\partial T_M$ (4) (/°F)
A: 525 - 2125° F (Reference)	2287.5	663.7	- 1.23E-5
B: 525 - 1325° F (% variation)[2]	2027.4 (-11.4)	601.5 (-9.4)	- 1.39E-5 (13.0)
C: 525 - 3500° F (% variation)[2]	2656.4 (16.1)	750.6 (13.1)	- 1.06E-5 (-13.8)

[1] Feedback parameters listed on Table 6.5

[2] $\%\ \text{Variation} = \frac{\text{Case Value - Reference Value}}{\text{Reference Value}} \times 100$

[3] Metal temperature rise in hot channel from 0.0 seconds to 0.05 seconds.

[4] Temperature coefficient of reactivity; calculated from steady state runs.

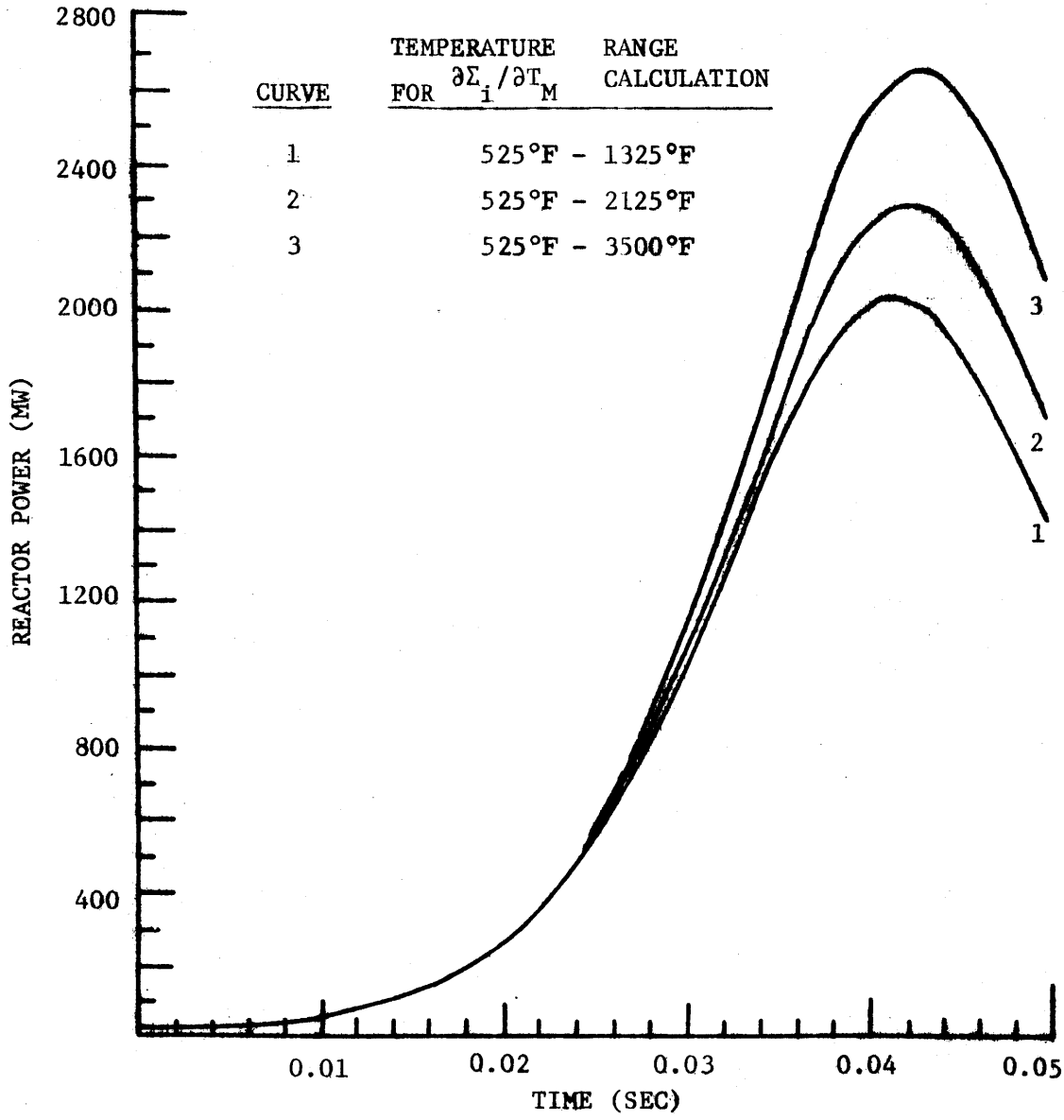

FIG. 6.6: METAL FEEDBACK SENSITIVITY: ALL LINEAR PARAMETERS.

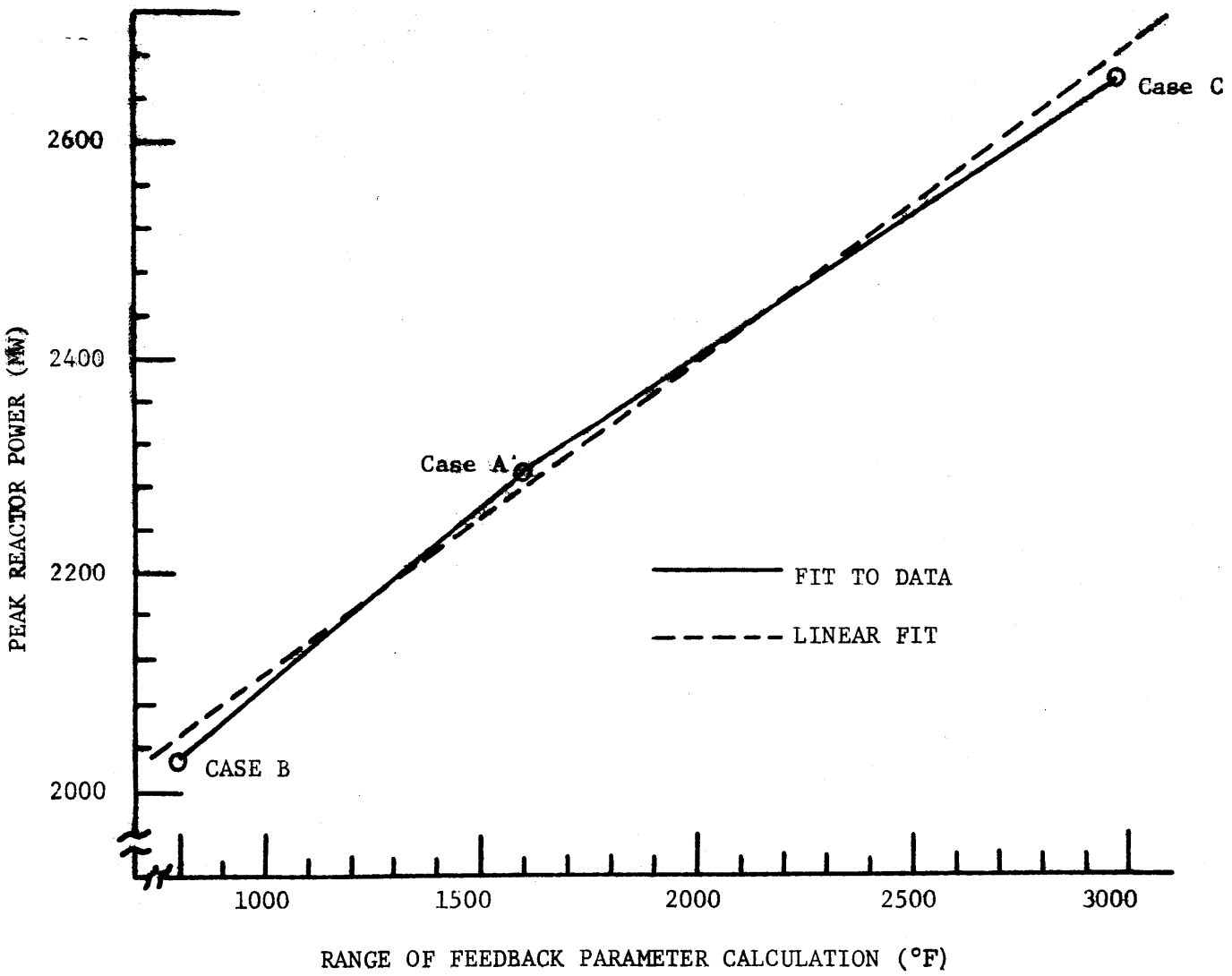

FIG. 6.7: PEAK POWER VS. TEMPERATURE RANGE OF FEEDBACK PARAMETER CALCULATION.

range over which the feedback parameters were evaluated. The curve is close to being linear. Numerically, this graph infers that an 800° F difference in the range of feedback parameter calculation will result in a relative error of 10% in peak powers.

Only results pertaining to linear cross section changes have been discussed thus far. The next step involved representing the cross section-temperature behavior by higher order polynomials, specifically a fourth-order curve and a quadratic.

As displayed by Eq. (6.1), cross sections are currently updated in MEKIN by

$$\Sigma_i(T_M) = \Sigma_i^* + C_3 \, (T_M - T_M^*), \qquad (6.6)$$

where $C_3 = {}^{\partial \Sigma_i}/_{\partial T_M}$. e_c and T_c dependence has been dropped because all test cases in this section have C_1 and C_2 of Eq. (6.1) set to zero. Quadratic and fourth-order approximations require calculations of the form:

$$\Sigma_i(T_M) = \Sigma_i^* + C_3 \, (T_M - T_M^*) + C_3' \, (T_M - T_M^*)^2 \qquad (6.7)$$

and

$$\begin{aligned} \Sigma_i(T_M) = \Sigma_i^* &+ C_3 \, (T_M - T_M^*) \\ &+ C_3' \, (T_M - T_M^*)^2 \\ &+ C_3'' \, (T_M - T_M^*)^3 \\ &+ C_3''' \, (T_M - T_M^*)^4, \end{aligned} \qquad (6.8)$$

where C_3', C_3'', and C_3''' are the coefficients of higher order terms. Attention was restricted to the group one capture cross section. The five data points in Fig. 6.1 were fit to quadratic

and fourth order curves, where each of the five points was weighted equally. The fits are plotted and the corresponding coefficients are listed on Figs. 6.8 and 6.9. Note that the zero order coefficients are slightly different from the reference cross section because the fits were not exact.

In order to implement these equations in the MEKIN code, a temporary modification of SUBROUTINE CROSU1 was necessary. Appendix E gives the programming details.

When comparing the results of the quadratic fit to the fourth order fit, peak powers differed by 6% and the fuel temperature rises in the hot assembly disagreed by 5%. Power vs. time is plotted on Fig. 6.10 for both cases, and further details are given in Table 6.7. As expected, these curves fall between the upper and lower power peaks from the linear approximations of $\partial \Sigma_{c1} / T_M$ shown on Fig. 6.2.

These results must be interpreted carefully. For one thing, they indicate that the solution is sensitive to the order of the polynomial fit. However, the peak power differences were far less when comparing the quadratic to the fourth-order results (6%) than when comparing the extreme linear approximations (34%). In all fairness to the linear cases, a feedback parameter would be chosen between the extremes, and when input to MEKIN, deviation from the exact answer would be less than 34%. Unfortunately, this data deals with only one feedback parameter. Further qualitative conclusions may be unwarranted.

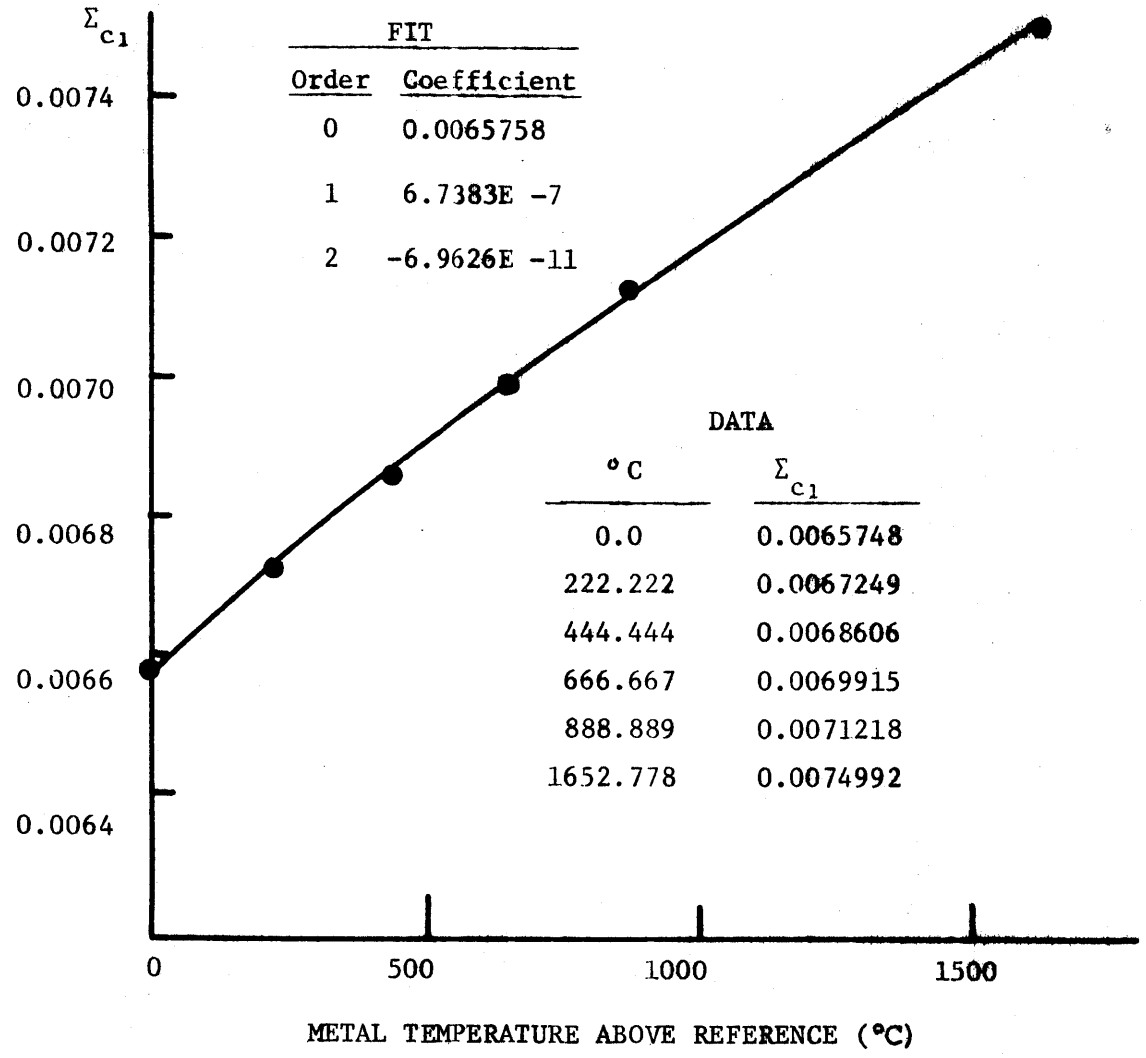

FIG. 6.8: QUADRATIC FIT TO Σ_{c_1} DATA.

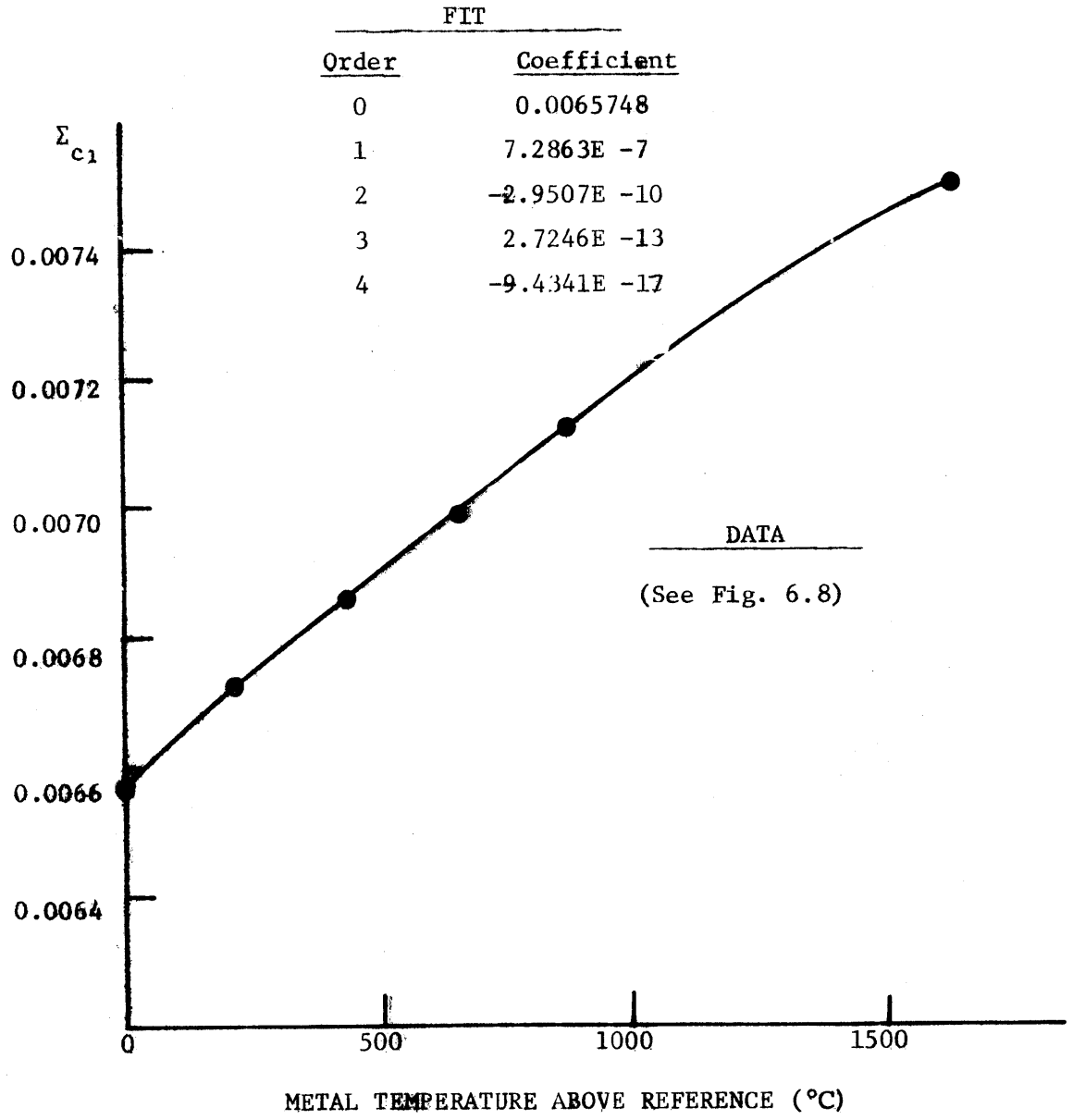

FIG. 6.9: FOURTH - ORDER FIT TO Σ_{c1} DATA.

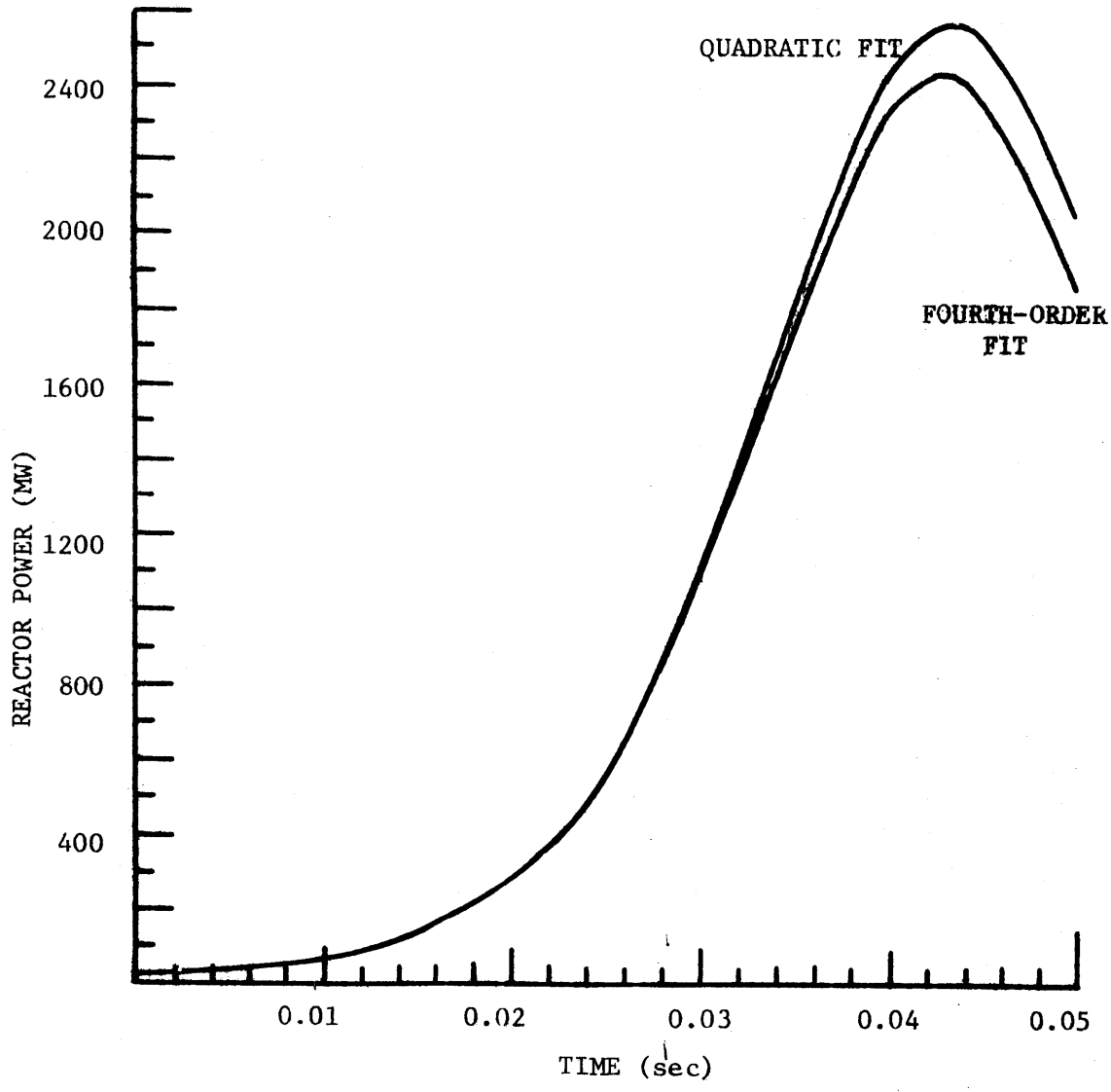

FIG. 6.10: METAL FEEDBACK SENSITIVITY: QUADRATIC AND FOURTH-ORDER FITS.

TABLE 6.7.

NON-LINEAR FEEDBACK - RESULTS.

Case	Peak Power (MW)	ΔT_M (2) (°F)
Fourth-order polynomial	2425.7	697.9
Quadratic	2568.5	730.5
(% variation')	(5.9)	(4.7)

[1] % variation = $\frac{\text{Quadratic Value - Fourth-Order Value}}{\text{Fourth-Order Value}}$ x 100

[2] Metal temperature rise in hot channel from 0.0 seconds to 0.05 seconds.

6.3 COOLANT FEEDBACK SENSITIVITY

Up to this point, the feedback parameter study has only dealt with those parameters associated with fuel temperature. The sensitivity of the coolant cross section feedback parameter (i.e., the $\partial\Sigma_i/\partial T_c$, $\partial\Sigma_i/\partial e_c$) is addressed here.

In order to observe significant feedback in the coolant, a slow reactivitiy insertion rate is necessary; otherwise, doppler feedback in the fuel will stop the power rise before the coolant is adequately effected. For this reason, a very slow rod withdrawal was used. (9 $^{cm}/_{sec}$, a rod worth double the delayed neutron fraction). The reactor was Model 7 of Appendix B. Coolant density changes the most rapidly in the two-phase state, so boiling was induced by the input of a high coolant inlet temperature.

In developing a test transient, a neutronics-only calculation was the initial step. As shown on Fig. 6.11, the neutronics-only power-time behavior is well behaved with tight time steps at the start and coarse time steps as the transient evolves. However, when this set of time steps was used for the same model with thermal-hydraulic feedback, the results were unacceptable (Compare Figs. 6.11 and 6.12; the only difference between the two cases is the time step size, yet the solutions differ greatly). Even with a significant tightening of the time step size, non-physical power-time oscillations remain. Furthermore, these oscillations are

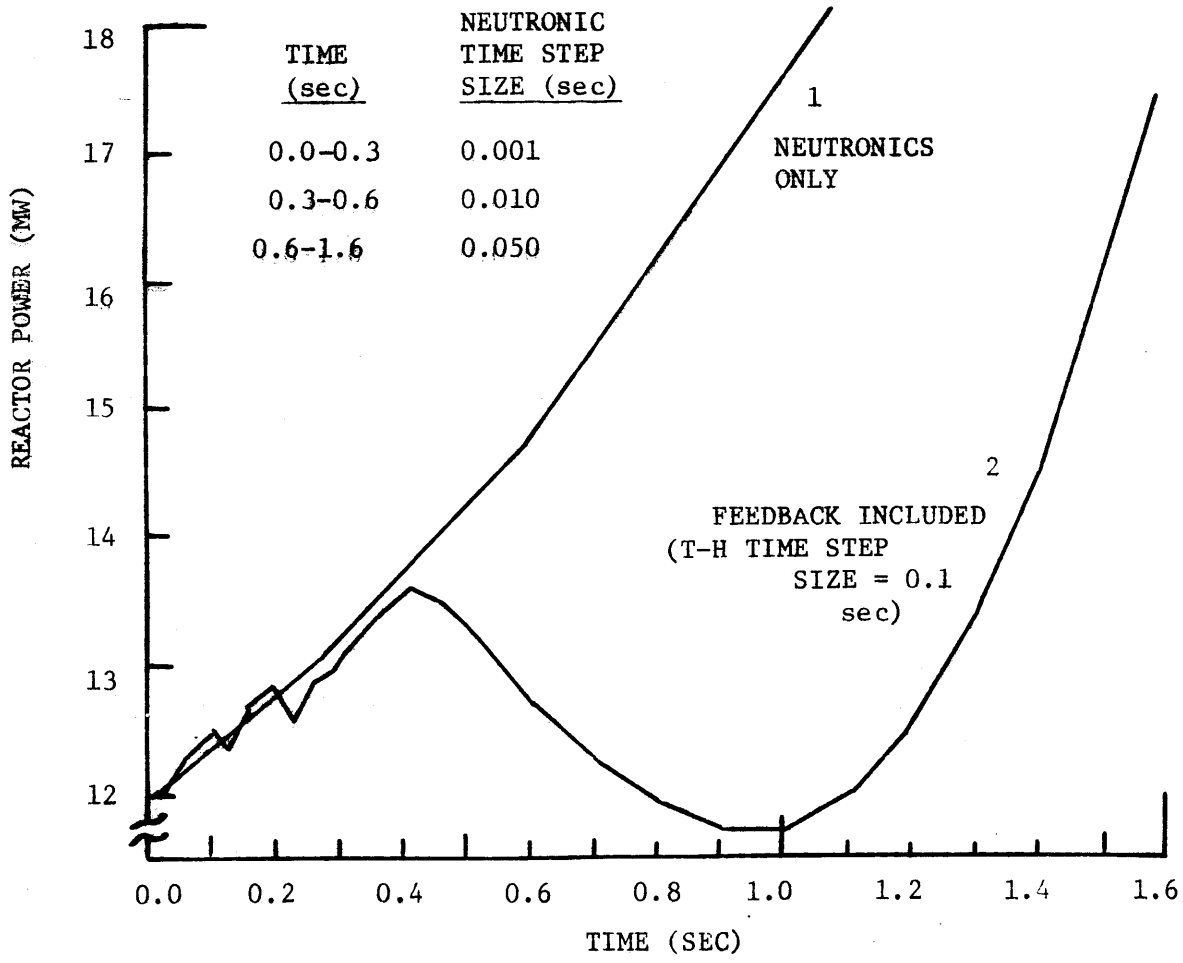

FIG. 6.11. EFFECT OF COARSE TIME STEPS.

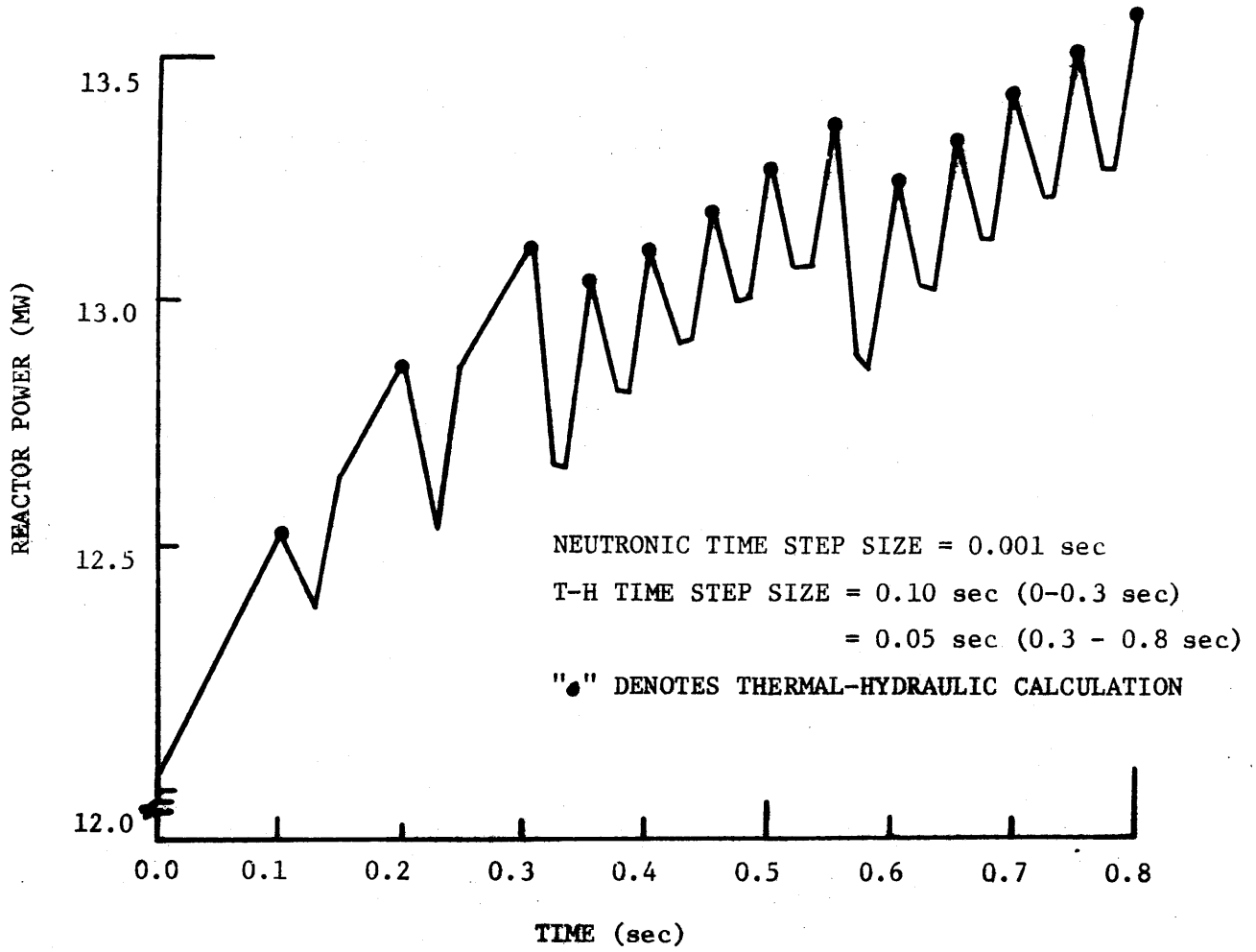

FIG. 6.12: EFFECT OF DECREASING THE NEUTRONIC TIME STEP SIZE.

not dampened as the transient evolves (see Fig. 6.12). The "dips" in the curve can be explained by the interfacing of the neutronics with the thermal hydraulics. Note how each dip involves several neutronic calculations, but only one thermal hydraulic time step. Because the cross sections are updated only after thermal-hydraulic calculations, large thermal-hydraulic time steps lead to large step-insertions of reactivity. (In calculating temperature changes and energy deposition, COBRA extrapolates the current power back to the previous thermal-hydraulic calculation.) These reactivity insertions cause problems for the intermediate neutronics calculations. Such perturbations instantaneously change the reactor period, while the neutronics solution technique (NSADE method) predicts a constant period. The resulting curve is shown on Fig. 6.12.

In an attempt to achieve a more reasonable power-time behavior, a thermal hydraulic calculation was performed with every neutronic calculation. Results show an improved, yet still suspicious, curve (see Fig. 6.13). Note how both feedback curves initially start above the neutronics-only curve. This should be expected because the steady state power distributions differ. For this reason, the control rod is being withdrawn from a relatively more important region in the feedback cases. A disturbing feature is the lack of agreement between the two feedback curves up to .1 sec. The suspected

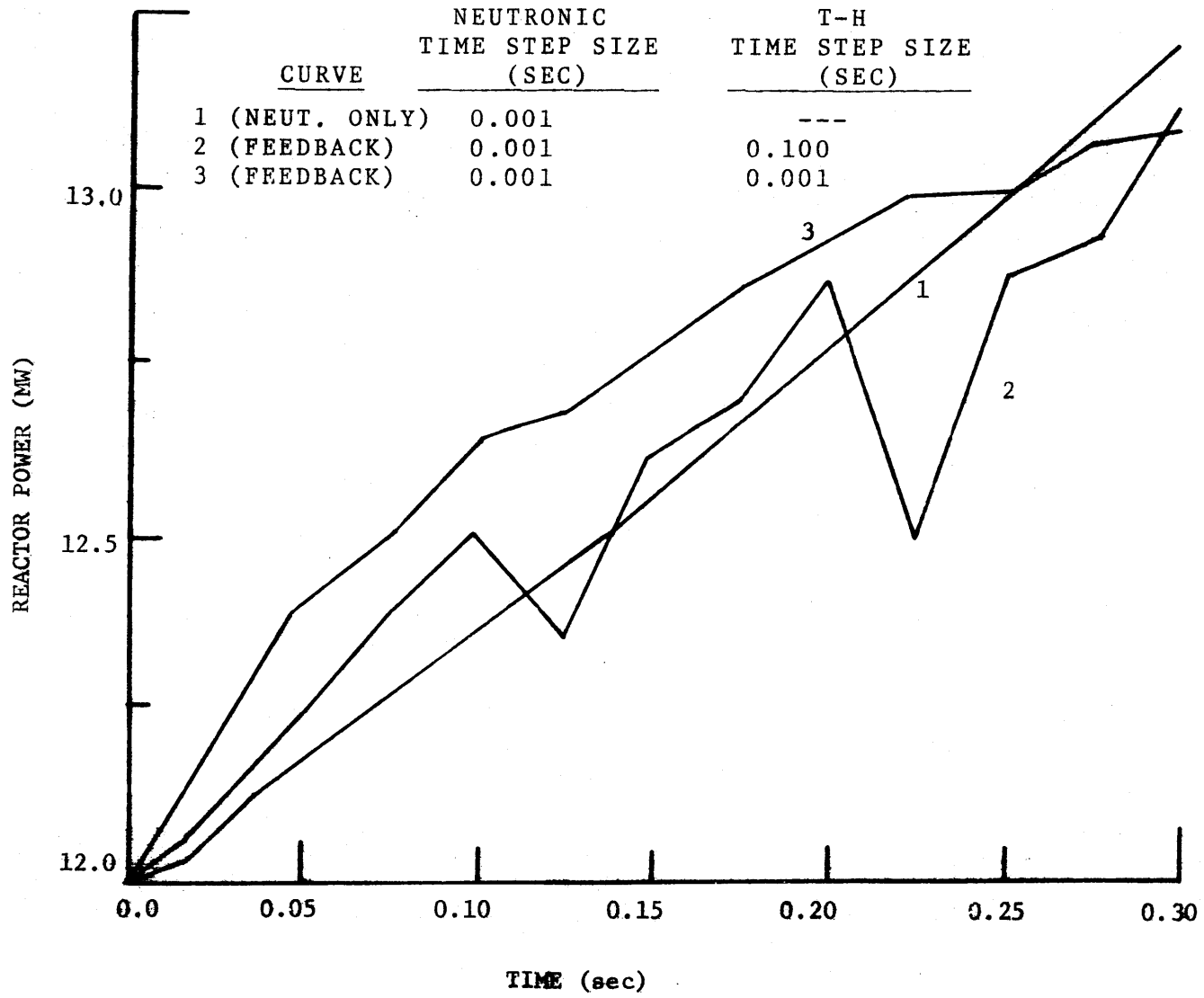

FIG. 6.13: EFFECT OF DECREASING THE THERMAL-HYDRAULIC TIME STEP SIZE.

problem involves the convergence of the COBRA solution. Concerning the interval from 0 - 0.3 sec, note the agreement in reactor power at 0.3 seconds for the two feedback cases. However, the power-time curves do not tell the whole story as energy deposition, indicated by fuel temperature rise, differs by almost 25% (see Table 6.8). Efforts using this transient were halted here because expenses become prohibitive for such small thermal-hydraulic time steps. Keep in mind that the original purpose of this transient involved a feedback parameter sensitivity, and for meaningful results, well behaved power-time behavior is essential.

As an alternative approach to investigating the sensitivity of the coolant feedback parameters, a series of steady state calculations was performed. Model 7 of Appendix B served as the reactor. The coolant inlet temperature was chosen close to saturation to permit significant boiling. The variable parameters were the $\partial\Sigma_i/\partial\rho_c$ and all input values were based on a pressurized water reactor assembly with a burnup of 11,481 MWD/MT and an initial enrichment of 2.73% U-235. The fuel feedback parameters were identical in all calculations. The $\partial\Sigma_i/\partial T_c$ were set to zero because these inputs have no effect in boiling conditions.

Previous work (see Section 6.1) indicated that the scattering feedback parameter ($\partial\Sigma_s^{1\to2}/\partial\rho_c$) should be expected to have a larger effect on the solution that the other coolant feedback terms. For this reason, the initial cost of runs

TABLE 6.8.

SOLUTION BEHAVIOR OF A SLOW TRANSIENT WITH FEEDBACK.

	Δt_N[2]=.001 sec Δt_{t-H}[3]=.001 sec	Δt_N[2]=.001 sec Δt_{T-H}[3]=.1 sec
Power at 0 seconds (MW)	12.0000	12.0000
Power at .3 seconds (MW)	13.0952	13.1156
Average period (sec)	3.4349	3.3748
% difference[4] of period	--	-1.75
$\bar{T}$ at 0 seconds' (°F)	1922.88	1922.88
$\bar{T}$ at .3 seconds' (°F)	1926.70	1927.65
$\bar{T}'$ (°F)	3.82	4.77
% difference[4] of $\bar{T}'$	--	24.90

[1]Average fuel temperature in hottest region

[2]Neutronic time step size

[3]Thermal-hydraulic time step size

[4]$\frac{\text{Column 2 value - Column 1 value}}{\text{Column 1 value}} \times 100$

involved varying only $\partial \Sigma_s^{1\to 2} / \partial e_c$. This process was repeated for several different levels of boiling. (The level of boiling was altered by varying the coolant flow rate.) This combination of computer runs yielded the curves of K-effective vs. outlet coolant density shown on Figs. 6.14. The average slopes of these lines estimate density coefficients of reactivity as a function of $\partial \Sigma_s^{1\to 2} / \partial e_c$. The coefficients vary by as much as 14% (see Table 6.9), indicating a noticeable sensitivity.

The next set of calculations consisted of varying the coolant feedback parameters as a group. To accomplish this task, three groups of coolant feedback terms were calculated over three different density ranges. Using the procedure described in the previous paragraph, the temperature coefficients of reactivity varied by as much as 32%. See Fig. 6.15 and Table 6.10.

Thus, when coolant density exhibits the dominant reactivity feedback effect, the solution is sensitive to the linear approximation of cross section-coolant density behavior.

6.4 USER APPLICATIONS OF THE FEEDBACK PARAMETER SENSITIVITY

When selecting a set of cross section feedback parameters for input to the MEKIN code, the user faces two problems not encountered when choosing a neutronic mesh size and a neutronic time step size. First, in an initial calculation there is no sure way of avoiding error due to the feedback parameters while uncertainty in the neutronic finite difference

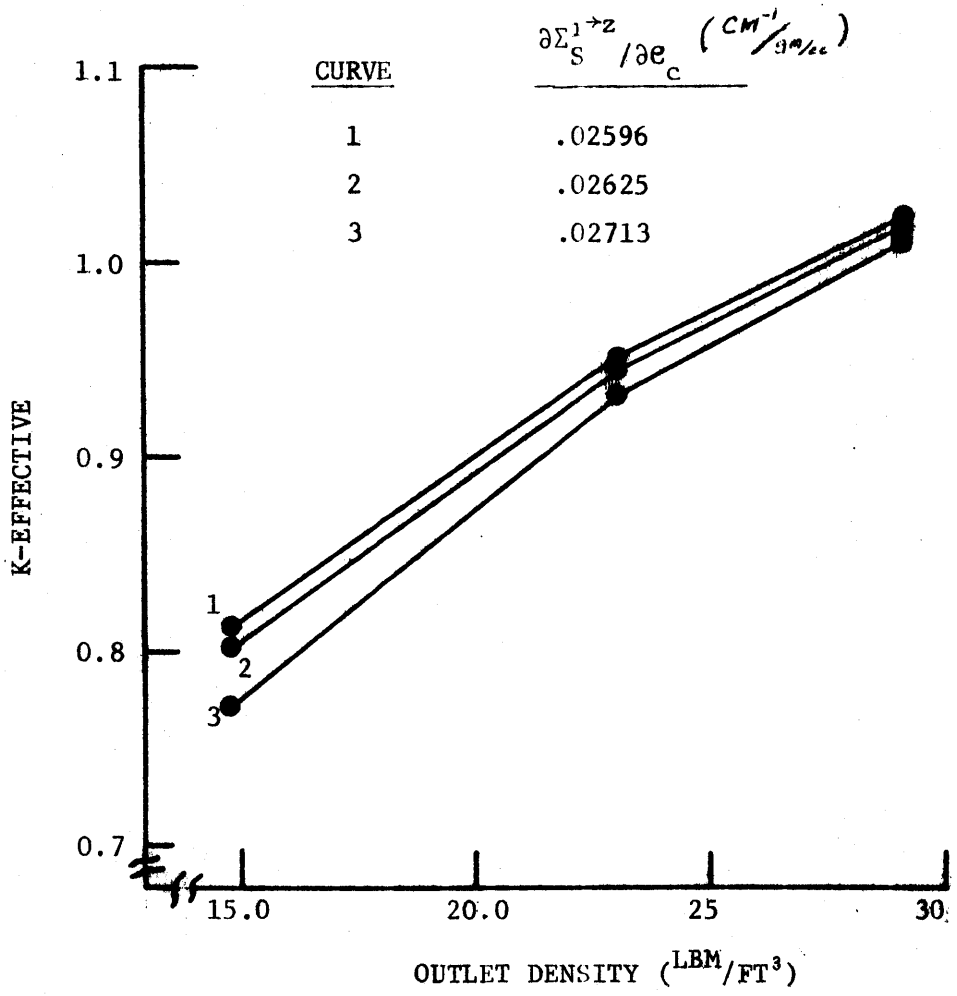

FIG. 6.14: COOLANT FEEDBACK SENSITIVITY: $\partial\Sigma_S^{1\to2}/\partial e_c$ VARIED.

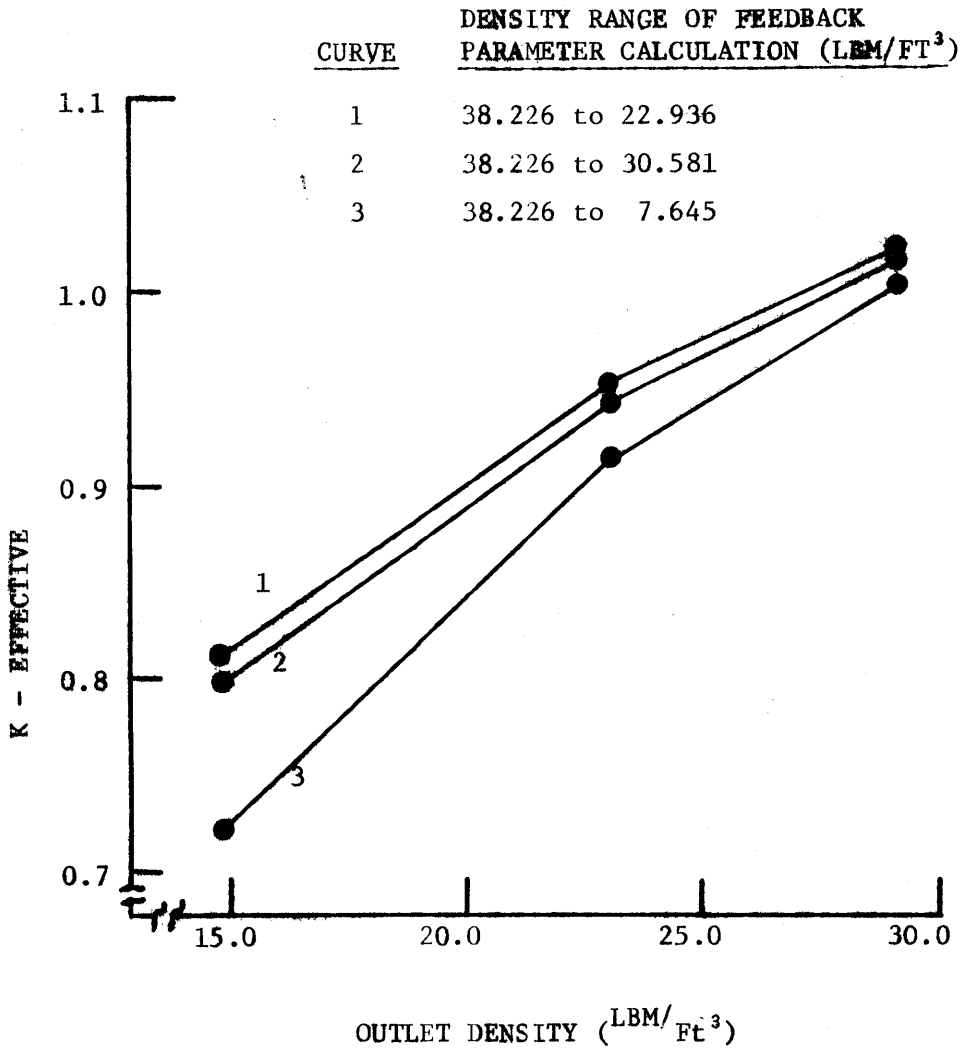

FIG. 6.15: COOLANT FEEDBACK SENSITVITY: ALL PARAMETERS VARIED.

TABLE 6.9.

DENSITY COEFFICIENT OF REACTIVITY AS A FUNCTION OF $\partial\Sigma_s^{1\to2}/\partial e_c$.

$\partial\Sigma_s^{1\to2}/\partial e_c$	$\Delta K/\Delta e_c$ (LBM/FT^3)	% Difference from Reference
.02596 (reference)	.01478	--
.02625	.01526	3.25
.02713	.01685	14.01

TABLE 6.10.

DENSITY COEFFICIENT OF REACTIVITY AS A FUNCTION OF THE SET OF COOLANT FEEDBACK PARAMETERS.

Density Range of Feedback Parameter Calculation (LBM/FT^3)	$\Delta K/\Delta e_c$ (LBM/FT^3)	% Difference from Reference
38.226 to 22.936 (reference)	.01478	--
38.226 to 30.581	.01531	3.59
38.226 to 7.645	.01963	32.81

calculations can always be eliminated by choosing a tight enough spatial mesh and time step. Second, generating a set of feedback parameters requires calculations prior to using MEKIN.

As a first approximation for accurate answers, the linear feedback parameters can be calculated over the same reactor averaged temperature rise that the transient actually follows. The problem with this criteria is that the user must know the answer before it is computed. As a partial solution to this problem, Fig. 6.7 suggests two transient calculations and linear interpolation. Unfortunately, this procedure still does not promise the best solution because non-linear temperature cross section behavior is approximated by linear functions. If all feedback parameters in the reactor are identical, feedback can be represented by higher oder polynomials as outlined in Appendix E.

The user must do some background work before a set of cross section feedback parameters is ready for input to MEKIN. Appendix D provides the use of the LEOPARD code as an example. As mentioned in Section 6.1 the feedback parameters are dependent on material compositions as well as temperature. For example, past studies involving the MEKIN code have used parameters significantly different from those employed in this project (see Table 6.11). Properties such as burnup and initial enrichment must be adequately considered while preparing input for a code like LEOPARD. Under no

circumstances should the MEKIN user blindly extract feedback parameters from a previous study.

Table 6.11 illustrates extreme cases, but smaller differences in burnup and initial enrichment also cause noticeable changes in the feedback parameters. Table 6.12 gives an indication of the relative importance of temperature range, burnup, and initial enrichment. Each case involved holding two of these variables identical with the reference while the third was varied as shown. Although temperature range appears to have the most sensitivity, the others should not be ignored.

6.5 IMPLICATIONS OF THE FEEDBACK PARAMETER SENSITIVITY

The results presented in this chapter pose several implications. First, reactor power level and thermal-hydraulic energy deposition are both sensitive to the linear cross section feedback parameters. Second, these inputs have no mechanism to guarantee accuracy (within 10%). This situation is different in the previous two chapters, where decreasing the neutronic spatial mesh interval and tightening the time step size cause convergence to better answers. Third, representation of the cross section-temperature behavior by higher order polynomials (i.e., quadratic, cubic, etc.) is one means for improvement. However, such a modification does not remove importance from the preliminary calculations used to generate the feedback parameters.

Data storage is a potential drawback in the event of

TABLE 6.11.

FEEDBACK PARAMETER COMPARISON,

$(cm^{-1}/^{\circ}C)$

Feedback Parameter	Case A[1]	Case B[2]	Case C[3]
$\partial D_1^{-1}/\partial T_M$	+0.331E-5	-0.660E-5	-0.880E-5
$\partial \Sigma_{c1}/\partial T_M$	+0.616E-6	+0.330E-6	+0.143E-6
$\partial \Sigma_{f1}/\partial T_M$	+0.407E-7	-0.570E-7	-0.230E-7
$\partial D_2^{-1}/\partial T_M$	+0.134E-4	-0.260E-5	-0.153E-5
$\partial \Sigma_{c2}/\partial T_M$	+0.614E-6	-0.380E-6	-0.131E-6
$\partial \Sigma_{f2}/\partial T_M$	+0.108E-5	-0.100E-5	-0.277E-6
$\partial \Sigma_s^{1\to 2}/\partial T_M$	-0.353E-6	-0.850E-7	-0.130E-6

[1]This project, PWR assembly, 6000 MWD/MT of burnup.

[2]Ref. 20, PWR assembly, no burnup.

[3]Ref. 21, BWR assembly, no burnup.

TABLE 6.12.

EFFECT OF BURNUP, INITIAL ENRICHMENT, ON TEMPERATURE RANGE ON FEEDBACK PARAMETERS.

$(cm^{-1}/{}^{\circ}C)$

Feedback Parameter	Reference Value	% Difference from Reference[4]		
		Temperature[1] Range Varied	Burnup[2] Varied	Enrichment[3] Varied
$\partial D1^{-1}/\partial T_M$	0.331E-5	55.0	1.5	4.0
$\partial \Sigma c1/\partial T_M$	0.616E-6	4.4	7.8	1.2
$\partial \Sigma f1/\partial T_M$	0.407E-7	25.3	4.4	7.9
$\partial D2^{-1}/\partial T_M$	0.134E-4	26.1	1.5	6.0
$\partial \Sigma c2/\partial T_M$	0.614E-6	22.6	7.3	5.5
$\partial \Sigma f2/\partial T_M$	0.108E-5	22.2	0.0	11.1
$\partial \Sigma_s^{1\to 2}/\partial T_M$	-0.353E-6	5.1	7.4	.8

[1]Reference temperature range = 525° F - 2125° F, varied to 525° F - 1325° F.

[2]Reference burnup = 6000 MWD/MT, varied to 11,481 MWD/MT.

[3]Reference initial enrichment - 2.73% U-235, varied to 3.03% U-235.

[4]% difference = $\left| \frac{\text{Case Parameter} - \text{Reference Parameter}}{\text{Reference Feedback Parameter}} \right| \times 100$

of implementing an alternate means of representing cross section-temperature behavior in the MEKIN code. This is particularly true for problems involving many sets of material compositions (i.e., the N8 input cards) because a complete set of feedback parameters is required for every composition. Consequently, difficulties might arise for a modification such as a fourth order polynomial equation for all cross sections with respect to all three thermal properties. On a more positive note, several options exist where additional storage requirements are negligible. For example, a quadratic, or possibly a higher order polynomial, could replace the linear approximation for only the most important feedback parameters (i.e., $\partial\Sigma c_1/\partial T_m$, $\partial\Sigma f_2/\partial T_m$, $\partial\Sigma s^{1\rightarrow 2}/\partial e_c$). In any case, the results of this project appear to encourage further investigation of methods to replace the linear cross section feedback representation.

CHAPTER 7

CONCLUSIONS AND RECOMMENDATIONS

Based on the results of the three preceding chapters, the solution generated by the MEKIN code is rather sensitive to neutronic spatial mesh size, neutronic time step size, and the linear cross section feedback parameters. The user may encounter problems if these sensitivities are not properly considered.

As theory predicts, the neutronic finite difference solution is most sensitive to mesh size for problems which are spatially long and which contain significant region to region material discontinuities. Fortunately, for these extreme cases, the steady state power distribution converges to better answers in a somewhat linear manner as the mesh size is decreased. However, large problems which demand a high degree of accuracy may be prohibitively expensive. For time dependent calculations, errors induced by mesh size grow as the transient evolves. The main reason for this growth appears to be the sensitivity of rod worth to mesh size.

Neutronic time step size was found to be dependent on the rate of change of the frequency ($\frac{d\omega}{dt}$) as well as the frequency (ω) itself. In fact, much smaller time steps were needed than originally anticipated when the power-time behavior deviated from an exponential. This makes the NSADE method less attractive from an economic point of view. Fortunately, the solution converged to better answers as the time step was tightened. An automatic time step selector would help avoid such problems

as non-physical oscillations, but the requirement for extremely small time steps would remain. If the NSADE method is to be modified, the frequency transform may be the place to start.

Power level and energy deposition were both found to be very sensitive to the linear approximation of cross-section temperature feedback. This was true when the parameters were varied individually and as a group. Perhaps more interesting than the exact level of sensitivity is the fact that the linear feedback approximation cannot be depended upon, apriori, to give highly accurate answers (i.e., within 10%). Representing the cross section-temperature behavior by a higher order polynomial appears to reduce the uncertainty. This conclusion encourages future efforts to improve the method by which cross sections are updated with temperature and density. Regardless of the coupling of temperature to cross sections in MEKIN, the feedback parameters, and therefore the solution, are also sensitive to the preliminary calculations.

If economy must be tied with accuracy in MEKIN calculations, additional studies should involve modifications or new methods for solving the steady state and transient neutron diffusion equations. At the same time, the reader and future researchers should never forget that this project has only investigated several aspects of the MEKIN code. Thus, when striving for an accurate answer through a MEKIN calculation, the entire code must be considered.

On a more positive note, the results presented here quantify errors and bracket uncertainties with respect to several important input parameters. Consequently, this work can provide a users' guide for selecting neutronic spatial mesh intervals, choosing time step sizes, and determining the cross section feedback parameters.

REFERENCES

1. Barry, R. F., "LEOPARD - A Spectrum Dependent Non-Spatial Depletion Code for the IBM-7094," WCAP-3269-26, Westinghouse Electric Co. (1963).

2. Bowring, R. W., J. W. Stewart, R. A. Shober, and R. N. Sims, "MEKIN: MIT-EPRI Nuclear Reactor Core Kinetics Code," Research Project 227, Computer Code Manual, Massachusetts Institute of Technology (1975).

3. Breen, R. J., "A One-Group Model for Thermal Activation Calculations," Nucl. Sci. Eng. 9, 91 (1961).

4. Cadwell, W. R., "PDQ-7 Reference Manual," WAPD-TM-678, Bettis Atomic Power Laboratory (1967).

5. Clark, M., and K. F. Hansen, Numerical Methods of Reactor Analysis. New York: Academic Press, 1964.

6. Fergusen, D. R., and K. F. Hansen, "Solution of the Space-Dependent Reactor Kinetics Equations in Three-Dimensions," Ph.D. Thesis, Department of Nuclear Engineering, Massachusetts Institute of Technology, MIT-3903-4, MITNE-132 (1971).

7. Fowler, T. B., D. R. Vondy, and G. W. Cunningham, "Nuclear Reactor Core Analysis Code: CITATION," ORNL-TM-2496, Oak Ridge National Laboratory (1971).

8. Greenspan, H., C. N. Kelber, D. Okrent, Computational Methods in Reactor Physics. New York: Gorden and Breach, 1969.

9. Henry, A. F., Nuclear-Reactor Analysis, Cambridge, Mass.: MIT Press, 1975.

10. Kalambokas, P. C., and A. F. Henry, "Replacement of Reflectors by Albedo Type Boundary Conditions," Ph.D. Thesis, Department of Nuclear Engineering, Massachusetts Institute of Technology (1975).

11. Kast, S. J., and K. F. Hansen, "Solution of the Reactor Kinetics Equations in Two Dimensions by Finite Difference Methods," S. M. Thesis, Department of Nuclear Engineering, Massachusetts Institute of Technology (1970).

12. Lamarsh, J. R., Introduction to Nuclear Reactor Theory. Reading, Mass.: Addison-Wesley Publishing Company (1966).

13. Reed, W. H., and K. F. Hansen, "Finite Difference Techniques for the Solution of the Reactor Kinetics Equations," Sc.D. Thesis, Department of Nuclear Engineering, Massachusetts Institute of Technology, MITNE-100 (1966).

14. Rowe, D. S., "Cobra IIIC: A Digital Computer Program for Steady State and Transient Thermal-Hydraulic Analysis of Rod Bundle Nuclear Fuel Elements," BNWL-1695 (1973).

15. Science Applications, Inc., "Dynamic Analysis of Scrammed Power Reactors Interim Informal Report," SAI/SR-147-PA (1976).

16. Shober, R. A., and A. F. Henry, "Nonlinear Methods for Solving the Diffusion Equation," Ph.D. Thesis, Department of Nuclear Engineering, Massachusetts Institute of Technology (1976).

17. Sims, R. N., and A. F. Henry, "A Coarse-Mesh Nodal Diffusion Method Based on Response Matrix Considerations," Department of Nuclear Engineering, Massachusetts Institute of Technology (1977).

18. Solan, G. M., "Neutronic Analysis of a Proposed Plutonium Recycle Assembly," Nucl. Eng. Thesis, Department of Nuclear Engineering, Massachusetts Institute of Technology, MITNE-175 (1975).

19. Stewart, J. W., and K. F. Hansen, "Finite Difference Equations for the MEKIN Code," MEKIN, Program Development Notes, Massachusetts Institute of Technology (1975).

20. Stewart, J. W., "Linear Correlations of Neutron Cross Sections with Thermal-Hydraulic State Variables for MEKIN Testing," MEKIN, Program Development Notes, Massachusetts Institute of Technology (1975).

21. Valente, J. U. and K. F. Hansen, "Multidimensional Modeling of the Rod Drop Accident," Nucl. Eng. Thesis, Department of Nuclear Engineering, Massachusetts Institute of Technology (1975).

APPENDIX A

SPECIAL EXAMPLES INVOLVING INPUT PREPARATION

A.1 THE USE OF MIXED NUMBER DENSITY CROSS SECTIONS IN MEKIN

As a data base for test problems, mixed number density (MND) data was provided for the thermal spectrum. A discussion of mixed number density theory and its application to test problems is presented in the following paragraphs.

Flux and current continuity are the conventional boundary conditions when using regionwise thermal constants in the standard diffusion equation. For one group,

$$-\nabla\cdot\bar{D}\nabla\bar{\phi} + \bar{\Sigma}_a\bar{\phi} = S. \qquad (A.1)$$

The unknown variable is $\bar{\phi}$ (region averaged flux), while $\bar{D}$ (average diffusion coefficient) and $\bar{\Sigma}_a$ (average absorption cross section) are user inputs. S is a constant source term. Usually, $\bar{D}$ and $\bar{\Sigma}_a$ are averaged over the Wigner-Wilkens spectrum. Such an approach leads to discontinuity of activation ($\sigma\phi$) at boundaries because microscopic cross sections are different in each region. As a result, thermal flux peaking near water gaps may be underestimated.(3)

For a $\frac{1}{v}$ absorber, continuity of activation implies continuity of number density:

$$\sigma(E)\phi(E)dE \simeq \int\frac{1}{V(E)}\phi(E)dE = \int N(E)\bar{dE} = \bar{N}, \qquad (A.2)$$

where $\sigma(E)$ = energy dependent cross section,

$\phi(E)$ = energy dependent neutron flux,

$V(E)$ = energy dependent neutron velocity,

$N(E)$ = energy dependent neutron density.

Thus, the standard diffusion equation (A.1) may be rewritten in

one group as:

$$-\nabla\cdot\overline{DV}\,\nabla\,\overline{N} + \overline{\Sigma_a V}\,\overline{N} = S. \tag{A.3}$$

Required inputs become:

$$\overline{DV} = \frac{\int_\varepsilon D(E)\ \nabla\ \phi(r,E)\ dE}{\int_\varepsilon \frac{1}{V(E)}\ \nabla\ \phi(r,E)\ dE} = \frac{\overline{D}}{(\frac{\overline{1}}{V})}$$

and

$$\overline{\Sigma_a V} = \frac{\int_\varepsilon \Sigma_a(E)\ \phi(r,E)\ dE}{\int_\varepsilon \frac{1}{V(E)}\ \phi(r,E)\ dE} = \frac{\overline{\Sigma_a}}{(\frac{\overline{1}}{V})}. \tag{A.4}$$

Note that these terms need not be averaged over identical spectrums. Advanced codes (3) indicate that the leakage coefficients are most accurately obtained by averaging over the maxwellian model. Conversely, the absorption coefficients are best obtained by averaging over the Wigner-Wilkens spectrum. The difference can be attributed to the fact that leakage is tightly linked to neutrons in the water gap, where the spectrum is softer than in the fuel. With the above considerations, the diffusion equation can take the form:

$$-\frac{\overline{D}_{max}}{(\frac{\overline{1}}{V})_{max}}\nabla^2\overline{N} + \frac{\Sigma_{a_{WW}}}{(\frac{\overline{1}}{V})_{WW}}\overline{N} = S. \tag{A.5}$$

Such a form is the foundation for the MND section of LEOPARD. Since the maxwellian model represents a softer spectrum than the Wigner-Wilkens model, peaking near water channels no longer suffers a large underestimation. (3)

For the test problems of this project, flux weighted cross sections were generated with the use of LEOPARD and PDQ. LEOPARD

can be employed to compute and print both conventional and MND spectrum averaged cross sections. Then, spacial weighting of the constants can be done by running PDQ. However, in the particular data base for this project, only the MND constants are spatially weighted.

MEKIN was programmed to solve a semi-discrete form of the transient diffusion equation. For the thermal group: (only two terms are given in order to simplify the following explanation):

$$v^{-1} \frac{\partial}{dt} \phi_{ijK} = - \Sigma_R \phi_{ijK} + \text{etc.}, \qquad (A.6)$$

where ϕ_{ijK} = thermal flux at mesh point ijK,

v^{-1} = inverse of average thermal neutron velocity,

Σ_R = thermal removal cross section (cm^{-1}) of a homogeneous neutronic region ($\Sigma_c + \Sigma_f$)

ϕ_{ijk} is the unknown, while v^{-1} and Σ_R are user inputs. Σ_R can always have the conventional spectrum, spacial averaged form ($\overline{\Sigma}_a$ in Eq. (A.1)). MND data can be used only if Eq.(A.6) can be transformed into a mathematically equivalent equation with $\overline{N}_{ijK}$ as the unknown. Proper conditions exist only if $\frac{\partial \phi_{ijK}}{\partial t} = 0$ as in the static representation of Eq. (1.A). However, $\frac{\partial \phi ijK}{\partial t} \neq 0$ in a MEKIN transient.

The previous two paragraphs indicate a paradox: only MND constants will be spacially weighted by PDQ, but these constants can not be fed into a MEKIN transient analysis. Fortunately,

LEOPARD will print $(\frac{1}{v})_{max}$ and $(\frac{1}{v})_{ww}$, the average normalized inverse velocities for the maxwellian and Wigner-Wilkens distributions. MEKIN input can then be determined as follows: (Recall that in LEOPARD the leakage coefficient is averaged over the maxwellian spectrum and the absorption coefficients over the Wigner-Wilkens spectrum.).

[MND constant from PDQ] x [the appropriate $(\frac{1}{v})$] = [MEKIN input parameter],

$$\left.\begin{aligned}
&\frac{\bar{D}_{max}}{(\frac{\bar{1}}{v})_{max}} \times (\frac{\bar{1}}{v})_{max} = \bar{D}(cm), \\
&\left[\frac{\bar{\Sigma}_{a\ w.w.}}{(\frac{\bar{1}}{v})_{w.w.}} - \frac{\bar{\Sigma}_{f\ w.w.}}{(\frac{\bar{1}}{v})_{w.w.}}\right] \times (\frac{\bar{1}}{v})_{w.w.} = \bar{\Sigma}_{c}(cm^{-1}), \\
&\left[\frac{\bar{\Sigma}_{f\ w.w.}}{(\frac{\bar{1}}{v})_{w.w.}}\right] \times (\frac{\bar{1}}{v})_{w.w.} = \bar{\Sigma}_{f}\ (cm^{-1}).
\end{aligned}\right\} \quad (A.7)$$

$\bar{D}$, $\bar{\Sigma}_c$, and $\bar{\Sigma}_f$ can be the thermal group constants of a homogeneous neutronic region which are supplied to MEKIN.

A.2 REFLECTOR ALBEDOES IN MEKIN

Below is a brief explanation of the application of albedoes in MEKIN.

According to Volume 1, Part 1, p. 56 of the MEKIN manual:

$$\begin{aligned}
J_1(x)_I &= \alpha_{11}\,\phi_1(x)_I\ , \\
J_2(x)_I &= \alpha_{21}\,\phi_1(x)_I + \alpha_{22}\,\phi_2(x)_I\ ,
\end{aligned} \quad (A.8)$$

or, $$\underline{J} = \underline{\underline{\alpha}}\,\underline{\phi}\,, \tag{A.8}$$

where, ϕ_g = group flux at interface.

J_g = group current at interface,

α_{11} = group 1 albedo,

α_{22} = group 2 albedo,

α_{21} = transfer albedo (group 1 to group 2).

One method of calculating an appropriate set of albedoes it the procedure developed by P. Kalambokas (see Vol. 22, p. 597 of the MEKIN manual). The formulas involve only reflector constants such that:

$$\begin{aligned} \bar{\alpha}_{11} &= f_1(\text{reflector constants}), \\ \bar{\alpha}_{22} &= f_2(\text{reflector constants}), \\ \bar{\alpha}_{21} &= f_3(\text{reflector constants}), \end{aligned} \tag{A.10}$$

where Kalambokas defines:

$$\begin{aligned} \phi_1 &= \bar{\alpha}_{11} J_1\,, \\ \phi_2 &= \bar{\alpha}_{21} J_1 + \alpha_{22} J_2\,, \end{aligned} \tag{A.11}$$

or, $$\underline{\Phi} = \underline{\underline{\bar{\alpha}}}\,\underline{J}\,. \tag{A.12}$$

To convert these albedoes to the form necessary for MEKIN input, note that:

$$\begin{aligned} \underline{\phi} &= \underline{\underline{\bar{\alpha}}}\,\underline{J}\,, \\ \underline{J} &= \underline{\underline{\bar{\alpha}}}^{-1}\,\underline{\phi}\,. \end{aligned} \tag{A.13}$$

From Eqs. (A.9) and (A.13),

$$\underline{\underline{\bar{\alpha}}}^{-1} = \underline{\underline{\alpha}}\,, \tag{A.14}$$

$$\bar{\bar{\alpha}}^{-1} = \frac{\text{adjoint } \bar{\bar{\alpha}}}{\det. \bar{\bar{\alpha}}}$$

$$= \frac{\text{adj.}\begin{bmatrix} \bar{\alpha}_{11} & 0 \\ \alpha_{21} & \alpha_{22} \end{bmatrix}}{\det.\begin{bmatrix} \bar{\alpha}_{11} & 0 \\ \alpha_{21} & \alpha_{22} \end{bmatrix}}$$

$$= \frac{\begin{bmatrix} \bar{\alpha}_{22} & 0 \\ -\alpha_{21} & \alpha_{11} \end{bmatrix}}{\frac{1}{\bar{\alpha}_{11}\,\bar{\alpha}_{22}}} .$$

Thus, the elements of $(\bar{\bar{\alpha}})^{-1}$ relate to those of $\bar{\bar{\alpha}}$ such that:

$$\alpha_{11} = \frac{1}{\bar{\alpha}_{11}} ,$$

$$\alpha_{22} = \frac{1}{\bar{\alpha}_{22}} , \qquad \text{(A.15)}$$

$$\alpha_{21} \quad \frac{-\bar{\alpha}_{21}}{\bar{\alpha}_{11}\,\bar{\alpha}_{22}} .$$

Small test problems were used to verify that the albedoes in MEKIN are employed described above. From a qualitative viewpoint, very low albedoes model reflected boundary conditions and very high albedoes cause the flux to approach zero at the interface. Both results are physically consistent with Eq. (A.8) where $\alpha \approx \frac{J}{\phi}$. However, reference 9, pp. 531-533 suggests that the magnitude of the albedoes must be less than 1/2 at interfaces where diffusion theory is considered valid.

For most of the test problems in this thesis, the albedoes were calculated by Kalambokas's method (10). The reactor for which the data was approximated is a large PWR having an effec-

tive horizontal reflector of one inch of stainless steel shroud followed by five inches of water. The horizontal albedoes were calculated from the following equations in terms of reflector constants:

$$\alpha_{gg} \equiv \frac{C_g^S \cdot S_g^R \cdot (L_g^R/D_g^R) + C_g^R \cdot S_g^S \cdot (L_g^S/D_g^S)}{(L_g^R/D_g^R) \cdot (D_g^S/L_g^S) \cdot S_g^S \cdot S_g^R + C_g^S \cdot C_g^R}; \quad g=1,2,$$

$$\alpha_{21} \equiv \alpha_{11} \cdot \Omega_1 - \alpha_{22} \cdot \Omega_2 ,$$

$$\Omega_1 \equiv [(C_1^S - C_2^S) \cdot r^S \cdot \frac{L_1^R}{D_1^R} \cdot S_1^R + C_2^S \cdot \frac{r^R}{D_1^R} \cdot (L_1^R S_1^R - L_2^R S_2^R) + \tag{A.16}$$

$$+ C_1^R \cdot \frac{r^S}{D_1^S} \cdot (L_1^S S_1^S - L_2^S S_2^S) + (C_1^R - C_2^R) \cdot r^R \cdot \frac{L_2^S}{D_2^S} \cdot S_2^S \cdot \frac{D_2^R}{D_1^R}] /$$

$$/[\text{Numerator of } \alpha_{11}],$$

$$\Omega_2 \equiv [(\frac{S_1^S}{L_1^S} - \frac{S_2^S}{L_2^S}) \cdot r^S \cdot D_2^S \cdot S_1^R \cdot \frac{L_1^R}{L_1^R} + S_2^S \frac{r^R}{D_1^R} \frac{D_2^S}{L_2^S} (L_1^R S_1^R - L_2^R S_2^R) +$$

$$+ (C_1^S - C_2^S) \cdot r^S \cdot \frac{D_2^S}{D_2^S} C_1^R + C_2^S \cdot (C_2^R - C_2^R) \cdot r^R \cdot \frac{D_2^R}{D_1^R}] / \tag{A.17}$$

$$/[\text{Denominator of } \alpha_{11}],$$

$$\left.\begin{aligned} C_g^z &\equiv \cosh(\frac{\Delta_z}{L_{gz}}) \\ S_g^z &\equiv \sinh(\frac{\Delta_z}{L_{gz}}) \end{aligned}\right\} \quad g = 1, 2; \ z = \text{zone}, \tag{A.19}$$

$$r^z \equiv \frac{\Sigma_{1\to 2_z} / D_{2z}}{\frac{1}{L^2_{2z}} \frac{1}{L^2_{2z}}} , \qquad (A.20)$$

$$L^2_{gz} = \frac{D_{gz}}{\Sigma_{gaz}} , \qquad (A.21)$$

Δ_z = zone thickness,

$z = \begin{cases} S = \text{steel} \\ R = \text{light water} \end{cases}$.

Above and below the core, no shroud exists, but equipment (nozzles, etc.) means that the top and bottom reflectors are more than just water. Therefore, homogenized constants will be used in calculating the vertical albedoes from the following equaitons:

$$\alpha_{11} \equiv \frac{L_1}{D_1} \tanh \left(\frac{\Delta}{L_1}\right) , \qquad (A.22)$$

$$\alpha_{22} \equiv \frac{L_2}{L_2} \tanh \frac{\Delta}{L_2} , \qquad (A.23)$$

$$\alpha_{21} \equiv \frac{\Sigma_{1\to 2}}{D_1\Sigma_2 - D_2\Sigma_1} \cdot \left(D_1\alpha_{11} - D_2 \cdot \alpha_{22}\right) , \qquad (A.24)$$

Although these formulas are not exact, a "reflector represented by albedoes leads to extremely accurate flux and power distributions for large, shrouded reactors." (10) Calculations produced the following set of albedoes at the indicated reflector core interfaces:

	TOP	BOTTOM	HORIZONTAL
α_{11}	.045	.051	.105
α_{22}	.132	.169	.203
α_{21}	- .0396	-.0204	-.0067

.

APPENDIX B

REACTOR MODELS FOR TEST CASES

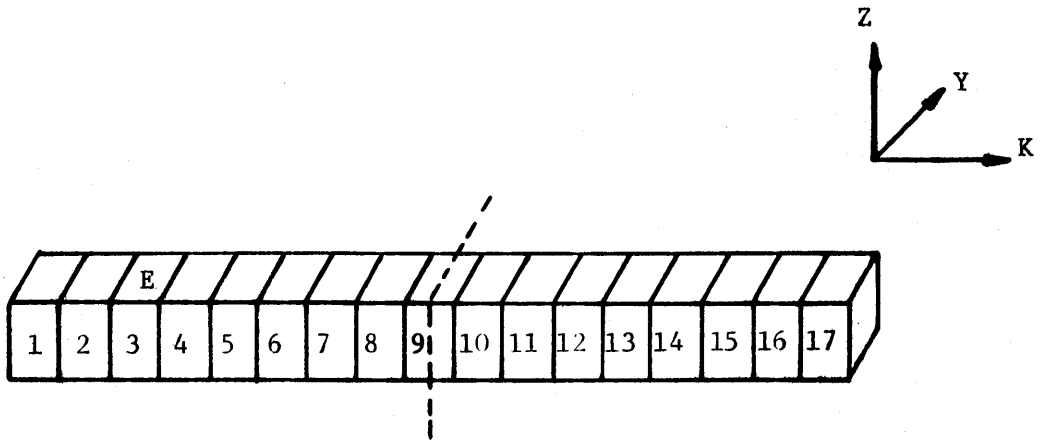

Reactor Data:

region dimensions: 20.8 x 20.8 x 29.8 cm^3

steady state power: 5 MW

boundary conditions: albedoes on ends, reflecting on top, bottom and sides

2 neutron energy groups.

Transient Data:

rod worth: $\simeq 0.6 \times \beta$

rod location: Channel E

ejection time: 0.005 seconds

6 precursor groups.

FIG. B.1.

MODEL 1.

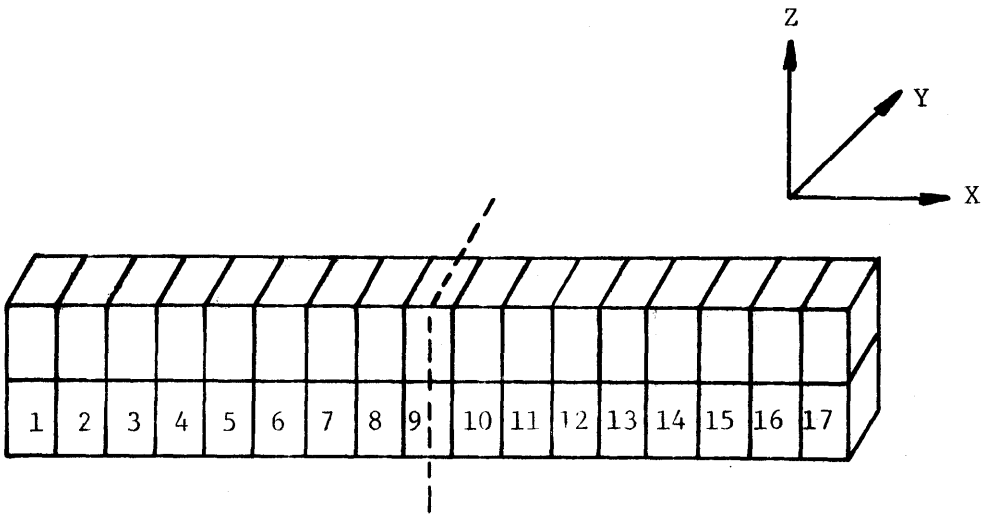

REACTOR DATA

region dimensions: 20.8 x 20.8 x 29.8 cm^3

steady state power: 40 MW

boundary conditions: albedoes on ends, reflecting on top, bottom and sides

2 neutron energy groups.

FIG. B.2.

MODEL 2.

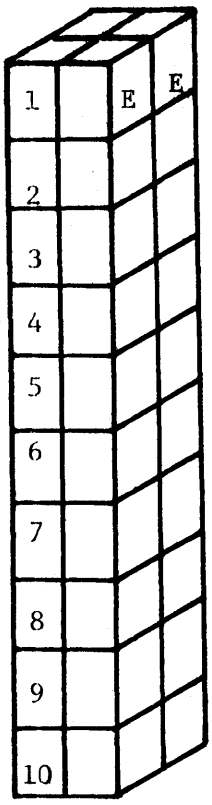

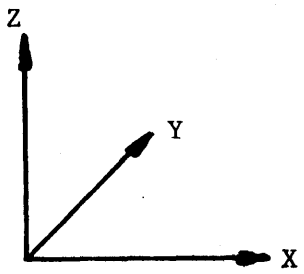

REACTOR DATA

region dimensions: 20.8 x 20.8 x 29.8 cm^3

steady state power: 47 MW

boundary conditions: different albedoes on top and bottom, reflecting on all sides

2 neutron energy groups.

TRANSIENT DATA

total rod worth: $\$ 0.6 \times \beta$

rod location: E channels

ejection time: 0.01 seconds

6 precursor groups.

FIG. B.3. MODEL 3.

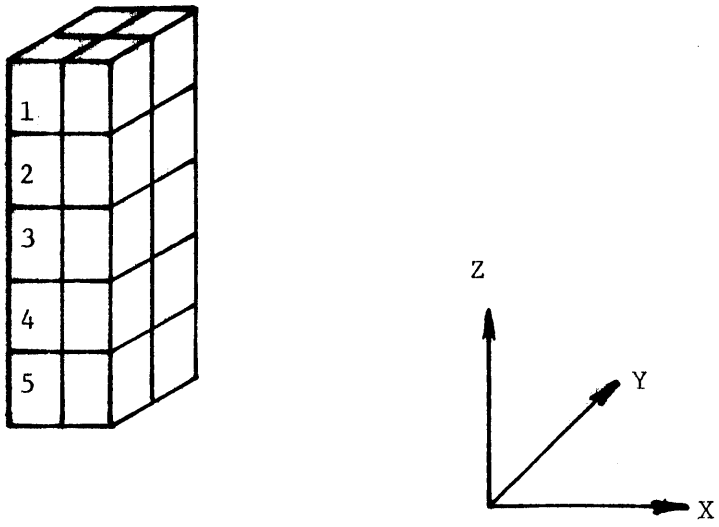

REACTOR DATA

region dimensions: 20.8 x 20.8 x 29.8 cm^3

steady state power: 18.8 MW

boundary conditions: albedoes on bottom, reflecting on top and all sides

2 neutron energy groups.

FIG. B.4.

MODEL 4.

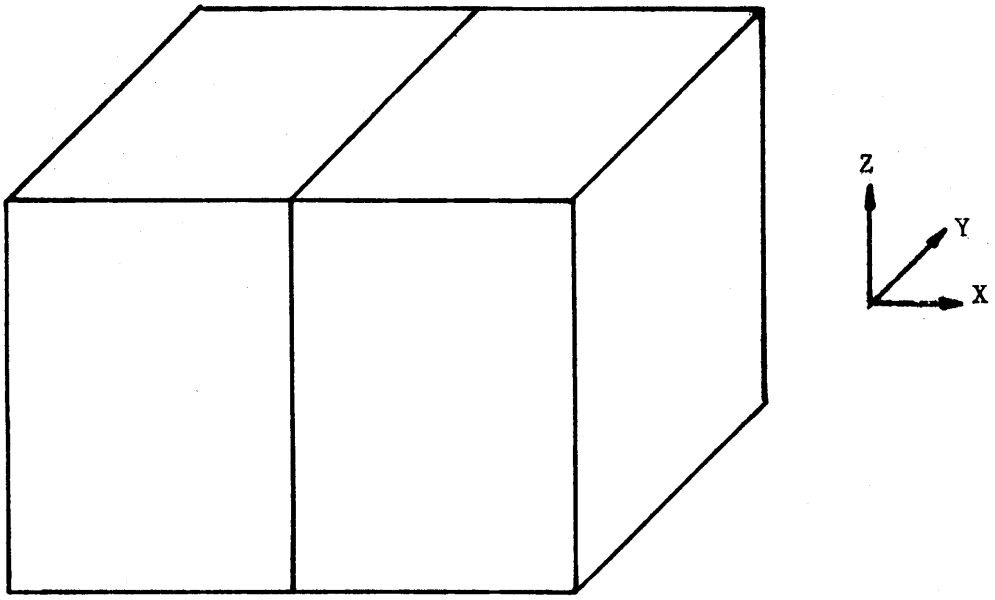

REACTOR DATA

region dimensions: 20.8 x 20.8 x 29.8 cm^3

steady state power: 2 MW

boundary conditions: (case dependent)

2 neutron energy groups.

FIG. B.5.

MODEL 5.

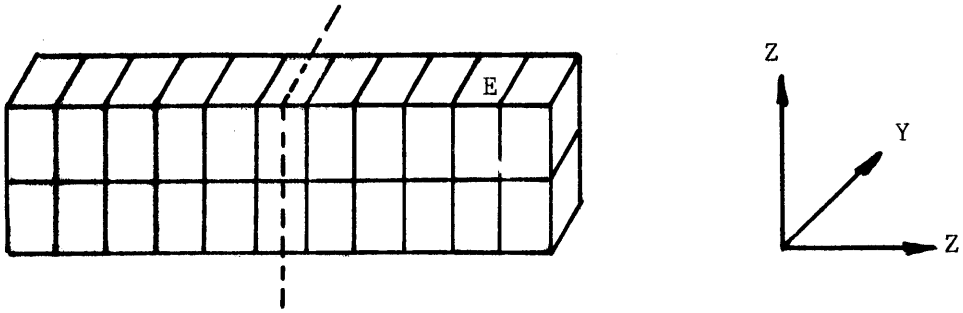

REACTOR DATA

reactor dimensions: 20.8 x 20.8 x 29.8 cm^3

steady state power: 26 MW

boundary conditions: albedoes on ends, reflecting on sides, top and bottom

2 neutron energy groups.

TRANSIENT DATA

rod worth: $\simeq 2 \times \beta$

rod location: channel E

ejection time: 0.01 seconds

1 precursor group.

FIG. B.6.

MODEL 6.

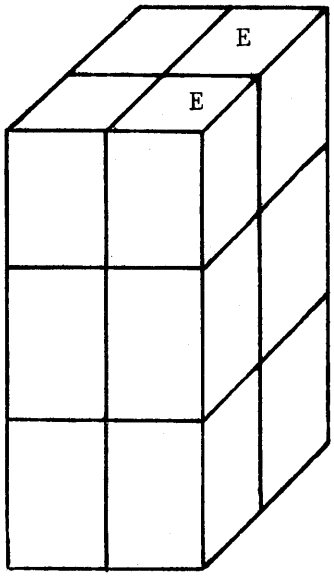

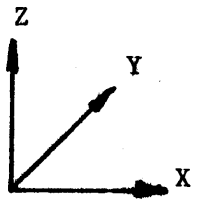

REACTOR DATA

region dimensions: 20.8 x 20.8 x 29.8 cm^3

steady state power: 12 MW

boundary conditions: albedoes on top and bottom, reflecting on bottom, reflecting on all sides

2 neutron energy groups.

TRANSIENT DATA

total rod worth: $\simeq 2 \times \beta$

rod location: E channels

withdrawal time: 10.0 seconds

1 precursor group.

FIG. B.7.

MODEL 7.

APPENDIX C

MESH SENSITIVITY TEST CASE RESULTS

The tables of this appendix consist of the power distributions of each test case in Chapter 4 and the errors incurred as the mesh spacing was varied. In steady state, total reactor power is a user input while the power distribution represents the neutronic solution. The sum of all region powers yields the total reactor power. For example, the sum of the 10 region powers on Fig. C.6 corresponds to one-fourth of the total reactor power of a 40 region reactor (Model 3 of Appendix B). For the neutronics-only cases, the input power levels were somewhat arbitrary. For the cases involving thermal-hydraulic feedback, the power represents a fraction of a PWR's operating power level, This fraction is identical to the volume of the model divided by the volume of a full core. This effort was undertaken to assure a reasonable amount of feedback.

For each region, error is measured by

$$\% \text{ error} = \frac{\text{case power} - \text{reference power}}{\text{reference power}} \times 100,$$

where the reference power corresponds to the solution of the smallest mesh interval for the given case.

TABLE C.1

HORIZONTAL SPACIAL MESH SENSITIVITY: CASE 1

CASE DESCRIPTION (CASE 1): MODEL 1 OF APPENDIX B, STEADY STATE, NEUTRONICS-ONLY, ALL REGIONS IDENTICAL.

	REFERENCE POWERS (MW x 10)	PERCENTAGE DIFFERENCE* FROM REFERENCE (%)		
Region	2.6cm MESH	3.5 cm	5.2cm	10.4cm
1	0.7912	0.36	1.06	2.62
2	1.5263	0.11	0.31	0.73
3	2.2045	0.05	0.13	0.28
4	2.8169	0.01	0.02	0.04
5	3.3450	-0.01	-0.04	-0.10
6	3.7731	-0.03	-0.08	-0.19
7	4.0884	-0.04	-0.11	-0.25
8	4.2814	-0.05	-0.12	-0.28
9	4.3464	-0.05	-0.13	-0.29
10				
11				
12	(SYMMETRY ABOUT REGION 9)			
13				
14				
15				
16				
17				

$$* \ \% \text{ DIFFERENCE} = \frac{\text{CASE POWER} - \text{REFERENCE POWER}}{\text{REFERENCE POWER}} \times 100$$

TABLE C.2

HORIZONTAL SPACIAL MESH SENSITIVITY: CASE 2

CASE DESCRIPTION (CASE 2): MODEL 1 OF APPENDIX B, STEADY STATE, NEUTRONICS-ONLY, ALL REGIONS IDENTICAL EXCEPT # 3 (ROD WITHDRAWN)

	REFERENCE POWERS (MW X 10)	PERCENTAGE DIFFERENCES* FROM REFERENCE (%)		
Region	2.6 cm MESH	3.5 cm	5.2 cm	10.4 cm
1	1.6329	0.49	1.34	3.98
2	3.1926	0.22	0.55	1.99
3	4.6263	0.30	0.84	3.31
4	4.6246	0.11	0.21	0.90
5	4.4860	0.07	0.11	0.47
6	4.3186	0.02	-0.03	-0.03
7	4.1126	-0.03	-0.16	-0.46
8	3.8699	-0.08	-0.26	-0.84
9	3.5926	-0.12	-0.34	-1.16
10	3.2833	-0.16	-0.40	-1.42
11	2.9446	-0.19	-0.45	-1.62
12	2.5797	-0.21	-0.48	-1.78
13	2.1917	-0.23	-0.48	-1.87
14	1.7842	-0.24	-0.47	-1.88
15	1.3608	-0.23	-0.40	-1.77
16	0.9252	-1.26	-0.24	-1.42
17	0.4746	.05	0.48	0.35

$$* \ \% \text{ DIFFERENCE} = \frac{\text{CASE POWER} - \text{REFERENCE POWER}}{\text{REFERENCE POWER}} \times 100$$

TABLE C.3

HORIZONTAL SPACIAL MESH SENSITIVITY: CASE 3

CASE DESCRIPTION (CASE 3): MODEL 1 OF APPENDIX B, STEADY STATE, NEUTRONICS-ONLY, MATERIAL COMPOSITIONS VARY FROM REGION TO REGION

	REFERENCE POWERS (MW X 10)	PERCENTAGE DIFFERENCES FROM REFERENCE (%)		
Region	1.3 cm MESH	2.6 cm	5.2 cm	10.4 cm
1	5.3254	0.86	2.88	6.72
2	5.9229	0.50	1.44	2.40
3	3.7514	-0.46	-1.90	-6.64
4	3.3263	-0.34	-1.29	-4.01
5	4.3263	-0.70	-1.75	-1.03
6	1.6625	-0.64	-1.93	-3.75
7	0.3785	-1.33	-4.49	-10.61
8	0.2176	-0.36	-0.44	-2.31
9	0.2136	-0.76	-1.71	-0.26
10				
11				
12				
13	(SYMMETRY ABOUT REGION 9)			
14				
15				
16				
17				

$$*\% \text{ DIFFERENCE} = \frac{\text{CASE POWER} - \text{REFERENCE POWER}}{\text{REFERENCE POWER}} \times 100$$

TABLE C.4

HORIZONTAL SPACIAL MESH SENSITIVITY: CASE 4

CASE DESCRIPTION (CASE 4): MODEL 2 OF APPENDIX B, STEADY STATE, FEEDBACK INCLUDED, ALL REGIONS IDENTICAL

	REFERENCE POWERS (MW)	PERCENTAGE DIFFERENCES* FROM REFERENCE (%)	
Region	2.6 cm MESH	5.2 cm	10.4 cm
1	0.4214	1.30	2.80
2	0.7706	0.48	0.70
3	1.0367	0.24	0.15
4	1.2296	0.09	-0.09
5	1.3629	-0.04	-0.21
6	1.4508	-0.14	-0.27
7	1.5054	-0.23	-0.30
8	1.5349	-0.28	-0.30
9	1.5443	-0.30	-0.30
10			
11			
12			
13			
14			
15	(SYMMETRY ABOUT REGION 9)		
16			
17			

* % DIFFERENCE = $\frac{\text{CASE POWER - REFERENCE POWER}}{\text{REFERENCE POWER}} \times 100$

TABLE C.5

HORIZONTAL SPACIAL MESH SENSITIVITY: CASE 5

CASE DESCRIPTION (CASE 5): MODEL 2 OF APPENDIX B, STEADY STATE, FEEDBACK INCLUDED, SAME MATERIAL COMPOSITIONS AS CASE 3

	REFERENCE POWERS (MW)	PERCENTAGE DIFFERENCES* FROM REFERENCE (%)	
Region	2.6 cm MESH	5.2 cm	10.4 cm
1	1.8527	1.29	3.70
2	2.1086	0.44	0.56
3	1.4449	-1.37	-5.20
4	1.4139	-0.29	-1.77
5	1.8591	-0.24	-1.46
6	0.7662	-0.21	-0.40
7	0.1934	-2.04	-6.60
8	0.1463	1.11	5.84
9	0.1586	0.28	3.74
10			
11			
12			
13	(SYMMETRY ABOUT REGION 9)		
14			
15			
16			
17			

*% DIFFERENCE = $\frac{\text{CASE POWER - REFERENCE POWER}}{\text{REFERENCE POWER}} \times 100$

TABLE C.6

AXIAL SPACIAL MESH SENSITIVITY: 10 REGIONS

CASE DESCRIPTION: MODEL 3 OF APPENDIX B, STEADY STATE, NEUTRONICS ONLY, MATERIAL COMPOSITIONS VARIED FROM REGION TO REGION

	REFERENCE POWERS (MW)	PERCENTAGE DIFFERENCES* FROM REFERENCE (%)		
Region	7.2 cm MESH	9.6 cm	14.5 cm	29.0 cm
1	1.2457	-2.21	-4.64	-4.13
2	1.5108	-1.21	-2.65	-3.31
3	1.5736	-0.60	-1.39	-2.33
4	1.5352	-0.09	-0.27	-0.89
5	1.4268	0.34	0.65	0.27
6	1.2740	0.68	1.43	1.25
7	1.0976	0.99	2.12	2.16
8	0.9105	1.28	2.77	3.19
9	0.7099	1.57	3.51	4.87
10	0.4660	2.04	4.89	9.58

$$* \ \% \text{ DIFFERENCE} = \frac{\text{CASE POWER} - \text{REFERENCE POWER}}{\text{REFERENCE POWER}} \times 100$$

TABLE C.7

AXIAL SPACIAL MESH SENSITIVITY: 5 REGIONS

CASE DESCRIPTION: MODEL 4 OF APPENDIX B, STEADY STATE, NEUTRONICS-ONLY, MATERIAL COMPOSITIONS VARY FROM REGION TO REGION

	REFERENCE POWERS (MW)	PERCENTAGE DIFFERENCES* FROM REFERENCE (%)			
Region	4.1 cm MESH	7.2 cm	9.6 cm	14.5 cm	29.0 cm
1	1.1958	-0.20	-0.32	-0.54	-1.23
2	1.1297	-0.15	-0.26	-0.47	-1.21
3	1.0040	-0.05	-0.11	-0.23	-0.77
4	0.8202	0.13	0.21	0.34	0.64
5	0.5503	0.65	1.11	2.03	5.60

$$* \ \% \text{ DIFFERENCE} = \frac{\text{CASE POWER} - \text{REFERENCE POWER}}{\text{REFERENCE POWER}} \times 100$$

TABLE C.8

HORIZONTAL SPACIAL MESH SENSITIVITY: TRANSIENT

CASE DESCRIPTION: MODEL 1 OF APPENDIX B, TRANSIENT, NEUTRONICS-ONLY, MATERIAL COMPOSITIONS VARY FROM REGION TO REGION, AT 0.03 SECONDS

	REFERENCE POWERS (MW)	PERCENTAGE DIFFERENCES FROM REFERENCE (%)	
Region	2.6 cm MESH	5.2 cm	10.4 cm
1	1.4847	-1.99	-9.05
2	1.6709	-3.08	-12.60
3	1.1021	-5.12	-18.37
4	0.9134	-4.76	-17.11
5	1.1401	-8.28	-13.89
6	0.4318	-4.97	-16.27
7	0.0948	-6.70	-21.39
8	0.0469	-3.35	-9.66
9	0.0361	-3.55	-9.05
10	0.0278	-1.68	-3.15
11	0.0380	-3.42	-10.10
12	0.1632	-1.39	-3.40
13	0.4224	-0.64	0.02
14	0.3282	-1.03	-3.95
15	0.3759	-1.47	-5.82
16	0.6044	0.91	1.72
17	0.5489	2.01	5.76
TOTAL REACTOR	9.4318	-2.83	-10.23

APPENDIX D

FEEDBACK PARAMETER GENERATION WITH THE LEOPARD CODE

All cross section feedback parameters employed in this project were obtained by using LEOPARD (1), a spectrum dependent computer code. The user supplies only geometry, compositions for either an assembly or single pin, and temperatures. The paragraphs that follow consist of an explanation of the manner in which LEOPARD has been and can be applied to input preparation for MEKIN.

With respect to the metal (fuel and clad) temperature, relevant inputs to LEOPARD are the average fuel temperature (T_f), the effective resonance temperature (T_r), and the average clad temperature (T_k). In a LEOPARD calculation, T_r is used to determine the Doppler contribution to the U-238 resonance integral, while T_f and T_k correct dimensions and number densities (1). If these parameters are varied as a group with all other inputs held constant, the metal temperature-cross section behavior can be predicted. The linear feedback parameters (i.e., $\partial\Sigma_i/\partial T_M$ of Eq. (6.1)) can then be estimated from this data. As a first approximation, T_f can be assigned the same value of T_r (21).

Regarding the coolant, the situation is more complicated because two inputs are involved, C_1 and C_2 of Eq. (6.1). Average coolant temperature (T_c) and system pressure are LEOPARD user

inputs, while the corresponding average coolant density (ρ_c) is calculated in the code. Holding the system pressure constant and varying the coolant temperature in subcooled conditions, the cross section behavior is a function of both T_c and ρ_c. The effects cannot be separated with only subcooled coolant data. To accommodate the input for MEKIN, $\partial\Sigma_i/\partial T_c$ could be set to zero and an "effective" $\partial\Sigma_i/\partial\rho_c$ would account for both coolant temperature and coolant density changes. In equation form,

$$\partial\Sigma_i^*/\partial\rho_c\Big|_p = \partial\Sigma_i/\partial\rho_c\Big|_{TP} + \partial T_c/\partial\rho_c\Big|_p \; \partial\Sigma/\partial T_c\Big|_{p\rho}, \quad \text{(D.1)}$$

where T, P, and C represent coolant temperature, pressure, and density. Unfortunately, this procedure breaks down when boiling occurs because temperature is no longer changing. However, LEOPARD can be used to predict the cross section-coolant density behavior in boiling conditions. Coolant temperature and pressure must be specified at saturation, while the variable input becomes the void fraction (i.e., the fraction of moderator volume which is in void form). From this data, $\partial\Sigma_i/\partial\rho_c\Big|_{TP}$ of Eq. (D.1) can be estimated for boiling conditions. Assuming this term has the same linear value in subcooled and boiling regimes, $\partial\Sigma_i/\partial T_c\Big|_{p\rho}$ of Eq. (D.1) can be found by

$$\partial\Sigma_i/\partial T_c\Big|_{p\rho} = \frac{\partial\Sigma_i^*/\partial\rho_c\Big|_p - \partial\Sigma_i/\partial\rho_c\Big|_{pT}}{\partial T_c/\partial\rho_c\Big|_p} \quad \text{(D.2)}$$

Thus, $\partial \Sigma i / \partial e_c \Big|_{PT}$ and $\partial \Sigma i / \partial T_c \Big|_{Pe}$ can be input to MEKIN for C_1 and C_2 of Eq. (6.1). However, the reader should be aware that LEOPARD was developed for pressurized water reactors with a subcooled moderator. For this reason, the accuracy of calculations with LEOPARD is questionable under conditions of high void fractions.

APPENDIX E

MODIFICATION OF THE CROSS SECTION FEEDBACK PROCEDURE

As mentioned in Section 6.2, a temporary modification of SUBROUTINE CROUSUI was necessary in order to represent the cross section-temperature behavior by higher order polynomials. The entire subroutine is listed on the following pages and changes should be made on cards 36760 to 36790. In the particular example presented here, the group one capture cross section was represented by the quadratic fit shown on Fig. 6.9. This modification consisted of replacing the operation performed by card 36770 by the operation of card 36775. With respect to the group two feedback parameters, the same procedure can be applied to SUBROUTINE CROSU2.

This method has several limitations. First, this subroutine must be recompiled every time a non-linear polynomial is studied. Second, this procedure forces the polynomial to apply to all regions of the core. The programming required to make this technique a general user option was beyond the scope of this project.

```
      SUBROUTINE CROSU1(ND3,CROS,STATE,COPR,PERT,IPRT)                  00035600
C                                                                       00035610
C                                                                       00035620
C=====OBJECTIVE:    UPDATE GROUP 1 CROS BLOCK FOR AXIAL SEGMENT ND3     00035630
C                                                                       00035640
C=====CALLED FROM:  SIGGEN                                            00035650
C                                                                       00035660
C=====CALLS TO:     NONE                                              00035670
C                                                                       00035680
C=====BLOCKS USED:  NONE, EXCEPT THROUGH ARGUMENT LIST                00035690
C                                                                       00035700
C=====COMMON AND TYPING INFORMATION                                   00035710
C                                                                       00035720
C---------BLANK COMMON                                                00035730
      COMMON         DATA(1)                                          00035740
CIBM                                                                  00035750
      REAL*8         DDAT(1),XKEFF                                    00035760
CIBM                                                                  00035770
CCDC                                                                  00035780
C     DIMENSION      DDAT(1)                                          00035790
CCDC                                                                  00035800
      INTEGER        IDAT(1)                                          00035810
      EQUIVALENCE    (DATA(1),DDAT(1),IDAT(1))                        00035820
C                                                                     00035830
C---------INTEGER LIMITS                                              00035840
      COMMON/LIMITS/    NBXX  ,ND1X  ,ND2X  ,ND3X  ,NP1X  ,NP2X  ,   00035850
     1    NP3X  ,NRGX  ,NTHRGX,NTHBXX,NTH3X ,NPBX  ,NPBDX ,NPPX  ,   00035860
     3    IQCONX,MX    ,NALBX ,ND3GX ,NCOEFX,NPP3X ,NGANGX,ICRDX ,   00035870
     2    NPTX  ,NGIX  ,NDFX  ,NP3GX ,NP3FX ,       NCPX  ,NCORX ,   00035880
     4    NTIMDX,NPWFX ,NINT1X,NINT2X,NINT3X,NCF1DX,NSLN1X,NCFPKX,   00035890
     5    NSLNPX,NALX  ,NDMNX ,NNPRTX,NINTXX,NINTYX                    00035900
C                                                                     00035910
C---------SCALARS AND FIXED-LENGTH ARRAYS                             00035920
      COMMON/FIXED/     XKEFF ,ICENTR,NSYM  ,PITCH ,HX    ,HY    ,   00035930
     1    HXI   ,HYI   ,HAREA ,ZMAX  ,BSQDT ,YXE   ,YIO   ,AMDAXE,   00035940
     2    ITSTEP,TIME  ,TIMEO ,DT    ,DTI   ,HT    ,HTI   ,ITHSTP,   00035950
```

```
     3    TIMTH ,TIMTHO,DTTH  ,DTTHI ,NSWITC,SCRIT1,SCRIT2,OMEGMX,      00035960
     4    OMEGMN,OMEGDF,NDMN  ,ITHC  ,INEUTC,INIT  ,IEDSSR,IEDSSP,      00035970
     5    ISSXEN,ITERX ,EPSSPR,EPSSK ,OMGP  ,IBCT  ,IBCB  ,KORGD ,      00035980
     6    DSG3  ,RVOL  ,ITH3B ,ITH3T ,DZP3  ,FCSAT ,PWRT0 ,PWRD0 ,      00035990
     7    PWRF0 ,PWRT  ,PWRD  ,PWRF  ,PWRTO ,PWRDO ,PWRFO ,PTIME0,      00036000
     8    PALFAP,IRODS ,NCRDRV,IDRIVE,ISCRAM,PSCRAM,PRSCRM,FSCRM ,      00036010
     9    TSCRM ,ICRDR ,ICRSC ,IN    ,IOUT  ,ILAST ,ICROS ,IDSKED,      00036020
     A    TDECAY,LTTH  ,LTPR  ,LTDS  ,IDECAY,ICNVSS,TDRIVE,NTIMD ,      00036030
     B    DIFMAX,         BETAF(6),AMDA(6),TFINAL(10),NNTPD(10),        00036040
     C    NTHFRQ(10),PTHMAX(10),IPRNTF(10),IDSKF(10),IPRNTL(10),        00036050
     D    TITLE(20)                                                     00036060
C                                                                       00036070
C---------DATA BLOCK NAMES & DATA TYPES                                 00036080
      COMMON/NAMES/     NAMLX ,WNBOX ,WND1T ,WND2T ,WNTHB ,WNB1T ,      00036090
     1    WNB2T ,WISTR ,WIEND ,WNPPS ,WNP1T ,WNP2T ,WNP3T ,WTMET ,      00036100
     2    WTCOL ,WDCOL ,WFLUX ,WFLXO ,WPRFC ,WXEN0 ,WSRC  ,WSRC1 ,      00036110
     3    WSRC2 ,WOMEG ,WCROS ,WQFMB ,WQCON ,WBETA ,WNCMP ,WCORR ,      00036120
     4    WALBT ,WALBR ,WALBX ,WALBY ,WCOFF ,WCOFX ,WCOFY ,             00036130
     5    WPWME ,WPWCO ,WPWRT ,WPWD0 ,WCFAX ,WCFAY ,WCFAZ ,WNCRB ,      00036140
     6    WCRMS ,WNCPD ,WPWFC ,WTPWF ,WINT1 ,WINT2 ,WINT3 ,WCF1D ,      00036150
     7    WSLN1 ,WOMG1 ,WCFPK ,WSLNP ,WPWRF ,WINTX ,WINTY ,WXPRT ,      00036160
     8    WTF1D,WTFPK,WTHD1,WTHD2,WGFAC,ITYPE(65)                       00036170
C                                                                       00036180
C---------ORIGINS OF CORE-CONTAINED BLOCKS                              00036190
      COMMON/ORIGIN/    KNBOX ,KND1T ,KND2T ,KNTHB ,KNB1T ,KNB2T ,      00036200
     1    KISTR ,KIEND ,KNPPS ,KNP1T ,KNP2T ,KNP3T ,KTPWF ,KOMG1 ,      00036210
     2    KCFPK ,KSLNP                                                  00036220
C                                                                       00036230
C                                                                       00036240
      COMMON/CONSTS/ IZERO ,IONE  ,ITWO  ,ITHREE,IFOUR ,IFIVE ,ISIX  ,  00036250
     1         ISEVEN,IEIGHT,ININE ,ITEN  ,ZERO  ,ONE   ,TWO   ,THREE ,  00036260
     2         FOUR  ,FIVE  ,SIX   ,SEVEN ,EIGHT ,XNINE ,TEN   ,HALF  ,  00036270
     3         THIRD ,QUARTR,EIGHTH                                     00036280
C                                                                       00036290
C                                                                       00036300
C                                                                       00036310
```

```
C                                                                       00036320
C                                                                       00036330
C                                                                       00036340
CIBM                                                                    00036350
      DOUBLE PRECISION  XKI                                             00036360
CIBM                                                                    00036370
C                                                                       00036380
C                                                                       00036390
      XKI=ONE                                                           00036400
      IF(ITSTEP.GT.IZERO)  XKI=ONE/XKEFF                                00036410
      DIMENSION IPRT(7,1)                                               00036420
      DIMENSION  CROS(NBXX,1),STATE(6,1),CORR(NCORX,1),PERT(7,1)        00036430
C                                                                       00036440
C=====LOOP OVER BOXES                                                   00036450
C                                                                       00036460
      DO 100  NBX=1,NBXX                                                00036470
      NCP=STATE(1,NBX)                                                  00036480
C                                                                       00036490
C-----SET BASE VALUES                                                   00036500
C                                                                       00036510
      SIGS=ZERO                                                         00036520
      IF(NGIX.EQ.ITWO)                                                  00036530
     1SIGS = CORR(40,NCP)                                               00036540
      SIGC = CORR(11,NCP)                                               00036550
      SIGF = CORR(15,NCP)                                               00036560
      DI   = CORR( 7,NCP)                                               00036570
      SIGX = CORR(20,NCP)                                               00036580
      XNU  = CORR(19,NCP)                                               00036590
      VI   = CORR(21,NCP)                                               00036600
      BET  = CORR( 4,NCP)                                               00036610
C                                                                       00036620
C-----INCLUDE T-H FEEDBACK, IF ANY                                      00036630
C                                                                       00036640
      IF(ITHC.EQ.IZERO)  GO TO 110                                      00036650
      E2 = STATE(2,NBX)                                                 00036660
      E3 = STATE(3,NBX)                                                 00036670
```

```
      E4 = STATE(4,NBX)                                                  00036680
      E20= CORR(1,NCP)                                                   00036690
      E30= CORR(2,NCP)                                                   00036700
      E40= CORR(3,NCP)                                                   00036710
      D2 =-E20 + E2                                                      00036720
      D3 =-E30 + E3                                                      00036730
      D4 =-E40 + E4                                                      00036740
      IF(NGIX.EQ.ITWO)                                                   00036750
     1SIGS = SIGS + CORR(41,NCP)*D2 + CORR(42,NCP)*D3 + CORR(43,NCP)*D4  00036760
C*****     L      6-10-77  CRAIG       NEW X-SEC UPDATING   (NEW CARDS O)
C     SIGC = SIGC + CORR(12,NCP)*D2 + CORR(13,NCP)*D3 + CORR(14,NCP)*D4  00036770
      SIGC = .00000104 + (6.73828E-7)*D4 + (-6.96264E-11)*(D4**2) +SIGC  00036775
      SIGF = SIGF + CORR(16,NCP)*D2 + CORR(17,NCP)*D3 + CORR(18,NCP)*D4  00036780
      DI   = DI   + CORR( 8,NCP)*D2 + CORR( 9,NCP)*D3 + CORR(10,NCP)*D4  00036790
C                                                                        00036800
C-----FORM D                                                             00036810
C                                                                        00036820
 110  D = ONE/DI                                                         00036830
C                                                                        00036840
C-----INCLUDE ZENON, IF ANY                                              00036850
C                                                                        00036860
      IF(ISSXEN.EQ.IZERO)  GO TO 120                                     00036870
      SIGC=SIGC+STATE(5,NBX)*SIGX                                        00036880
C                                                                        00036890
C-----INCLUDE CONTROL, IF ANY                                            00036900
C                                                                        00036910
 120  IF(IRODS.EQ.IZERO)  GO TO 130                                      00036920
      IF(NGIX.EQ.ITWO)                                                   00036930
     1SIGS = SIGS + CORR(47,NCP) * STATE(6,NBX)                          00036940
      D    = D    + CORR(22,NCP) * STATE(6,NBX)                         00036950
      SIGC = SIGC + CORR(23,NCP) * STATE(6,NBX)                          00036960
      SIGF = SIGF + CORR(24,NCP) * STATE(6,NBX)                          00036970
C                                                                        00036980
C=====INCLUDE EXTERNAL NEUTRONICS PERTURBATIONS, IF ANY                  00036990
C                                                                        00037000
 130  IF(NNPRTX.EQ.IZERO)  GO TO 150                                     00037010
```

```
      DO 200  NNPRT=1,NNPRTX                                          00037020
      MCP =IPRT(1,NNPRT)                                              00037030
      MCOR=IPRT(2,NNPRT)                                              00037040
      V   =PERT(7,NNPRT)                                              00037050
      IF(MCP.NE.NCP)  GO TO 200                                       00037060
      IF(MCOR.EQ.IONE)   D=D+V                                        00037070
      IF(MCOR.EQ.ITWO)   SIGC=SIGC+V                                  00037080
      IF(MCOR.EQ.ITHREE)  SIGF=SIGF+V                                 00037090
      IF(MCOR.EQ.IFOUR)  XNU=XNU+V                                    00037100
 200  CONTINUE                                                        00037110
C                                                                     00037120
C=====STORE IN CROS                                                   00037130
C                                                                     00037140
 150  CROS(NBX,1) = D                                                 00037150
      CROS(NBX,2) = SIGC+SIGF+SIGS                                    00037160
      CROS(NBX,3) = SIGF                                              00037170
      CROS(NBX,4) = SIGF*XNU*XKI                                      00037180
      CROS(NBX,5) = SIGX                                              00037190
      CROS(NBX,6) = VI                                                00037200
      CROS(NBX,7) = BET                                               00037210
      NRG=NBX+NBXX*ND3                                                00037220
      IF(D   )  901,901,310                                           00037230
 310  IF(SIGC)  902,320,320                                           00037240
 320  IF(SIGF)  903,330,330                                           00037250
 330  IF(SIGX)  904,340,340                                           00037260
 340  IF(BET )  905,350,350                                           00037270
 350  IF(XNU )  906,360,360                                           00037280
 360  IF(VI  )  907,370,370                                           00037290
 370  CONTINUE                                                        00037300
C                                                                     00037310
C=====INCLUDE TRANSVERSE BUCKLING IF NDMNX=2                          00037320
C                                                                     00037330
      IF(NDMNX.EQ.ITHREE)  GO TO 140                                  00037340
      CROS(NBX,2) = CROS(NBX,2) + D*BSQDT                             00037350
C                                                                     00037360
C=====END LOOP OVER NBX                                               00037370
```

```
C                                                                       00037380
 140  CONTINUE                                                          00037390
 100  CONTINUE                                                          00037400
C                                                                       00037410
C=====FINISHED                                                          00037420
C                                                                       00037430
      RETURN                                                            00037440
 901  WRITE(6,9010)  NRG,NCP,D    ,(STATE(I,NBX),I=2,7)                00037450
      GO TO 999                                                         00037460
 902  WRITE(6,9020)  NRG,NCP,SIGC,(STATE(I,NBX),I=2,7)                 00037470
      GO TO 999                                                         00037480
 903  WRITE(6,9030)  NRG,NCP,SIGF,(STATE(I,NBX),I=2,7)                 00037490
      GO TO 999                                                         00037500
 904  WRITE(6,9040)  NRG,NCP,SIGX,(STATE(I,NBX),I=2,7)                 00037510
      GO TO 999                                                         00037520
 905  WRITE(6,9050)  NRG,NCP,BET ,(STATE(I,NBX),I=2,7)                 00037530
      GO TO 999                                                         00037540
 906  WRITE(6,9060)  NRG,NCP,XNU ,(STATE(I,NBX),I=2,7)                 00037550
      GO TO 999                                                         00037560
 907  WRITE(6,9070)  NRG,NCP,VI  ,(STATE(I,NBX),I=2,7)                 00037570
      GO TO 999                                                         00037580
 999  STOP 1                                                            00037590
 9010 FORMAT(1H0,50(1H*)//10X,39HCROSS SECTION PROCESSING ERROR.  REGION00037600
     1,I5,12H COMPOSITION,I5, 9H GROUP 1 //                             00037610
     210X,37HD                    IS NEGATIVE OR ZERO    /              00037620
     310X, 28HCOOLANT DENSITY (GM/CC)    = ,1PE12.5/                    00037630
     410X, 28HCOOLANT TEMPERATURE (O C) = ,1PE12.5/                     00037640
     510X, 28HMETAL   TEMPERATURE (O C) = ,1PE12.5/                     00037650
     610X, 28HXENON CONC. (ATOM/B-CM)    = ,1PE12.5/                    00037660
     710X, 28HCONTROL ROD FRACTION       = ,1PE12.5)                    00037670
 9020 FORMAT(1H0,50(1H*)//10X,39HCROSS SECTION PROCESSING ERROR.  REGION00037680
     1,I5,12H COMPOSITION,I5, 9H GROUP 1 //                             00037690
     210X,37HCAPTURE XSECTION IS NEGATIVE          /                    00037700
     310X, 28HCOOLANT DENSITY (GM/CC)    = ,1PE12.5/                    00037710
     410X, 28HCOOLANT TEMPERATURE (O C) = ,1PE12.5/                     00037720
     510X, 28HMETAL   TEMPERATURE (O C) = ,1PE12.5/                     00037730
```

OCT

```
    610X, 28HXENON CONC. (ATOM/B-CM)    = ,1PE12.5/                          00037740
    710X, 28HCONTROL ROD FRACTION       = ,1PE12.5)                          00037750
9030 FORMAT(1H0,50(1H*)//10X,39HCROSS SECTION PROCESSING ERROR.  REGION00037760
    1,I5,12H COMPOSITION,I5, 9H GROUP 1 //                                   00037770
    210X,37HFISSION XSECTION IS NEGATIVE            /                        00037780
    310X, 28HCOOLANT DENSITY (GM/CC)    = ,1PE12.5/                          00037790
    410X, 28HCOOLANT TEMPERATURE (O C) = ,1PE12.5/                           00037800
    510X, 28HMETAL   TEMPERATURE (O C) = ,1PE12.5/                           00037810
    610X, 28HXENON CONC. (ATOM/B-CM)    = ,1PE12.5/                          00037820
    710X, 28HCONTROL ROD FRACTION       = ,1PE12.5)                          00037830
9040 FORMAT(1H0,50(1H*)//10X,39HCROSS SECTION PROCESSING ERROR.  REGION00037840
    1,I5,12H COMPOSITION,I5, 9H GROUP 1 //                                   00037850
    210X,37HXENON   XSECTION IS NEGATIVE            /                        00037860
    310X, 28HCOOLANT DENSITY (GM/CC)    = ,1PE12.5/                          00037870
    410X, 28HCOOLANT TEMPERATURE (O C) = ,1PE12.5/                           00037880
    510X, 28HMETAL   TEMPERATURE (O C) = ,1PE12.5/                           00037890
    610X, 28HXENON CONC. (ATOM/B-CM)    = ,1PE12.5/                          00037900
    710X, 28HCONTROL ROD FRACTION       = ,1PE12.5)                          00037910
9050 FORMAT(1H0,50(1H*)//10X,39HCROSS SECTION PROCESSING ERROR.  REGION00037920
    1,I5,12H COMPOSITION,I5, 9H GROUP 1 //                                   00037930
    210X,37HDELAYED FRACTION IS NEGATIVE            /                        00037940
    310X, 28HCOOLANT DENSITY (GM/CC)    = ,1PE12.5/                          00037950
    410X, 28HCOOLANT TEMPERATURE (O C) = ,1PE12.5/                           00037960
    510X, 28HMETAL   TEMPERATURE (O C) = ,1PE12.5/                           00037970
    610X, 28HXENON CONC. (ATOM/B-CM)    = ,1PE12.5/                          00037980
    710X, 28HCONTROL ROD FRACTION       = ,1PE12.5)                          00037990
9060 FORMAT(1H0,50(1H*)//10X,39HCROSS SECTION PROCESSING ERROR.  REGION00038000
    1,I5,12H COMPOSITION,I5, 9H GROUP 1 //                                   00038010
    210X,37HNU                  IS NEGATIVE         /                        00038020
    310X, 28HCOOLANT DENSITY (GM/CC)    = ,1PE12.5/                          00038030
    410X, 28HCOOLANT TEMPERATURE (O C) = ,1PE12.5/                           00038040
    510X, 28HMETAL   TEMPERATURE (O C) = ,1PE12.5/                           00038050
    610X, 28HXENON CONC. (ATOM/B-CM)    = ,1PE12.5/                          00038060
    710X, 28HCONTROL ROD FRACTION       = ,1PE12.5)                          00038070
9070 FORMAT(1H0,50(1H*)//10X,39HCROSS SECTION PROCESSING ERROR.  REGION00038080
    1,I5,12H COMPOSITION,I5, 9H GROUP 1 //                                   00038090
```

```
     210X,37HINVERSE VELOCITY IS NEGATIVE                /                00038100
     310X, 28HCOOLANT DENSITY (GM/CC)    = ,1PE12.5/                       00038110
     410X, 28HCOOLANT TEMPERATURE (O C) = ,1PE12.5/                        00038120
     510X, 28HMETAL   TEMPERATURE (O C) = ,1PE12.5/                        00038130
     610X, 28HXENON CONC. (ATOM/B-CM)    = ,1PE12.5/                       00038140
     710X, 28HCONTROL ROD FRACTION       = ,1PE12.5)                       00038150
C                                                                          00038160
C=====END                                                                  00038170
C                                                                          00038180
      END                                                                  00038190
```

NUCLEAR ENGINEERING
READING ROOM - M.I.T.